The Dissertation Committee for Ann Thijs Certifies that this is the approved version of the following dissertation:

BIOTIC AND ABIOTIC CONTROLS ON CARBON DYNAMICS IN A CENTRAL TEXAS ENCROACHING SAVANNA

Committee:

Christine Hawkes, Co-Supervisor

Marcy Litvak, Co-Supervisor

Mathew Leibold

Thomas Juenger

Zong-Liang Yang

Thomas Boutton

BIOTIC AND ABIOTIC CONTROLS ON CARBON DYNAMICS IN A CENTRAL TEXAS ENCROACHING SAVANNA

by

Ann Thijs, M.S.

Dissertation

Presented to the Faculty of the Graduate School of

The University of Texas at Austin

in Partial Fulfillment

of the Requirements

for the Degree of

Doctor of Philosophy

The University of Texas at Austin

December 2014

Dedication

Voor mijn kinderen – Annalies en Xander – dat ze mogen opgroeien, gelukkig zijn en genieten van deze wonderbare wereld.

Acknowledgements

I am very grateful for my supervisors, Marcy Litvak and Christine Hawkes, for their continued advice and support throughout my years as a graduate student. Thank you to Tamara Basham, Sheri Knight and Lauren Colangelo for help with fieldwork. At Freeman Ranch, I want to thank JP Bach and Chris Thomas for their logistical support and practical advice.

Courses taught by Camille Parmesan, Libby Stern and Zong-Liang Yang at UT Austin shaped my thinking. I met a great group of people with similar research interests through the SIRFER stable isotope course at the University of Utah, as well as the Advanced Study Program at the National Center for Atmospheric Research. From this larger group of people, I especially want to thank Joseph Berry for his help with the biochemical models and Chun-Ta Lai for his help with the scaling exercise.

On a more personal note, I want to thank Ana Gonzalez, Mary Poteet, Sarah Hamman, Tamara Basham and Valerie Huguet, for being great friends and women in science during our time together at UT Austin. I want to thank my parents for their unconditional love and their support in all my endeavors. Last, but not least, endless thanks goes out to my husband, Peter Vancorenland, for loving me, believing in me and supporting me.

This research was made possible through financial support from the UT Austin EEB graduate program, the UT Austin Graduate School and a NASA Earth System Science Fellowship.

BIOTIC AND ABIOTIC CONTROLS ON CARBON DYNAMICS IN A CENTRAL TEXAS ENCROACHING SAVANNA

Ann Thijs, PhD

The University of Texas at Austin, 2014

Co-Supervisor: Christine Hawkes

Co-Supervisor: Marcy Litvak

Anthropogenic activities are responsible for increases in atmospheric CO_2 and climate change. These increases are partly counterbalanced by natural processes, such as carbon uptake in land surfaces. These processes are themselves subject to climate change, creating a coupled carbon-climate system. I investigated the carbon sink that woody encroachment represents, using a Central Texas savanna as study site, and studied how climatic factors influence this carbon sink.

Woody plant encroachment, a worldwide structural change in grassland and savanna ecosystems, alters many ecosystem properties, but the net effect on the carbon balance is uncertain. Woody encroachment represents one of the key uncertainties in the US carbon balance, and demands a more detailed understanding. To come to a process-based understanding of the encroachment effect on carbon dynamics, I analyzed patterns of carbon exchange using eddy-covariance technology. I expected the imbalance between carbon uptake and release processes associated with the encroaching trees specifically, to be responsible for the carbon sink. I also expected that the sink would vary in time, due to strong links between carbon fluxes and soil water in this semi-arid ecosystem. I further

studied the ecophysiology of the dominant species, as well as soil respiration processes under different vegetation types, and scaled these findings in space and time.

I found that the ecosystem was a significant carbon sink of 405 g C m^{-2} yr^{-1}. The encroaching trees increased photosynthesis by 180% and decreased soil respiration by 14%, compared to the grassland, resulting in a strong carbon sink due to the encroachment process. The encroaching process also altered carbon dynamics in relation to climatic drivers. The evergreen species Ashe juniper effectively lengthened the growing season and widened the temperature range over which the ecosystem acts as a carbon sink. The drought resistance of the encroaching trees reduced the sensitivity of this savanna to drought.

I conclude that encroachment in Central Texas savannas increased the carbon sink strength by increasing the carbon inputs into the ecosystem. Woody encroachment also reduced the sensitivity to climatic drivers. These two effects constitute a direct effect, as well as a negative feedback to the coupled carbon-climate system.

Table of Contents

List of Tables

List of Figures

CHAPTER 1: WOODY ENCROACHMENT ALTERS ECOSYSTEM PHOTOSYNTHETIC PATHWAYS, PHOTOSYNTHETIC CAPACITIES AND SENSITIVITY TO CLIMATIC DRIVERS

Abstract

Grasslands and savanna ecosystems around the world are being invaded by woody species and this shift in plant functional type has the potential to change ecosystem functioning dramatically. Net effects of woody encroachment on the carbon balance are hard to predict due to differences in climate zones, encroaching species physiology and ecohydrological considerations. The Edwards Plateau, an important karst aquifer in Central Texas, is undergoing woody encroachment, which raises questions about the importance of the region in the carbon balance of the US, as well as the effect of the encroachment process on water supply.

To come to a mechanistic understanding of the changes in carbon dynamics due to woody encroachment, we assessed differences in plant ecophysiological traits pertinent to photosynthetic carbon uptake, in a semi-arid savanna ecosystem undergoing encroachment by two species - the conifer *Juniperus ashei* and the nitrogen fixer *Prosopis glandulosa*. We evaluated differences between four plant functional types (conifer, nitrogen fixing tree, C4 grass and C3 grass) during two years of contrasting water availability, in the context of a coupled stomatal-biochemical photosynthesis model, and inferred sensitivity of the four species to climatic drivers.

The encroaching trees exhibited a higher drought resistance than the grasses, due to a deeper rooting system, and a wider temperature range for photosynthesis than the C4 grass species. These two fundamental differences, as well as the year-long activity of Ashe juniper, effectively lengthens the growing season of the ecosystem and predicts that the encroachment process adds significantly to the carbon uptake potential of this ecosystem.

Rising CO_2 concentrations and altered precipitation regimes predicted for this region, both favor the encroaching trees over the grassland species and suggests further progression of woody encroachment.

1. Introduction

Woody encroachment is causing pervasive change in ecosystem structure in grassland and savanna ecosystems around the world. Proposed mechanisms pertain either to local drivers, such as overgrazing and disturbance of the natural fire cycle (Archer et al. 1995, Van Auken 2000) or global drivers, such as rising CO_2 levels, altered precipitation regimes and nitrogen deposition (Polley et al. 1997, Bond and Midgley 2000, Gao and Reynolds 2003, Fensham et al. 2005, Wigley et al. 2010). Regardless of the cause, woody encroachment has the potential to alter fundamental ecosystem properties and processes, with consequences for both carbon balance (Houghton et al. 1999, Pacala et al. 2001) and hydrology (Huxman et al. 2005, Moore and Heilman 2011). Grasslands and savannas take up 28% of global land surface and represent 37% of global

net primary productivity (Grace et al. 2006). Due to the size of the biome, changes in carbon and water cycles in grasslands and savannas have potentially large feedbacks to the climate system.

Reported changes in ecosystem function triggered by woody encroachment have focused on different aspects of the carbon and water cycle, such as ecohydrology and ecophysiology (Huxman et al. 2005, Wilcox et al. 2005, Scott et al. 2006, Moore and Heilman 2011), biogeochemistry (Hibbard et al. 2003, McCulley et al. 2004, Cable et al. 2009) and biophysics (Kurc and Small 2004, Heilman et al. 2014). Known effects vary across sites, with increased or no effect on stream flow and ET, as well as increased or decreased total carbon storage (Jackson et al. 2002, Knapp et al. 2008, Barger et al. 2011). The large differences in functional types of encroaching species, together with their occurrence on different geological substrates and in different climate zones, make it hard to make generalizations about the net effect of woody encroachment on the carbon and water balance of ecosystems. A meta-analysis of 244 case studies, found that of the 43 response variables, most had a variable – positive to negative - response (Eldridge et al, 2011). Some general trends and frameworks are however emerging. Mean annual precipitation has been found to be a good predictor of changes in aboveground net primary productivity (Barger et al. 2011), while climate, landscape physiography and runoff mechanisms are determining factors in the outcome for the hydrological cycle (Moore and Heilman 2011). In the same meta-study, Eldridge (2011) found that characteristics of the encroaching species have a significant impact on both the structural and functional outcome of encroachment. Understanding the local-scale ecophysiology of

the encroaching species, as well as species that are being displaced, are therefore of utmost importance to make predictions at the local scale and will support mechanistic predictions about carbon and water exchange at larger scales.

The differences in carbon capturing mechanism between C3 and C4 species gives a first indication of how ecosystem processes and resource use efficiencies might be altered due to woody encroachment. At current levels of atmospheric CO_2, photorespiration reduces the overall photosynthetic efficiency in C3 plants, while the CO_2 concentrating mechanism in C4 plants allows for higher light use efficiency at higher temperatures (Ehleringer and Björkman, 1977), as well as higher water use efficiency (Osmond et al, 1982) and higher nitrogen use efficiency (Brown, 1978, Schmidt and Edwards, 1981).

Nevertheless, leaf-level metabolic advantages of C4 grass species over C3 tree species can be overridden at the ecosystem scale due to differences in phenology, rooting depth and nitrogen acquisition systems. Trees are generally deeper rooted than grasses (Walter 1954, Walker and Noy-Meir 1982, Schenk and Jackson 2002), which makes trees less susceptible to droughts. Differences in plant architecture and leaf area index can make tree-dominated systems more efficient in capturing CO_2 than C4-dominated sites (Knapp et al. 2008). Differences in phenology, temperature range of photosynthetic activity (Barron-Gafford et al. 2012), or drought resistance, allows trees to have longer, sometimes year-long, growing seasons, while the photosynthetic effort of C4 grasses is concentrated during well watered summer conditions. These three advantages of trees over grasses suggest that the process of woody encroachment provides ecosystems with a

stronger carbon uptake capacity, but at the same time, might have repercussions for the water balance of an ecosystem by increasing evapotranspiration and reducing recharge to aquifers and watersheds (Huxman et al. 2005, Moore and Heilman 2011).

In this study, we examine the ecophysiology of two encroaching tree species and two grassland species on the Edwards Plateau, a physiographic subdivision of the Great Plains in Central Texas, that has been classified as having a high woody encroachment carbon sink potential (Barger et al. 2011). The most common encroaching tree species in Central Texas is Ashe juniper (*Juniperus ashei* Buchholz), a drought-tolerant evergreen. Honey mesquite (*Prosopis glandulosa*) is also encroaching in this region, but only where deeper soils prevail (Eggemeyer and Schwinning 2009). The ecosystem under study is located on an extensive karst system, where the ability of woody species to access a stable supply of water, not accessible to the existing grasses, is questionable (Eggemeyer et al. 2009, Heilman et al. 2012, Schwinning 2013, Elkington et al. 2014).

We had two goals: (1) quantify differences in ecophysiological characteristics between the invading woody and existing herbaceous species and (2) develop a predictive model that effectively scales from the leaf to the ecosystem to quantify how the observed increase in woody species is likely to alter carbon uptake in this ecosystem. To meet our first objective, we quantified the photosynthetic performance of four different species (two existing herbaceous species, two invading woody species) over a two year period when weather conditions ranged from drought to well-watered, allowing us to determine the photosynthetic characteristics of the four dominant species and their sensitivity to climatic drivers. Based on differences in plant functional type, we predicted low

photosynthetic uptake rates and high water use efficiency for the encroaching conifer; and high photosynthetic uptake rates and low water use efficiency for the nitrogen fixing encroacher. We expected the C4 grass to have the best of worlds: high photosynthetic uptake rates and high water use efficiency. Based on the assumed differences in rooting depth, we predicted that the invading trees would be less sensitive to changes in soil water content than grasses, but would also experience drought effects due to lack of access to a perennial water source.

To address our second objective, we used the leaf level measurements from the first objective to parameterize biochemical models of C3 and C4 photosynthesis and included a dependence on soil water content. We used these models to predict how all four species are likely to respond to climatic variables. Whereas the leaf level measurements give us a good indication of what the species are doing at specific times, the more mechanistic biochemical models gives us predictive power to model what the different species will do at different times and under different climatic conditions.

2. Materials and methods

2.1. SITE DESCRIPTION

The research took place at the AmeriFlux site Freeman Ranch 2 (US-FR2; 29°56'N, 98°W) located in the Balcones Canyonlands subregion of the eastern Edwards Plateau in Central Texas (Litvak et al. 2011). The climate at the study site is characterized by mild, humid winters and hot, dry summers, when periods of dry heat are

interspersed by pulse rain events. Mean annual temperature is 19.6 °C and mean annual rainfall is 913.3 mm. Most of the region is occupied by upland habitats, which consist of savanna parkland with clusters of Plateau Live Oak (*Quercus virginiana var. fusiformis*) and Ashe juniper (*Juniperus ashei*) scattered in perennial grasslands. The study site is located in a former grassland, being encroached by Ashe juniper (*Juniperus ashei*) and Honey mesquite (*Prosopis glandulosa*). Historical aerial photographs show that the trees at the site are ~ 30 years old and that they comprised ~ 50% cover in 2008 (González 2010). The grassland vegetation at the site is indicative of heavy grazing and is dominated by the invasive C4 grass, King Ranch bluestem *(Bothriochloa ischaemum)*, with the C3 Texas wintergrass (*Nasella leuchotricha*) sub-dominant to rare.

The research area consists of a karst landscape which overlies and recharges the Edwards Aquifer. The soil at the site is Upland Rumple gravelly clay loam (Clayey-skeletal, mixed, active, thermic Typic Argiustolls) with weathered limestone (Bk horizon) at depths of ~1-2 m. The A horizon is ~20 cm thick and overlies a ~40 cm thick Bt1 horizon containing a high percentage of chert fragments. Below that is a Bt2 horizon containing few rock fragments (Barnes et al. 2000). Excavations showed the presence of roots throughout A and Bt horizons but limited penetration of roots into the Bk horizon (pers. comm. Susan Schwinning).

2.2. FOCAL SPECIES

We examined four different species, representing four different plant functional types*: Juniperus ashei* (Ashe juniper), a needle leaf evergreen, belonging to the family

Cuppressaceae; *Prosopis glandulosa* (Honey mesquite), a broadleaf nitrogen fixing deciduous tree; *Bothriochloa ischaemum* (King Ranch bluestem), an invasive C4 grass and *Nassella leuchotricha* (Texas wintergrass), a native perennial C3 grass. The first three species were chosen because of their dominance at the AmeriFlux tower site. Texas wintergrass was chosen because it is a native C3 grass, present at this site and very common in this ecoregion.

Ashe juniper, the most common encroacher in Central Texas, is native to northeastern Mexico and the south-central United States. Juniper species are drought tolerant and are among the most resistant species in the world to water-stress-induced xylem cavitation (Maherali et al. 2004). Ashe juniper is described as predominantly shallow-rooted with an expansive fibrous root system confined to thin soils (Hall 1952). The actual rooting depth of Ashe juniper seems to differ according to the underlying bedrock and geology. Tap roots of Ashe juniper have been observed in caves at 9–22 m depth in faulted karst regions, and stable isotope studies have shown that Ashe juniper can use deep water sources during the summer (McCole and Stern 2007). At other sites, rooting depth seems to be constrained and Ashe juniper does not seem to have access to a stable water source or affect streamflow (Wilcox 2002, Wilcox et al. 2005). Previous ecohydrological studies at our study site have shown reduced net photosynthetic uptake in Ashe juniper and reduced leaf water potentials during drought periods (Eggemeyer and Schwinning 2009, Elkington et al. 2014), as well as reduced sap flow during droughts (Elkington et al. 2014). Meteorological studies at our site and at a nearby juniper-oak woodland site, show rapid reductions in latent heat and increases in Bowen ratio in the

dry-down after a rainfall event (Litvak et al. 2011, Heilman et al. 2014). Taken together, this means that juniper does not have access to a perennial stable water source at our study site.

Honey mesquite is part of the *Prosopis* genus which includes several successful invaders in riparian areas, grasslands and savannas (Ansley et al. 2001, Asner et al. 2003, Throop and Archer 2007). Increases in Honey mesquite have altered productivity (Asner et al. 2003, Jenerette et al. 2009), the water budget, ecosystem physiology and biogeochemistry (Hibbard et al. 2001, McCulley et al. 2004, Liao et al. 2006, Scott et al. 2014) in other Southwestern savannas. Mesquite trees are winter-deciduous, drought-avoiding phreatophytes, and are capable of altering the ecosystem water balance in significant ways by maintaining high evapotranspiration rates by tapping into deeper water sources during droughts (Huxman et al. 2005, Scott et al. 2006, Throop et al. 2012). Although Honey mesquite is usually known to access deep water resources, ecohydrological studies at our study site have indicated that the root systems of Ashe juniper and Honey mesquite occupy the same soil space and do not seem to have access to a perennial stable water supply based on isotopic evidence, pre-dawn leaf potentials and sap flow measurements (Eggemeyer and Schwinning 2009, Elkington et al. 2014).

The dominant grassland species at our site is King Ranch Bluestem (*Bothriochloa ischaemum*), an invasive C4 perennial grass. King Ranch bluestem was introduced in the United States for pasture improvement and has since invaded grassland areas throughout Central Texas (Gabbard and Fowler 2007). Ecophysiological studies of King Ranch

bluestem have shown that the C4 grass exhibits drought response characteristics similar to other local C4 grass species (Basham 2013).

2.3. PHOTOSYNTHETIC MEASUREMENTS

Light response curves were collected monthly for all four species, as long as the species was photosynthetically active, using a portable infra-red gas analyzer (Li-6400, Li-Cor, Inc., Lincoln, NE, USA). CO_2 response curves were collected at five different time periods. The Li-6400 was calibrated each month using 0 and 400 ppm CO_2 standards and a dew point generator (Li-610, Li-Cor, Inc., Lincoln, NE, USA). CO_2 concentration inside the leaf chamber was held constant at 390 ppm CO_2 using CO_2 cartridges. Leaf temperature and humidity were held constant at ambient levels and incident photosynthetic radiation was varied between 2000 and 0 μmol $m^{-2}s^{-1}$. All measurements were made between 10AM and 2PM. We measured leaf area inside the cuvette using ImageJ image processing software on scanned leaves (Rasband, 1997-2014). For juniper, the half cylindrical leaf area was calculated by multiplying the projected leaf area with $\pi/2$ (Campbell and Norman 1998). The projected one-sided leaf area was used for the three other species in all calculations. A stomatal ratio of 1 was used for all species in the calculation of stomatal conductance and internal CO_2 concentration. A boundary layer conductance of 6 mol H_2O m^{-2} s^{-1} was used for juniper and a boundary layer conductance that scaled with leaf area and fan speed was used for the three other species. Leaf material was dried to constant weight at 70°C, weighed and ground for determination of specific leaf area and elemental and carbon isotopic composition (%C, %N, $\delta^{13}C$, University of Wyoming Stable Isotope Facility).

2.4. CALCULATING PHOTOSYNTHETIC PARAMETERS FROM LIGHT RESPONSE CURVES

We used a differential evolution algorithm in Matlab (MathWorks Inc., Natick, MA, USA) to fit three models to the individual light response curves: exponential, rectangular hyperbolic, and nonrectangular hyperbolic. The differential evolution algorithm with a normal least mean squares cost function was used because it converges faster and is more robust than the default nonlinear global optimization in Matlab (Storn and Price 1997). The Akaike Information Criterion (AIC) showed that the nonrectangular hyperbolic curve provided the best fit:

$$A(PAR) = \frac{\alpha PAR + A_{max} - \sqrt{(\alpha\ PAR + A_{max})^2 - 4\theta PAR\ A_{max}}}{2\theta} - R_d$$

This allowed us to estimate the parameters for light use efficiency (α; defined as the initial slope of the light response curve), gross photosynthesis at light saturation (Amax), curvature (θ) and respiration (Rd).

Instantaneous and intrinsic water use efficiency were calculated as An/E and An/G_s, respectively, where An is net carbon uptake, E is transpiration rate, and G_s is stomatal conductance. An, E and G_s were measured at saturated light conditions, in the 1500-2000 μmol PAR m^{-2} s^{-1} range of the light response curve. Nitrogen use efficiency was calculated as An/N [μmol CO_2 mol $N^{-1}s^{-1}$].

2.5. DATA ANALYSIS

We used SAS software (SAS Institute, Cary, NC, USA) PROC MIXED to evaluate differences between species in average leaf and photosynthetic characteristics. Ad hoc contrasts were used to compare species pairs.

We used single linear regression (SAS PROC GLM) analyses to investigate whether environmental drivers and leaf nitrogen content affected key physiological processes differently between the four focal species. Species was designated as a categorical variable and included as a factor in the model, as well as the interaction between species and the explaining variable. Differences in slopes were used to evaluate differences in response of species photosynthetic characteristics to climatic variables.

We also used multiple linear regression (SPSS) to investigate which climatic variables and leaf characteristics best described the observed variation in An, Gs and Rd per species (Table 4).

2.6. ESTIMATING PARAMETERS FOR THE COUPLED BIOCHEMICAL – STOMATAL CONDUCTANCE MODELS

Biochemical models of photosynthesis of C3 species (Farquhar 1989, Collatz et al. 1991) and C4 species (Collatz et al. 1992) form the plant physiological backbone of most biogeochemical models, ranging in scope from leaf-level, over canopy and regional models, to global coupled atmosphere-biosphere models (e.g. (Sellers et al. 1996b, Bonan et al. 2002).

We used the physiological leaf-level measurements, taken over a two year period in varying environmental conditions, to parameterize the C3 and C4 coupled biochemical-stomatal conductance models (Collatz et al. 1991, Collatz et al. 1992). The

biochemical models of photosynthesis work together with a model of stomatal conductance (Ball et al. 1987) to address the effect of atmospheric humidity on the opening of stomates, and provision of CO_2 to mesophyll cells for photosynthesis. During prolonged droughts however, other non-stomatal mechanisms, such as mesophyll conductance and decreased biochemical performance come into play. These effects can be incorporated in modeling exercises through a linear dependence of Rubisco capacity on either soil water deficit or leaf water potentials (Colello et al. 1998, Vico and Porporato 2008). This is intended to reproduce the effect, but does not represent the mechanism of water stress.

We estimated the Ball-Berry coefficients (Ball et al. 1987) to describe the response of stomatal conductance to the rate of net photosynthesis and the relative humidity and CO_2 mole fraction in the air at the leaf surface for all four species using linear regression. Only data points for which there was net carbon uptake, at sufficient light (PAR > 50 µmol m^{-2} s^{-1}) and CO_2 concentrations (Cs > 100 ppm), were used.

$$g_s = m\left(\frac{A_n \boldsymbol{h}_s}{C_s}\right) + b$$

The parameters of the C3 and C4 photosynthetic models (Appendix) were fitted using a Levenberg-Marquardt optimization in IDL 6.3 (Exelis Visual information Solutions, Boulder, CO, USA; Joseph Berry). Two separate parameter sets were determined for each species. In the first set, the entire data range was used, while for the second set only well-watered conditions were used, with measurements taken at volumetric soil water content over 15% (Heilman et al. 2009). To infer the drought

resistance and to allow the effects of soil water stress to be incorporated in the model, we used three different approaches (models A-C). The datasets were divided in monthly time periods of which the data was collected within a few days under similar climatic conditions. Separate V_m values were estimated for each time step, keeping the other parameters constant, with the first general parameter set for Models A and B, and the non-droughted parameter set for model C. For model A, V_m was not attenuated for SWC deficit and is thus the standard model. For model B, V_m values were regressed against the soil water content for the entire width of the soil water range. In Model C, V_m was regressed against the soil water content for the dry part of the soil water content range only (SWC < 0.15) and was held constant for higher soil water contents (SWC > 0.15). To evaluate the effectiveness of the different models, data was recalculated using the biochemical models with V_m values attenuated by soil water content.

2.7. ANCILLARY MEASUREMENTS

The plants we used for gas exchange measurements, were situated in the fetch area of the AmeriFlux site FR-2, where energy, water and CO_2 fluxes are being measured using the eddy covariance technique. Volumetric soil water content in the 0-10 cm soil layer was measured with ECH$_2$O probes (Decagon Devices, Inc., Pullman, WA, USA), in three soil pits located under the three primary vegetation types present at the tower site (grassland, Ashe juniper, Honey mesquite cover). The evaporative fraction was calculated for each day of the measurements as EF = Qe /(Qe + Qh) with Qe being the latent heat and Qh the sensible heat, integrated over the time of measurements (10AM-

2PM). For a more detailed description of instrumentation at the site, see Litvak et al. (2011).

3. Results

3.1 CLIMATE

In 2006 and 2007, the mean annual air temperature was 20.7 and 19.1 °C , respectively (Figure 1a). Total rainfall in 2006 was 815 mm, 10 % below normal and showed a bimodal distribution pattern with most of the rain occurring in spring and fall (Figure 1a). The summer months of 2006 were characterized as a severe drought based on the Palmer Z Drought Index, with a 60-day period without rain in July-August. In contrast, total precipitation in 2007 was 1514 mm, 65% above normal, and the summer months were categorized as moderately to extremely moist based on the Palmer Z Drought Index (NOAA website). The analysis of the energy balance of the site shows that 2006 was also drier from an atmospheric perspective, with higher vapor pressure deficits and lower evaporative fraction in the summer of 2006 (Heilman et al. 2012). The values of soil water content and evaporative fraction for the day of the measurements are given in Figure 1b.

3.2. LEAF-LEVEL MEASUREMENTS

3.2.1 Leaf characteristics

The two tree species, Ashe juniper and Honey mesquite, both had high carbon contents in their leaves, but differed significantly in nitrogen content. As a result, Ashe juniper foliage had high C/N leaf ratio, while vegetation in the nitrogen fixer, Honey mesquite, had a significantly lower C/N ratio (Table 1). Both grasses had low carbon and intermediate nitrogen content in their leaves, resulting in mid-range C/N ratios (Table 1). The specific leaf area (SLA) is higher for the grasses than the trees, which assumes a longer leaf lifespan for the trees (Table 1).

King Ranch bluestem had a low $\delta^{13}C$ ratio of -13.8 ‰, as expected for a C4 species. The C3 species had $\delta^{13}C$ values that fall in line with their expected water use efficiency, with a low value for the drought avoiding Honey mesquite (-27.3‰) and Texas wintergrass (-28.6‰) and a relatively high value for the drought tolerating juniper (-25.6‰)(Table1).

3.2.2. Photosynthetic measurements

Averaged over all measurements, King Ranch bluestem and Honey mesquite exhibited the largest net and gross photosynthetic carbon uptake (Table 2); Texas wintergrass had an intermediate value and Ashe juniper had generally low net and gross carbon uptake rates. This ranking was expected based on the photosynthetic pathway and the leaf nitrogen content of the C3 species.

The average dark respiration rate was highest for Honey mesquite, which follows from the photosynthetic uptake. King Ranch bluestem had a low average dark respiration rate despite its high carbon uptake rates. Ashe juniper had a relatively high average dark respiration rate, significantly higher than Texas wintergrass, explained by the assumed higher maintenance respiration that follows from the low specific leaf area (Table 2).

Stomatal conductance paralleled observed carbon uptake rates for the C3 species with low conductance values for Ashe juniper and high values for Texas wintergrass and Honey mesquite. King Ranch bluestem had an intermediate value, which was expected given that C4 species typically exhibit efficient carbon uptake at modest water loss. The average intrinsic water use efficiencies (A/g) were in line with photosynthetic uptake rates and stomatal conductance values. The C4 grass, King Ranch bluestem, exhibited the greatest intrinsic water use efficiency off all four species, but this did not differ significantly from the water use efficiency of Ashe juniper (Table 2). Honey mesquite balanced its high CO_2 uptake rates with high stomatal conductance and achieved an intermediate water use efficiency, while Texas wintergrass exhibited a low overall water use efficiency overall. King Ranch bluestem also exhibited the highest photosynthetic nitrogen use efficiency (PNUE) due to its C4 pathway (Bolton and Brown 1978, Sage and Pearcy 1987). Both tree species had a low PNUE, associated with their lower specific leaf area and assumed longer leaf life span (Reich et al. 1997).

Seasonal patterns of photosynthetic activity from 2006-2007 (Figure 2) were largely driven by two phenomena: (1) the seasonal temperature course, e.g. exhibited by the seasonal activity of the C4 species King Ranch bluestem and the gross photosynthetic uptake values of Ashe juniper; and (2) the water availability in the ecosystem. The summer drought of 2006 decreased photosynthetic activity in all four species, while the combination of high soil water availability and high temperatures in the summer of 2007 led to the highest uptake rates.

3.2.3. Sensitivity of photosynthesis to environmental drivers and leaf nitrogen content

Based on single factor regressions for all species combined (Table 3), almost half of the variation in net photosynthetic uptake was explained by relative humidity, with net photosynthesis in Honey mesquite having the strongest response to relative humidity (Table 3, Figure 3). This result was consistent for both tree species in the multiple regression analysis (Table 4), where relative humidity also explained most of the variation in net photosynthesis for the two tree species. In contrast, for the C3 grass and C4 grass species, most of the variation in net photosynthetic uptake was explained by nitrogen content and soil water content, respectively (Table 4).

Dark respiration for all species combined was best explained by leaf temperature (43%) and leaf nitrogen content of the leaves (41%, Table 3). In the multiple regression analysis for each species considered separately, most of the variation in dark respiration was explained by leaf nitrogen for the two tree species and leaf temperature for the grass species (Table 4). Ashe juniper showed the strongest response in dark respiration to increases in leaf nitrogen content (Table 3, Figure 3).

For all species combined, stomatal conductance showed the highest correlation with relative humidity (58%; Table 3). This was also the case for the two tree species, considered separately in multiple regressions, whereas soil water content was the main determinant in stomatal conductance for both the grass species (Table 4). Species differed in their response of stomatal conductance to relative humidity, with Honey mesquite and Texas wintergrass showing a stronger response than Ashe juniper and King Ranch bluestem (Table 3, Figure 3).

The intrinsic water use efficiency for all species combined was best explained by relative humidity (43.2%). While King Ranch bluestem showed a positive response in intrinsic WUE to relative humidity, the C3 species exhibited a negative response (Figure 3). Increases in relative humidity had a positive effect on both net photosynthesis and stomatal conductance, but must have had a slightly larger effect on stomatal conductance compared to net photosynthesis for the C3 species, explaining a negative response in intrinsic water use efficiency.

3.3 PARAMETERIZATION OF PHOTOSYNTHETIC MODELS

The parameterization of the coupled stomatal-photosynthesis model starts with determining the Ball-Berry coefficients. The coefficients (Table 5, Figure 4a) were consistent with the linear regressions and reflected what we would expect for the plant functional types. Ashe juniper and King Ranch bluestem exhibit a rather large initial stomatal conductance, but a shallow slope, meaning that they have a low stomatal response and operate under low stomatal conductance values. Honey mesquite and Texas wintergrass exhibit an intermediate initial stomatal conductance, but a large stomatal slope, resulting in a strong stomatal response and high conductance rates (Figure 4).

The overall parameterization of the biochemical models are given in Table 5 and default parameter values for the following biomes are given as comparison: needleleaf evergreen (~Ashe juniper), deciduous broadleaf (~Honey mesquite), C3 and C4 grassland (~Texas wintergrass and King Ranch bluestem) (Sellers et al. 1996a). Honey mesquite, Texas wintergrass, and Ashe juniper show respectively high, average, and low maximum rates of carboxylation ($V_{c,max}$) in both parameterizations, which correspond with the

relative nitrogen content in their leaves (Table 1). The first parameterization is based on measurements of the entire soil water content range, while the second is based on the non-drought part of the soil water range (SWC > 0.15).

Both encroaching tree species are well adapted/acclimated to functioning at high temperatures based on their high value for the heat stress parameter ('htti'), which determines the high temperature stress function (Appendix). Given that this is a high estimate for the heat stress parameter, we chose to set the heat stress parameter to 41ºC or 314K for all C3 species in further calculations and modeling (Chapter 4) (Campbell and Norman 1998). Texas wintergrass has an average heat stress parameter value, which is normal for a cool-season grass that is mostly dormant during the hot summer months (Magee 2002). As a warm season grass, King Ranch bluestem becomes active only at a higher temperature (modeled through a low temperature stress function, Appendix), but also has a relatively low heat stress parameter, resulting in a narrow optimum temperature range (Figure 4b).

The parameters 'Resp' is a scaling parameters and has to be interpreted in relation to the maximum rate of carboxylation, $V_{c,max}$. 'Resp' adjusts the rate of dark respiration, scaled as a fraction of $V_{c,max}$. In this view, the higher value for Ashe juniper and lower value for Honey mesquite seem normal given the low and high $V_{c,max}$ values respectively. Figure 4 shows the Ball-Berry relationship for the four species, as well as modeled response of net photosynthesis to temperature and soil water content.

3.4. EVALUATING $V_{C,MAX}$ SEASONALLY AND IN FUNCTION OF SWC

Ashe juniper had the least seasonal variation in normalized estimates of maximum rate of carboxylation (V_m values) (Figure 5). Juniper had high normalized V_m in April '06 and Jul-Aug '07 and an extreme low normalized V_m in Aug '06 – representing the times when deep soil water recharge and drought governed the ecosystem, respectively. Honey mesquite had the lowest normalized V_m values, at the beginning and end of the growing season, reflecting a possible leaf flush and leaf senescence of the deciduous species, but maintained a relatively high value during the summer drought of 2006 (August '06, Figure 5). The photosynthetic capacity of King Ranch bluestem was extremely impacted by the summer drought in August '06, but rebounded in October '06 after the autumn rains (Figure 5). Texas wintergrass was completely dormant during the summer of 2006.

When we inspect the seasonal V_m values in function of soil water content (Figure 6, approach A, B, and C), we can see that the maximum carboxylation rates of Honey mesquite and Ashe juniper were much less impacted by soil water content than the two grass species. Both tree species still had significant maximum carboxylation rates at lower soil water contents. In contrast, both grasses show a steep decline and photosynthesis completely halted with the wilting of the grassland (Figure 6, models B and C). Maximum carboxylation rates declined by 21-35% for Ashe juniper, 0-14% for Honey mesquite, and 50-100% for the grasses as the empirically measured soil water content approached zero (Table 4, Figure 5).

By estimating the seasonal maximum carboxylation rates (V_m), we eliminated the effect of other important climatic drivers, such as temperature and relative humidity,

which exert a strong influence on net photosynthesis and stomatal conductance. Our approach allowed us to rank the species according to their drought tolerance, with tolerance decreasing in the order: Honey mesquite, Ashe juniper, King Ranch bluestem, Texas wintergrass.

3.5. MODEL PERFORMANCE

Overall, the coupled stomatal-photosynthesis models explained 64 to 80% of all observed variation (Table 5). For the two grasses, the inclusion of soil water attenuation on maximum carboxylation rates, explained 6-7 % more of the observed variation. For the two encroaching tree species, there was only 1% improvement by including soil water effects in the model.

4. Discussion

The ecophysiological characterization and modeling of four plant functional types in savanna undergoing woody encroachment provides insights into changes in carbon dynamics as C3 trees displace grassland species. As trees encroach in Central Texas, carbon dynamics at the ecosystem level will most likely be shaped by the superior drought tolerance of trees over grasses, and the increased temperature range of photosynthetic activity of the invading C3 trees relative to the dominant C4 grass. Both of these factors should increase the growing season length in these savannas, which potentially will alter total carbon sequestered in these biomes.

4.1. DROUGHT TOLERANCE

The two-layer model of Walter (Walter 1954, Walker and Noy-Meir 1982, Ward et al. 2013), is an underpinning of savanna ecology and states that trees and grasses differ in rooting depth giving trees exclusive access to deep water layers. This early model for coexistence of trees and grasses has often been challenged (Sankaran et al. 2004) and is in its original sense not applicable to our study system, due to climatological, edaphic and anthropological considerations (see Ward et al. (2013) for an in-depth review of the original hypothesis). In karst systems, such as the Edwards Plateau, shallow soils are underlain by bedrock and therefore trees have uncertain rooting depths and access to deep water sources (Schwinning 2010). In karst systems, the subsoil is not the only layer contributing to the water holding capacity of the system, but fissures and cracks in the epikarst can also provide access to water (Schwinning 2010). However complicated the subsurface, we can still use the two-layer model as a working hypothesis for tree-grass differences, and assume trees have generally deeper roots and are less sensitive to decreases in soil water than grasses (Schenk and Jackson, 2002).

Our regression models showed a tree-grass dichotomy. Most of the variability in C4 grass net photosynthesis and stomatal conductance, as well as variability in stomatal conductance of the C3 grass, was explained by soil water content in the upper 10 cm of the soil profile. Net photosynthesis and stomatal conductance of both tree species were more strongly correlated to relative humidity (more so for Honey mesquite than Ashe juniper).

We attempted to remove the confounding effects of temperature and relative humidity on leaf net photosynthesis, by estimating the maximum carboxylation rate for discrete time steps and regressed it against soil water content. No obvious pattern was found for Honey mesquite, indicating that its maximum carboxylation rates were not impacted by decreases in soil water content in the upper 10 cm layers of the soil. More importantly, the maximum carboxylation rate for mesquite in the summer drought of 2006 was not as severely impacted as the other three species, when drought effects extended past the upper 10 cm of the soil profile (see Heilman et al. (2014) for details on energy balance analysis and estimated water storage capacity).

Our approach further showed that the seasonal maximum carboxylation rates of Ashe juniper were minimally impacted by soil water content, and both grass species showed a strong decline in fitted maximum carboxylation rates as a function of soil water content. Based on this analysis, we ranked the species resistance to drought as Honey mesquite > Ashe juniper > King Ranch bluestem > Texas wintergrass.

4.1.1. Drought response of grass species

The C3 grass species, Texas wintergrass, exhibited a classic drought avoidance strategy, characterized by high uptake rates and low water use efficiency to maximize its growth during favorable conditions in fall, winter and spring. It showed very rapid declines in net photosynthesis and maximum carboxylation rate in response to decreases in soil water content, and was fully dormant in the dry summer of 2006.

King Ranch bluestem is a classic C4 grass that concentrates its photosynthetic activity in the summer months, when it boasts high uptake rates and high water use efficiency. It is, however, also very sensitive to decreases in soil water content, and went almost fully dormant during the summer drought of 2006. It showed strong resilience and restored its green leaf area quickly after precipitation events following rains in September 2006 (Chapter 4). A greenhouse study has shown King Ranch bluestem to be similar in drought tolerance and resilience as other C4 grass species in the region (Basham 2013).

4.1.2. Two encroaching species compared

Besides their commonality in withstanding the summer drought of 2006, we found very distinct differences in the photosynthetic characteristics of the two encroaching tree species, as well as different strategies to withstand drought conditions.

Ashe juniper operated at low stomatal conductance, and had low nitrogen content in its leaves, resulting in low photosynthetic rates. Its water use efficiency is high, similar to the C4 grass, King Ranch bluestem. Ashe juniper shows very little seasonal variation in net photosynthesis or stomatal conductance, even during the summer drought of 2006. This steady rate of gas exchange has also been observed for Ashe juniper in other settings (Owens and Schreiber 1992, Bendevis et al. 2010). Ecohydrological studies at our site have shown very low pre-dawn leaf water potentials for Ashe juniper of ~-4 MPa during the summer drought of 2006 (Eggemeyer and Schwinning 2009) and down to -6 MPa in the summer drought of 2008 (Litvak et al. 2011), signaling that Ashe juniper did not have access to a perennial water source and did experience drought stress. Based on the high resistance to water-stress-induced xylem cavitation (Maherali et al. 2004, Kukowski et al. 2013), the low stomatal slope (Table 5), and the steady rate of gas exchange throughout

the summer of 2006, we conclude that Ashe juniper uses an anisohydric water strategy during droughts, meaning that it keeps it stomates open and continues to photosynthesize, even when this results in decreasing leaf water potentials. This has as corollary that it might function within narrow hydraulic safety margins during droughts, which makes it susceptible to catastrophic hydraulic failure during intense droughts (McDowell et al. 2008).

Honey mesquite on the other hand, has high photosynthetic uptake and stomatal conductance rates, but also has a very large stomatal slope (Ball-Berry coefficients, Table 5), meaning that it uses a more isohydric water strategy than Ashe juniper, and closes its stomates when the evaporative demand becomes high. An isotopic study at our study site showed that Honey mesquite and Ashe juniper used the same water source and had very similar pre-dawn leaf water potentials during the summer of 2006, indicating that neither species had access to a perennial water source and both experienced drought stress (Eggemeyer and Schwinning 2009). In a later study at our site, Honey mesquite did show higher pre-dawn leaf water potentials than Ashe juniper in the summer of 2008 (-2 MPa vs -6MPa, Litvak et al. (2011)). The isohydric water strategy is also reflected in strong seasonal fluctuations of net photosynthesis and stomatal conductance, e.g. Honey mesquite did have strongly reduced rates of net photosynthesis and stomatal conductance during the summer drought of 2006 (Figure 2). This is not contradictory to our earlier finding that its maximum carboxylation rate seemed least impacted by decreases in soil water content or summer drought. Rather, the stomatal response is an integral part of the coupled stomatal-biochemical photosynthesis model, and the isohydric strategy is

reflected by the large stomatal slope of Honey mesquite. The corollary of the isohydric strategy is that stomatal closure leads to decreased carbon uptake, which can lead to carbon starvation during extended drought periods (McDowell et al. 2008).

4.2. TEMPERATURE EFFECTS

We expected the C4 grasses to perform better at higher temperature, because its biochemical pathway has evolved specifically in response to decreasing atmospheric CO_2 concentrations at warm temperatures to reduce photorespiration (Sage 2004). Although our survey measurements were not specifically set up to study photosynthetic responses to temperature, we found that over the course of two years, the encroaching trees performed equally (well) at higher temperatures as the C4 grass. In the scatter plot of net photosynthesis against leaf temperature (Figure 3), we can see that Ashe juniper had a rather flat temperature response, while the optimum of the 'temperature envelope' was similar for Honey mesquite and King Ranch bluestem (~32ºC).

The parameterization of the photosynthetic models showed that the high temperature stress parameter for King Ranch bluestem was estimated to be 3-4 degrees lower than the commonly used value for C4 grasses (Table 5), which effectively reduces the temperature range for C4 photosynthesis in a modeling context. The high temperature stress parameters for the encroaching trees were estimated to be much higher than commonly used values, probably due a lack of data points in our dataset that represented decline in photosynthesis solely due to high temperatures. The high temperature stress parameter estimates for the C3 tree species were not used in further model evaluation or modeling exercises, because they result in a skewed temperature response of C3

photosynthesis. Instead a commonly used value of 314 K (~ 41 °C) was used (Campbell and Norman 1998).

These considerations only take the high temperature response into account, while the differences in photosynthesis at lower temperature might be more important in shaping the carbon dynamics of an encroaching ecosystem. C4 grasses do not photosynthesize at lower temperatures, which is modeled through a low temperature stress function in C4 photosynthetic models, which is absent in models of C3 photosynthesis (Figure 4, Appendix). It is this difference in temperature response that likely widens the ecophysiological temperature response function of the ecosystem – allowing carbon uptake at a wider range of temperatures compared to a C4 dominated grassland ecosystem. A recent study compared the temperature range of a grassland and a mesquite encroached woodland, and found the temperature range of net ecosystem productivity to be two or three times wider for the encroached site, compared to the grassland site, but only during drought periods (Barron-Gafford et al. 2012).

4.3. EXPECTED ECOSYSTEM LEVEL RESPONSES

In order to translate the leaf level species-specific differences to ecosystem level carbon fluxes, a scaling approach is needed (Chapter 4). At the ecosystem level, and on longer timescales, physiological processes might scale up differently based on canopy architecture and phenology. Specifically, the high leaf area index of Ashe juniper, its

drought tolerance and its year-round photosynthetic activity, might outweigh its low photosynthetic rate at the leaf level.

How differences between the two encroachers will scale up also depends on their leaf area and density at the encroaching savanna site. Based on their different strategies to cope with water stress (anisohydric Ashe juniper versus isohydric Honey mesquite), we predict that especially Ashe juniper will keep photosynthesizing during dry periods and will be responsible for a large part of carbon uptake during drought conditions. Overall, we expect the encroachment of both species to result in a considerable increase in the carbon uptake capacity, based on the drought resistance of the trees and the wider temperature range of photosynthetic uptake, which effectively lengthens the growing period of the ecosystem.

4.4. COUPLED STOMATAL-BIOCHEMICAL MODEL OF PHOTOSYNTHESIS

In order to scale the species specific differences in space and time, we parameterized the coupled stomatal biochemical models of C3 and C4 photosynthesis (Collatz et al. 1991, Collatz et al. 1992), and added a dependence on soil water content (Model B-C, Table 5). These models allow us to estimate photosynthetic uptake and stomatal conductance at any given combination of leaf temperature, light condition, relative humidity, atmospheric CO_2 level, and soil water content. In Chapter 4, we will use these models together with continuous micrometeorological data to assess photosynthetic rates in time, and use this together with vegetation structural data to

estimate ecosystem level contributions of the different plant functional types to the canopy photosynthetic flux.

The approach we took in incorporating soil water content to adjust the maximum carboxylation rate worked well in that it increased the amount of variation explained for the grass species, but there are some caveats to this approach. We used the 0-10 cm soil water content since it was readily available. This variable does not give any indications of water availability in deeper soil layers, or intensity and duration of drought (Schwinning et al. 2004). Another drought indicator variable, evaporative fraction, was investigated, but did not improve the results.

Another shortcoming of our approach is that we have not used seasonally variable maximum carboxylation rates. While this is acceptable for the evergreen Ashe juniper, the other species are deciduous and do show seasonality in their fitted maximum carboxylation rates that is unrelated to drought response (Figure 4). For example, Honey mesquite V_m values are the lowest in the beginning and at the end of the growing season and it has been shown that mesquite exhibits seasonal changes in physiology (Nilsen et al, 1983). Both grass species show a sharp increase in V_m values after the second leaf flush after the precipitation event in the fall of 2006. This may partly explain why more of the overall data of Ashe juniper is explained by the biochemical model than the three other species.

4.5. RESPONSE TO PREDICTED CLIMATE CHANGE

Based on the physiological characterization of the dominant species, we can deduce how the species might perform under predicted climate change conditions. Rising temperatures are expected to benefit C4 species, due to increases in photorespiration in C3 plants. We found no evidence in our physiological work that higher temperatures adversely affected the encroaching C3 species. Moreover, increases in CO_2 are expected to benefit C3 plants, and evergreens or species with more robust leaves (i.e., Ashe juniper) are more likely to have stronger increases in photosynthesis and intrinsic WUE under rising CO_2 concentrations (Niinemets et al. 2011).

Predictions for the water cycle in Central Texas are that precipitation intensity will increase, as well as number of consecutive dry days (IPCC 2007). The competitive advantage of C4 grasses at higher temperatures will likely be reduced under a predicted drier climate. We showed that the encroaching trees are much better at withstanding seasonal droughts than grasses – which constitutes the most important difference between grassland and encroaching species, given the predictions of future climate change for the region. Yet if summer droughts further increase in severity or duration, tree mortality might adversely affect woody encroachment due to hydraulic failure or carbon starvation (McDowell et al. 2008). After the conclusion of our study, a historic drought in 2011 resulted in the mortality of 100-500 million trees in Texas, with observed mortality rates of 6% for Ashe juniper at a nearby site (Kukowski et al. 2013). Nevertheless, the predicted altered precipitation regimes for this region and rising CO_2 concentrations together will favor the encroaching trees over the grassland species and suggests further progression of woody encroachment.

5. Conclusion

We characterized the photosynthetic performance of four species in an encroaching savanna ecosystem, and their sensitivity to climatic drivers to make inferences about changes in the carbon balance of an encroaching savanna site, as well as the future direction of the encroachment process under climate change predictions. Trees are more resistant to drought and function over wider temperature ranges, effectively lengthening the active growing season of the savanna ecosystem, and increasing the carbon uptake potential of the ecosystem. Distinct differences in how the two encroaching species deal with water stress further indicate that Ashe juniper is most likely to be responsible for both continued carbon uptake during droughts and the longer growing season in Central Texas encroaching savannas. Coupled stomatal-photosynthetic models of C3 and C4 photosynthesis with an included dependence on soil water content provide a flexible tool to scale leaf level physiology in time and space to the ecosystem level.

6. Figures

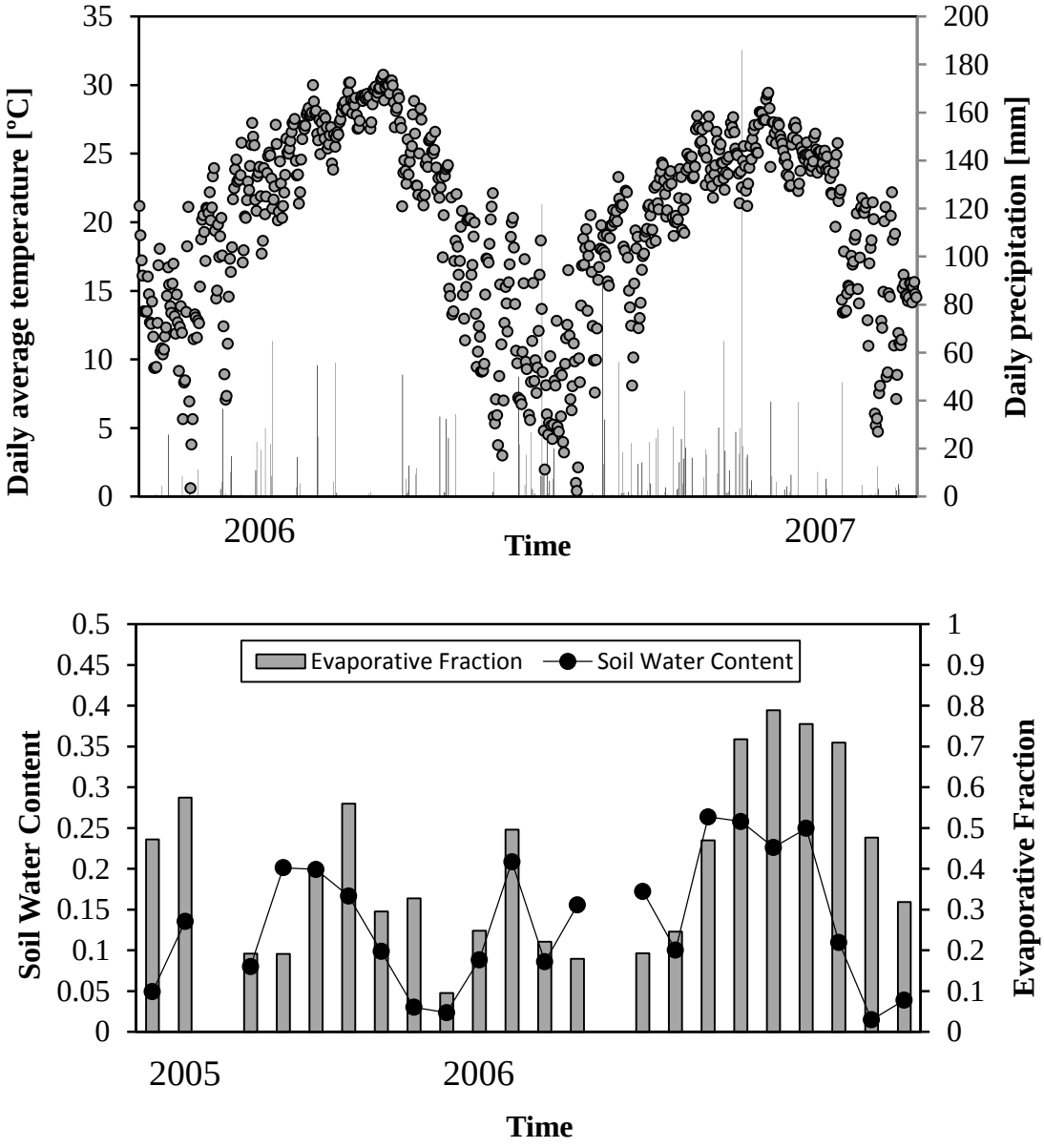

Figure 1.1: Climatic conditions during time of study. (a) Average daily temperature and precipitation distribution; (b) wetness indicators on days of leaf-level measurements: soil water content in the 0-10 cm soil layer and evaporative fraction.

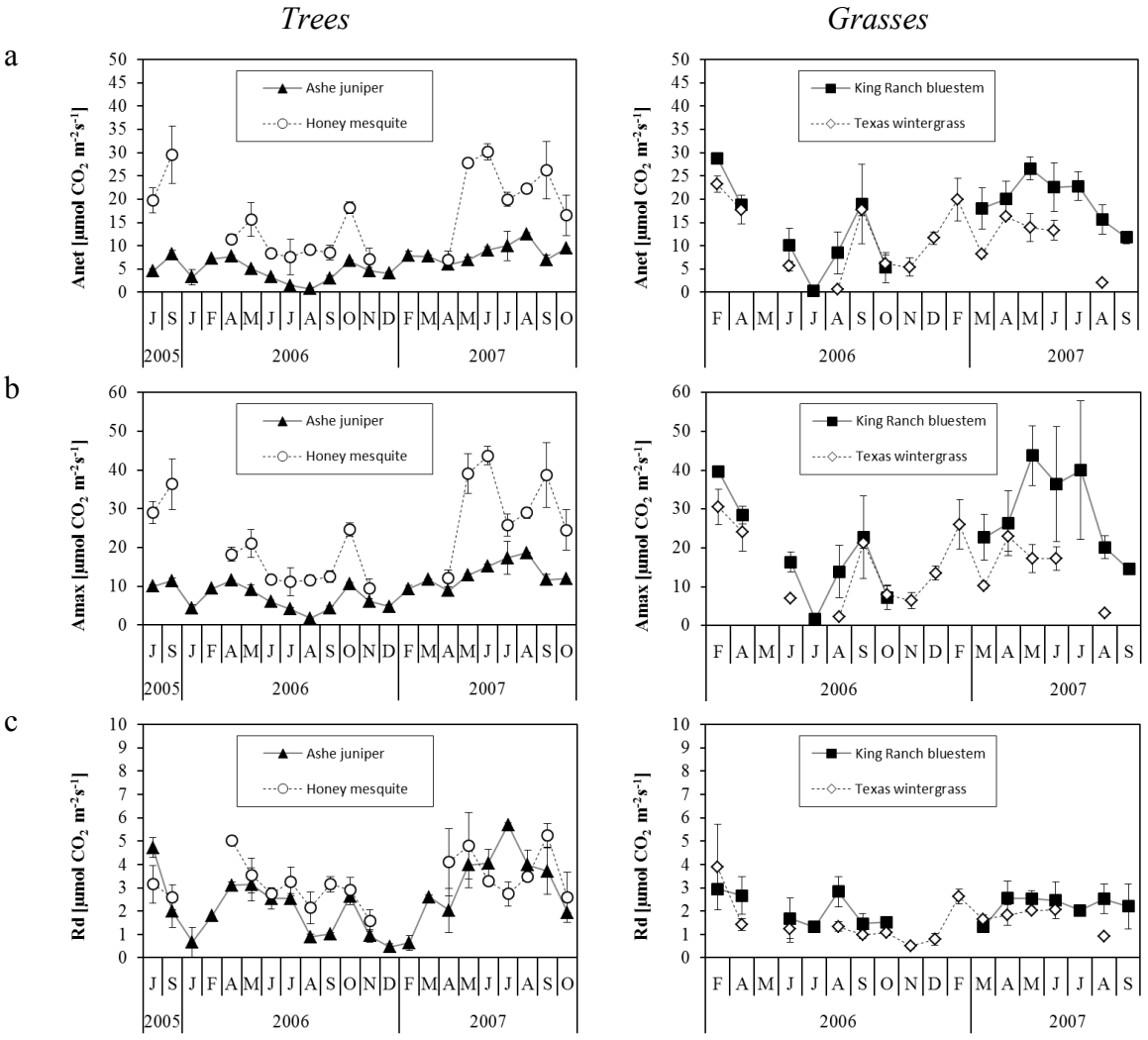

Figure 1.2: Seasonal pattern of photosynthetic characteristics of two tree species and two grass species. (a) Net photosynthesis at saturated light conditions; (b) Gross photosynthesis at saturated light conditions; (c) Dark respiration.

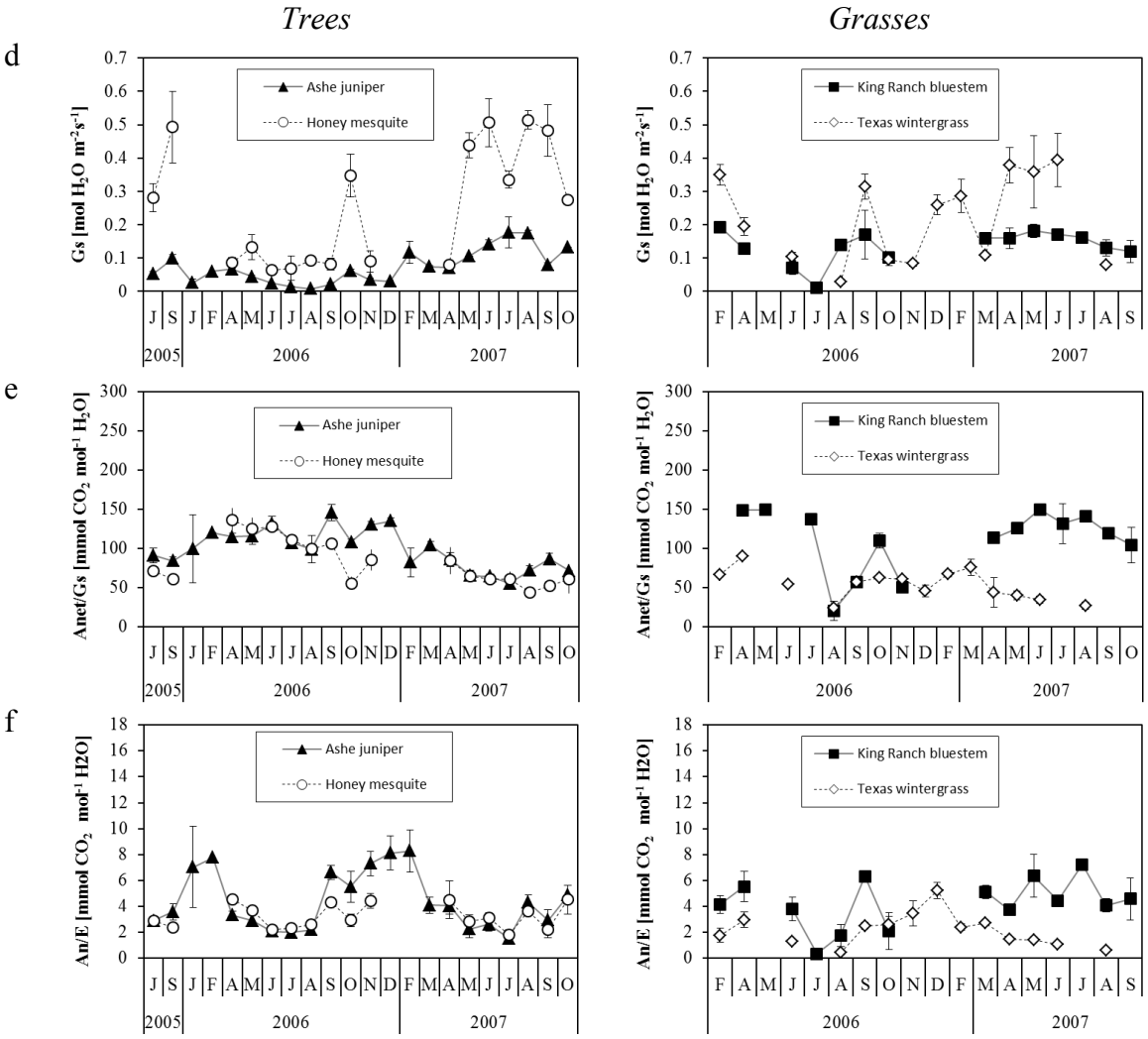

Figure 1.2 (continued): Seasonal pattern of photosynthetic characteristics of two tree species and two grass species. (d) Stomatal conductance at light saturation; (e) Intrinsic water use efficiency; (f) Instantaneous water use efficiency.

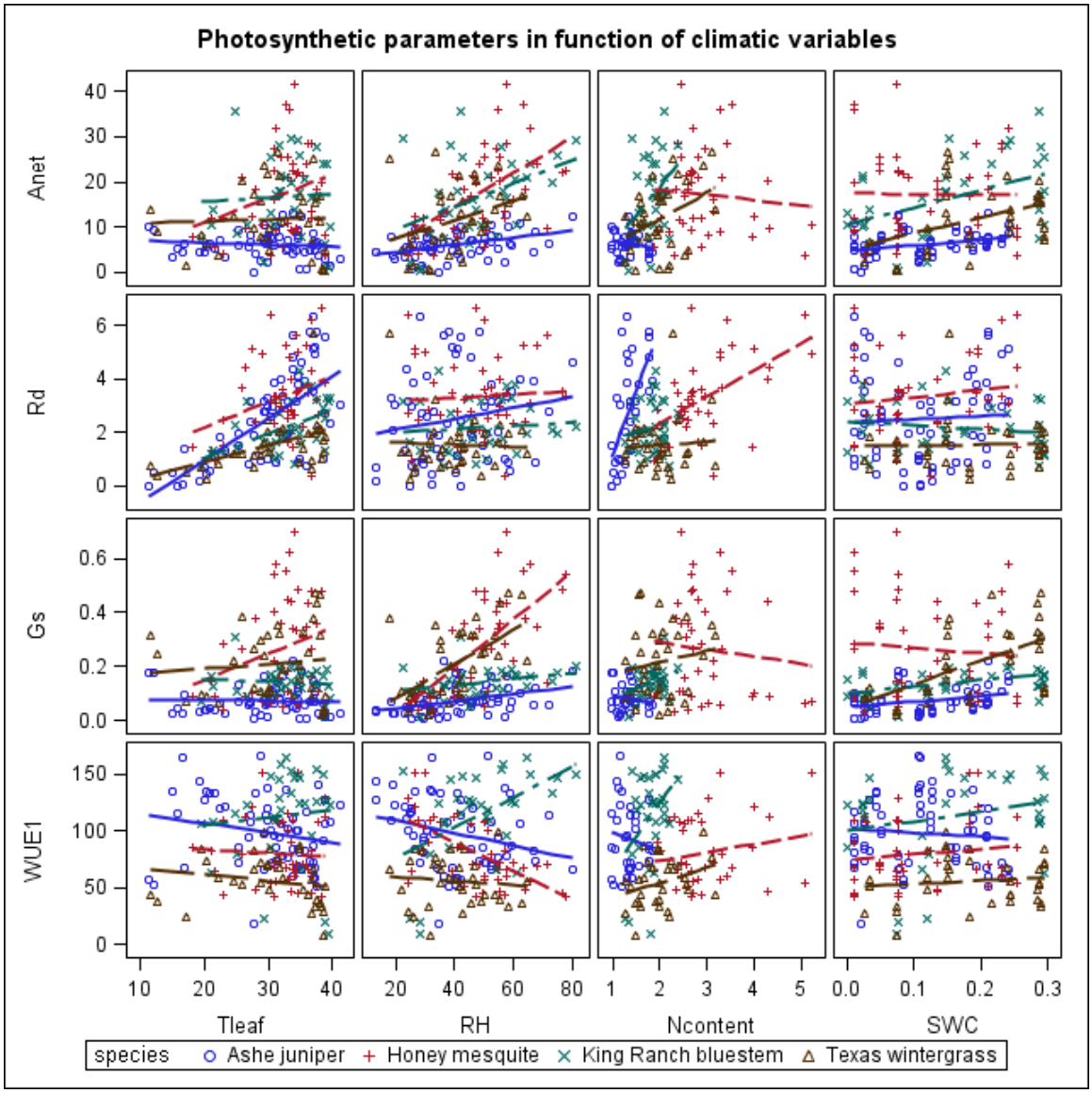

Figure 1.3: Single regression of photosynthetic parameters against climatic variables and leaf nitrogen content.

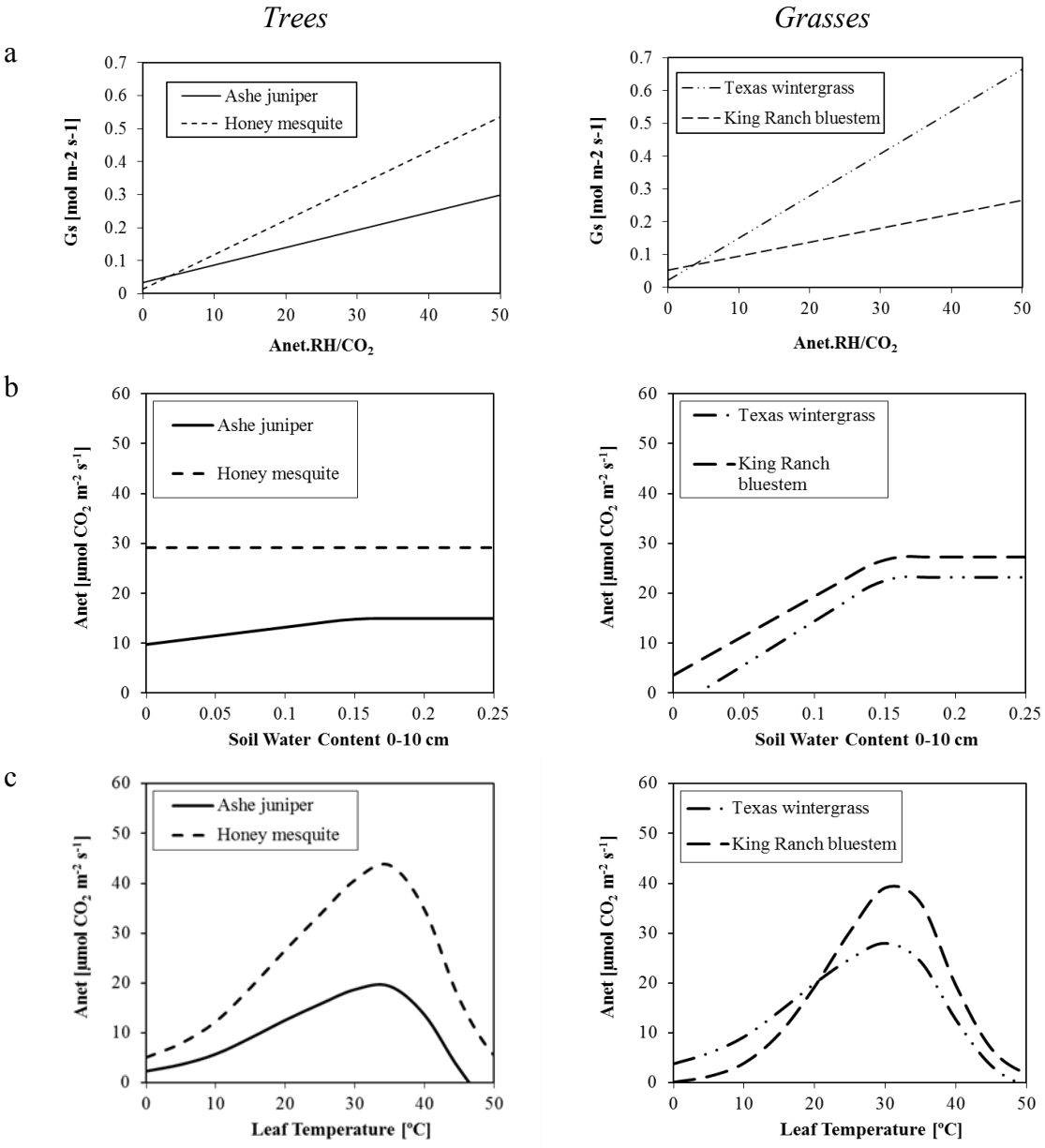

Figure 1.4: Coupled photosynthesis-stomatal model; (a) Stomatal conductance model according to Ball-Berry; (b) Net photosynthesis in function of soil water content (model C); (c) Net photosynthesis in function of leaf temperature. Standard conditions for b-c are 25ºC; 2000 µmol PAR m^{-2} s^{-1}; SWC > 15%; Ci = 300 ppm for C3 species and Ci =100 ppm for C4 species.

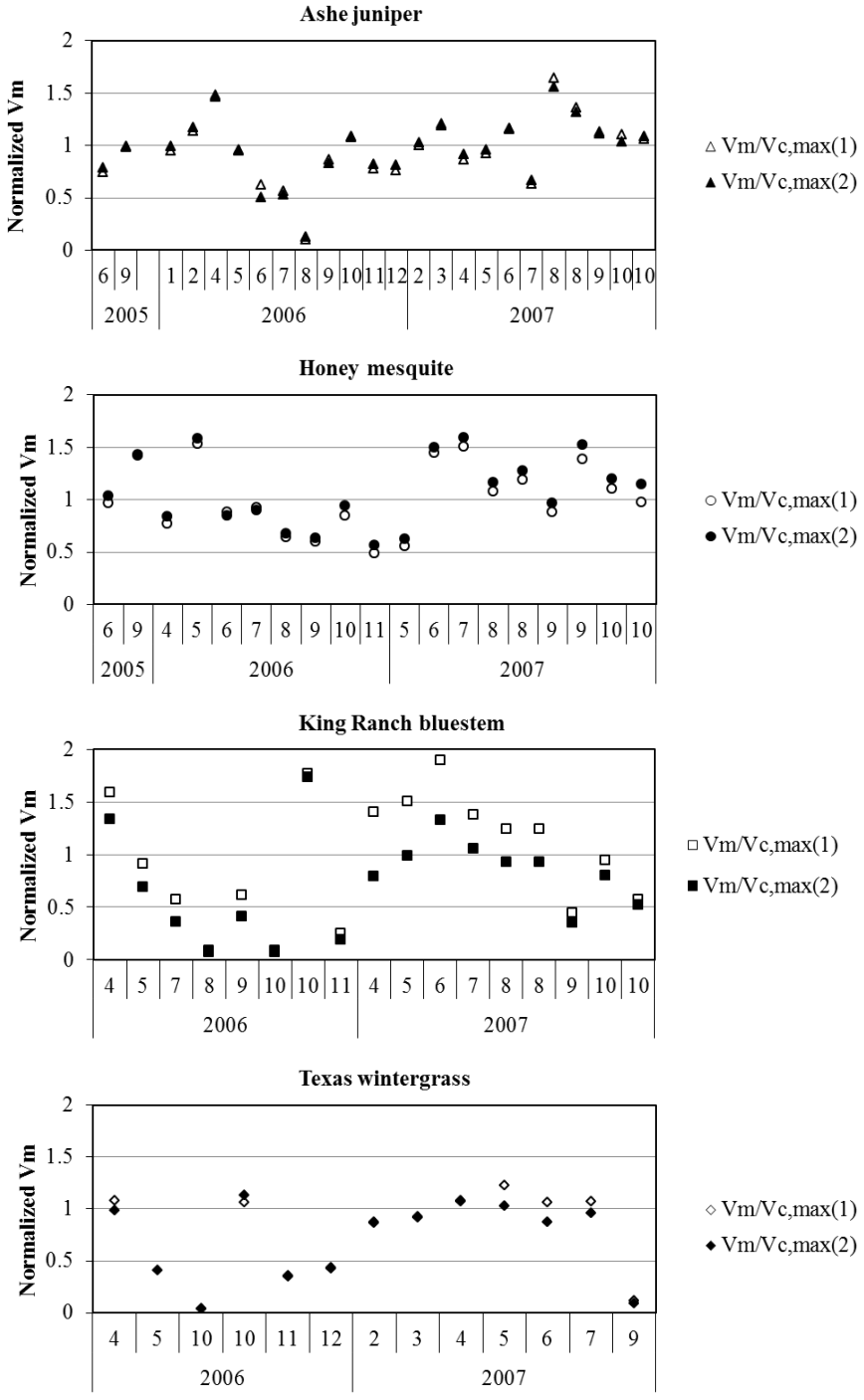

Figure 1.5: Seasonal variation in fitted Vm values.

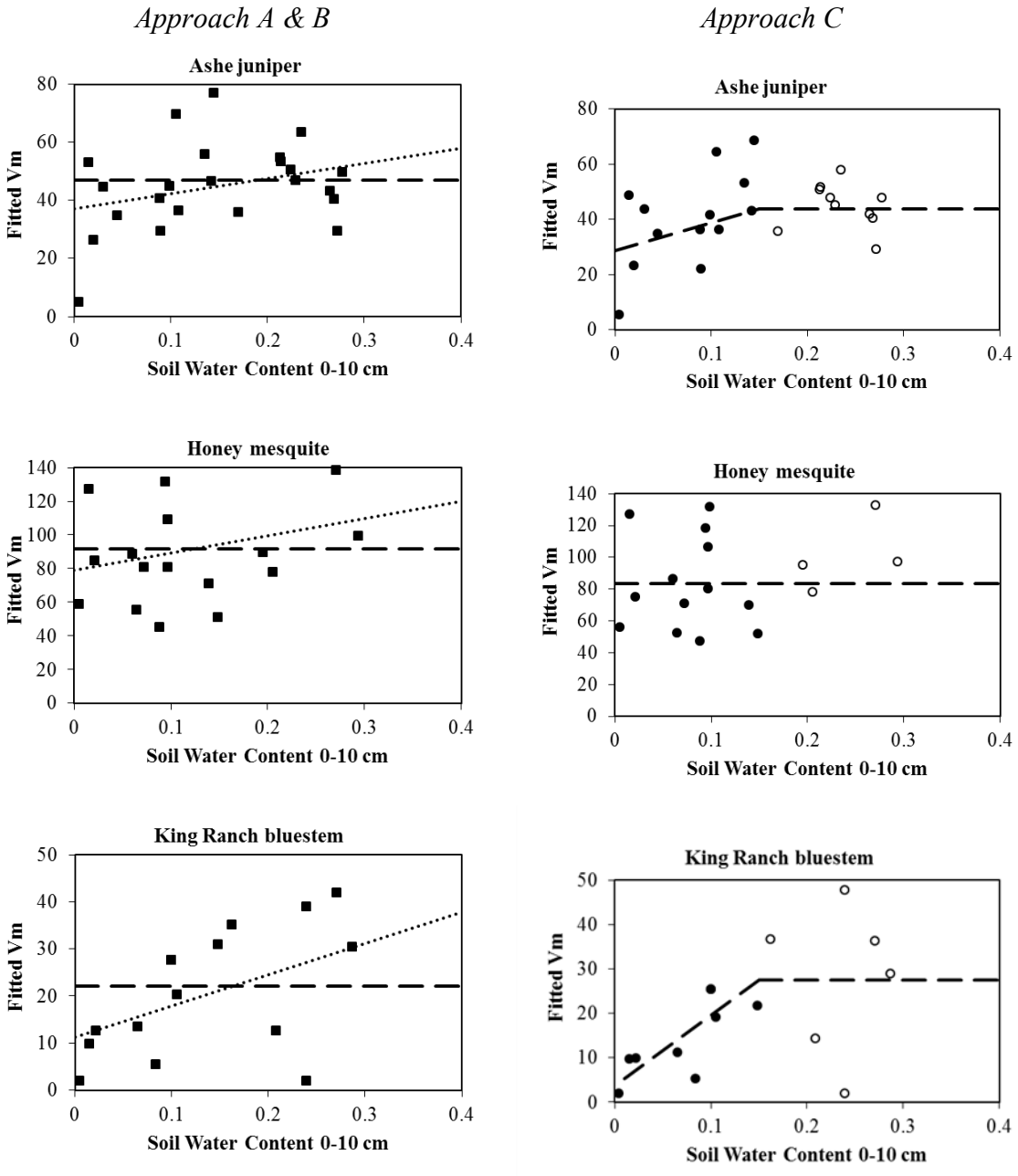

Figure 1.6: Fitted Vm values in function of soil water content 0-10 cm.

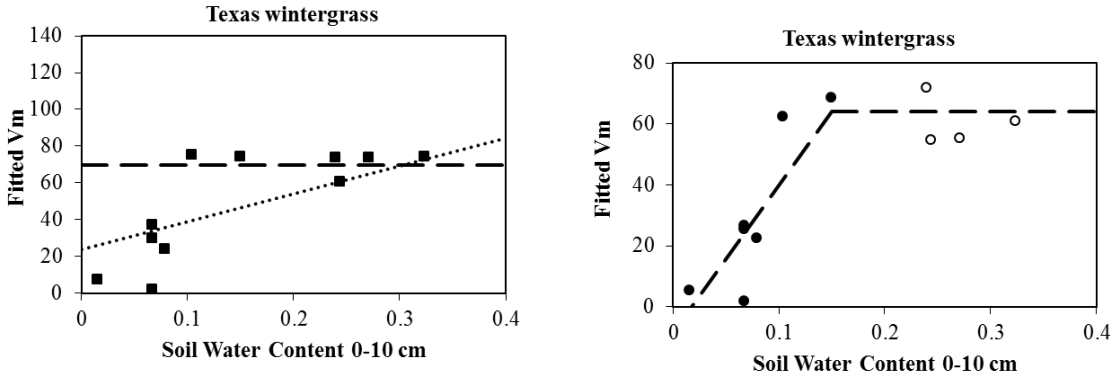

Figure 1.6 (continued): Fitted Vm values in function of soil water content 0-10 cm.

7. Tables

Table 1.1: Leaf characteristics of the four studies species

	N content [%]	**C content** [%]	**C/N** [-]	**δ13C** [‰]	**SLA** [cm2/g]
Ashe juniper	1.27 ± 0.11 (c)	48.0 ± 0.26 (a)	38.9 ± 1.20 (a)	-25.6 ± 0.20 (c)	64.82 ± 1.81 (a)
Honey mesquite	2.95 ± 0.11 (a)	47.9 ± 0.31 (a)	17.2 ± 1.15 (c)	-27.3 ± 0.22 (b)	88.13 ± 4.55 (a)
King Ranch bluestem	1.80 ± 0.12 (b)	44.4 ± 0.34 (b)	25.4 ± 1.27 (b)	-13.8 ± 0.24 (d)	181.78 ± 7.15 (c)
Texas wintergrass	1.95 ± 0.12 (b)	43.8 ± 0.34 (b)	23.9 ± 1.26 (b)	-28.6 ± 0.24 (a)	150.17 ± 4.72 (b)

Values are gives as average ± standard error. Significant differences between species, according to mixed model results, are denoted with different letters.

Table 1.2: Photosynthetic characteristics of the four studied species

		Ashe juniper	Honey mesquite	King Ranch bluestem	Texas wintergrass
Net Photosynthesis	Anet [umol CO2 m-2 s-1]	6.1 ± 1.34 (c)	17.0 ± 1.49 (a)	16.7 ± 1.62 (a, b)	11.8 ± 1.60 (b)
Gross Photosynthesis	Amax [umol CO2 m-2 s-1]	9.4 ± 1.90 (c)	23.6 ± 2.10 (a)	24.0 ± 2.27 (a)	15.2 ± 2.25 (b)
Dark Respiration	Rd [umol CO2 m-2 s-1]	2.51 ± 0.24 (b, c)	3.17 ± 0.27 (c)	1.98 ± 0.30 (a, b)	1.55 ± 0.29 (a)
Stomatal Conductance	Gs [mol H2O m-2 s-1]	0.073 ± 0.0239 (a)	0.258 ± 0.0267 (c)	0.136 ± 0.0290 (a, b)	0.219 ± 0.0289 (b, c)
Light Use Efficiency	alpha [umol CO2 umol PAR-1]	0.044 ± 0.0034 (a)	0.068 ± 0.0038 (b)	0.040 ± 0.0043 (a)	0.048 ± 0.0042 (a)
Intrinsic Water Use Efficiency	WUE1 [umol CO2 mol H2O-1]	98.7 ± 5.90 (c)	82.2 ± 6.73 (b)	113.1 ± 7.47 (b, c)	53.4 ± 7.41 (a)
Instantaneous Water Use Efficiency	WUE2 [umol CO2 mmol H2O-1]	4.41 ± 2.65 (a)	3.25 ± 1.18 (a, b)	4.42 ± 1.98 (a)	2.34 ± 1.41 (b)
Photosynthetic Nitrogen Use Efficiency	PNUE [umol CO2 mol N-1 s-1]	45.44 ± 3.52 (a)	74.72 ± 6.82 (a)	231.52 ± 21.48 (c)	124.62 ± 12.46 (b)

Values are gives as average ± standard error. Significant differences between species, according to mixed model results, are denoted with different letters.

Table 1.3: Single regression analysis of photosynthetic performance parameters against environmental drivers and leaf nitrogen content.

		Net Photosynthesis A_{net}	**Dark Respiration R_d**	**Stomatal Conductance G_s**	**Water Use Efficiency WUE**
Leaf Temperature	R^2 (F value)	0.345 (12.54) ***	**0.427 (17.80) *** **	0.346 (12.61)***	0.313 (10.88)***
	Species	0.67	1.68	0.81	1.35
	Tleaf	2.47	42.5***	2.75	0.36
	Species x Tleaf	1.68	2.9	2.14	0.68
Relative Humidity	R^2 (F value)	**0.483 (22.33) *** **	0.18 (5.36)***	**0.581 (33.17)*** **	**0.432 (18.17)*** **
	Species	0.49	0.85	4.16	8.13***
	RH	39.52***	0.73	65.18***	0.99
	Species x RH	4.45**	0.45	15.01***	11.78***
		(J<M)		(J, KR < N, M)	(KR > N , J; N>M)
Leaf N content	R^2 (F value)	0.304 (8.24)***	0.407 (12.92)***	0.257 (6.52)***	0.378 (11.48)***
	Species	3.61	4.09	1.8	2.51
	N	3.99	25.14***	0.16	4.26
	Species x N	3.59	7.85***	0.85	2.66
			(N, KR, M < J)		
Soil Water Content	R^2 (F value)	0.391 (15.34)***	0.175 (5.07)***	0.383 (14.83)***	0.316 (11.00)***
	Species	10.95***	1.92	14.6***	5.84**
	Tleaf	11.75**	0.3	7.52	1.41
	Species x Tleaf	2.22	0.44	3.92	1

Table 1.3 (continued): Single regression analysis of photosynthetic performance parameters against environmental drivers and leaf nitrogen content.

N= 174; R^2 and the overall F value for each regression are given, as well as the F values for the type III SS of the different terms. *** P<0.001, **P<0.01 *P<0.05. Values are Bonferroni corrected. For significant interaction terms, significant differences in regression slope between the species are indicated, with J = Ashe juniper, KR = King Ranch bluestem, M = Honey mesquite a nd N = Texas wintergrass.

Table 1.4: Multiple regression of key photosynthetic variables against environmental variables and leaf nitrogen content per species. Standardized coefficients (β) indicate relative importance of each variable in explaining variability in photosynthetic parameter.

	Net photosynthesis (Anet)			
	Ashe juniper	**Honey mesquite**	**Texas wintergrass**	**King Ranch bluestem**
Soil Water Content [%]	0.426	-	0.355	**0.402**
Relative humidity [%]	**0.457**	**0.591**	0.322	0.373
Leaf nitrogen content [gN m^{-2}]	-	-	**0.613**	-
Leaf temperature [ºC]	-	-	0.407	-
R^2 adjusted	0.299	0.33	0.432	0.288

	Stomatal conductance (gs)			
	Ashe juniper	**Honey mesquite**	**Texas wintergrass**	**King Ranch bluestem**
Soil Water Content [%]	0.397	-	**0.413**	**0.47**
Relative humidity [%]	**0.444**	**0.68**	0.41	-
Leaf nitrogen content [gN m^{-2}]	-	-	-	-
Leaf temperature [ºC]	-	-	-	-
R^2 adjusted	0.265	0.446	0.423	0.194

Table 1.4 continued

	Dark respiration (Rd)			
	Ashe juniper	**Honey mesquite**	**Texas wintergrass**	**King Ranch bluestem**
Soil Water Content [%]	0.295	-	-	-
Relative humidity [%]	-	-	-	-
Leaf nitrogen content [gN m^{-2}]	**0.529**	**0.596**	0.361	-
Leaf temperature [ºC]	0.368	0.422	**0.641**	**0.522**
R^2 adjusted	0.566	0.418	0.283	0.247

Table 1.5: Parameter estimates and performance of the C3 and C4 coupled photosynthesis – leaf conductance models.

Species	**Ashe juniper**			**Honey mesquite**			**King Ranch bluestem**			**Texas wintergrass**		
Number of data points	664			490			242			425		
Number of light response curves	58			42			24			35		
Number of Ci response curves	13			12			4			12		
Stomatal slope (m) [-]	5.33 (9)			10.41 (9)			4.26 (4)			12.89 (9)		
Minimum Stomatal Conductance (b) [mol m^{-2} s^{-1}]	0.033 (0.01)			0.014 (0.01)			0.053 (0.04)			0.021 (0.01)		
Parameterization 1 & 2	1	2	(biome 4)	1	2	(biome 2)	1	2	(biome 6)	1	2	(biome 9)
Maximum Rubisco Capacity ($V_{c,max}$) [mol m^{-2} s^{-1}]	47	44	(80)	92	83	(80)	22.1	27.4	(35.8)	70	64	(80)
High temperture stress factor (htti) [Kelvin]	333	333	(303)	333	333	(311)	309	310	(313)	312	316	(308)
Leaf respiration factor (Resp) [-]	0.031	0.040	(0.015)	0.019	0.019	(0.015)	0.056	0.057	(0.025)	0.0048	0.0077	(0.015)
Model	A	B	C	A	B	C	A	B	C	A	B	C
R^2	0.803	0.811	0.813	0.714	-	0.728	0.642	0.707	0.696	0.659	0.733	0.698
Intercept regression (Vm - SWC)	-	37.1	28.7	-	78.8	-	-	11.2	3.6	-	23.7	-8.7
Slope regresssion (Vm - SWC)	-	52.4	102.0	-	102.7	-	-	66.5	158.8	-	151.7	484.7

Default values for biome 4, 2, 6 and 9 from Sellers et al (1996) are given where applicable in parentheses (respectively needleleaf evergreen, broadleaf deciduous, C4 grassland and C3 grassland).

CHAPTER 2: LOWERED SOIL RESPIRATION AND LOWERED CLIMATIC SENSITIVITIES UNDER TWO DIFFERENT SAVANNA ENCROACHERS

Abstract

When grasslands and savanna ecosystems are invaded by woody species, the shift in plant functional type has the potential to change the carbon dynamics of these ecosystems significantly. Here we report on the effects of two different co-occurring encroaching species, Ashe juniper and nitrogen fixing Honey mesquite, on belowground carbon pools and respiration processes in a Central Texas savanna ecosystem, under the same climatic and edaphic factors.

Our specific objectives were to (1) compare soil respiration rates under both encroaching trees and in open grassland areas under different climatic conditions; (2) examine differences in soil carbon pools and microclimate under the two encroachers and grassland; (3) quantify the sensitivities of the respiration processes to soil temperature and soil moisture content, using five different models; and (4) use the models to estimate annual soil respiration flux under all three vegetation types for 2005-2006.

Soil respiration rates had similar seasonal patterns under all three vegetation types, with higher rates at warmer temperatures and higher soil moisture contents. Soil respiration was reduced by 3.5-20.5% and 9.8-22.7% annually under juniper and mesquite, respectively, compared to the adjacent grassland, with the largest differences observed during the active growing season. Up to 75% of the observed variation in respiration was explained by a logistic temperature model and a Lloyd & Taylor model, both combined with linear soil moisture dependence. Q_{10} values ranged from 2.13 under juniper to 2.78 in the grassland areas. Based on model results, soil respiration in grassland soils is more sensitive to soil moisture at high temperature, than in soils under both encroaching trees.

The shift from grassland to savanna in this ecosystem is accompanied by a reduction in soil respiration under both encroaching species. The decreased soil respiration and lower sensitivity to climatic factors under both encroachers, as well as increased SOC storage under juniper, all point in the direction that an increase in both Ashe juniper and Honey mesquite, increases the carbon sink strength of central Texas savannas.

1. Introduction

Semi-arid grasslands and savannas worldwide have undergone dramatic changes in the composition and structure of vegetation by an increase in the cover of woody species, due to a combination of anthropogenic activities and climate that favor C3 shrubs over C4 grasses (Archer 1990, Archer et al. 1995, Van Auken 2000). Woody encroachment is a widespread phenomenon, impacting a vast array of ecosystems in different climate zones, on different soil types and by many different species, making cross-ecosystem generalizations difficult (Eldridge et al. 2011). The latest estimates are that woody encroachment causes significant changes in ecosystem carbon pools, and estimates of the contribution of this land cover change to the US terrestrial carbon sink range from 60-130 Tg C yr^{-1}, or 25-46 % of the total US sink (Houghton et al. 1999, Pacala et al. 2001, King et al. 2007). Due to problems in bookkeeping methodology, scaling, and non-linearities in the encroachment process, these estimates are highly uncertain and errors associated with these numbers are larger than 100% (King et al. 2007).

In a recent overview study, considering large ranges of climatic and edaphic factors, mean annual precipitation (MAP) was found to be a good indicator of changes in aboveground net primary productivity (ANPP) following woody encroachment, whereas bulk density and clay content correlated with observed changes in soil organic carbon (SOC) (Barger et al. 2011). The encroaching species is also an important determinant, which are typically divided into two broad

classes, with arborescent conifers (e.g., juniper) categorized as trees, while the shrub category includes many different functional types, including the nitrogen fixing mesquite species. While these large scale correlations are useful scaling exercises, they provide little insight into the processes responsible for the changes in carbon pools.

Both the uptake and release of CO_2 between the land surface and atmosphere are expected to change when land cover changes (Raich and Tufekcioglu 2000, McCulley et al. 2004, Knapp et al. 2008). In ecosystems undergoing woody encroachment, generally C3 woody species replace C4 perennial grasses, and this change in plant functional type implies an increase in aboveground biomass, leaf area index, photosynthetic capacity, all of which can significantly alter rates of photosynthetic carbon uptake (Hughes et al. 2006, Knapp et al. 2008). Plant functional traits also have a strong direct and indirect control on soil carbon pools and processes. Phenology and growth rates regulate autotrophic respiration rates (Reich et al. 1997, Wright et al. 2004). In addition, a change in plant functional type, specifically a shift from C3 to C4 species, can alter soil carbon inputs from plants (Boutton et al. 1998, Cornwell et al. 2008), microbial diversity (Waldrop and Firestone 2006, Hollister et al. 2010), and soil microclimate (Smith and Johnson 2004), all of which can trigger a change in heterotrophic respiration rates.

Carbon uptake and respiration processes differ in both their sensitivity to climatic variables (Valentini et al. 2000), and primary physiological and ecological controls. Thus, it is critical to understand how woody encroachment alters both CO_2 uptake and release processes separately to make accurate predictions of how woody encroachment has altered ecosystem carbon balance, and how this is likely to change under future climate scenarios.

In this study, we took advantage of the co-occurrence of two encroachers, a coniferous tree species (Ashe juniper, *Juniperus ashei*, 'juniper' hereafter) and a nitrogen-fixing

deciduous shrub (Honey mesquite, *Prosopis glandulosa*, 'mesquite' hereafter), to study changes in soil organic carbon pools and respiration rates on the Edwards Plateau, a physiographic subdivision of the Great Plains in Central Texas. The Great Plains have been described as the bioclimatic region with the highest carbon sequestration potential due to woody encroachment, because of both changes in ANPP and SOC contributing to the sink (Barger et al. 2011). Despite their highly contrasting woody plant functional type, Ashe juniper and Honey mesquite are among the most prolific woody encroachers in North America. Prior studies have shown both increases and decreases, in both SOC pools and respiration rates, when wooded areas are compared to grassland areas (Biggs et al. 2002, Jackson et al. 2002, Jessup et al. 2003, Smith and Johnson 2003, McCulley et al. 2004, Smith and Johnson 2004, Liao et al. 2006, Neff et al. 2009, Cable et al. 2012, McCulley and Jackson 2012) suggesting that it is difficult to predict how soil organic carbon and respiration processes will respond to an increase in woody species. The occurrence of two important encroaching species at the same site, under the same edaphic and climatic conditions, makes this study site uniquely suited for studying changes in respiration processes and SOC pools associated with woody encroachment.

We measured soil respiration rates and quantified soil organic carbon pools under juniper, mesquite, and open grassland in Central Texas savanna recently invaded by juniper and mesquite. We then evaluated five different soil respiration models to quantify the abiotic controls on soil respiration, extend field measurements to annual sums, and predict the response of soil respiration to climate change. We hypothesized that the two woody species have differential effects on belowground carbon processes. Compared to grassland or mesquite, Ashe juniper has a lower leaf-level photosynthetic capacity, lower associated autotrophic respiration rates (Chapter 1), lower quality litter inputs, and an altered soil microclimate due to shading. These

factors should work in synergy to lower the overall soil respiration rate under Ashe juniper, and at the same time increase SOC storage. In contrast, Honey mesquite houses rhizobia that fix nitrogen and can increase soil fertility (Zitzer et al. 1996, Hibbard et al. 2001, Soper et al. 2014). We hypothesized that mesquite, contrary to juniper, will increase soil respiration rates and soil organic carbon pools, due to the additive effect of high autotrophic respiration rates associated with the high photosynthetic capacity of mesquite (Chapter 1) and its high quality inputs into the soil, which can sustain a large active soil microbial community. Finally, we predicted the temperature and moisture sensitivity of respiration to be lower under the encroaching tree species, compared to the grassland component. This is because photosynthesis in the dominant grassland species, King Ranch bluestem, has a narrow optimum temperature range, only occurs at higher temperatures, and depends on sufficient moisture. In contrast, both encroaching tree species have a broad temperature range, are partly decoupled from moisture in the upper soil layers, and juniper stays photosynthetically active throughout the whole year.

2. Materials and Methods

2.1. SITE DESCRIPTION

Our research was conducted at the AmeriFlux site Freeman Ranch 2 (US-FR2; 29°56'N, 98°W) located in the Balcones Canyonlands subregion of the eastern Edwards Plateau in Central Texas. The research area is in a karst landscape which overlies and recharges the Edwards Aquifer. Most of the region is occupied by savanna parkland of Plateau Live Oak (*Quercus virginiana var. fusiformis*) - Ashe juniper (*Juniperus ashei*) clusters interspersed in mixed C3/C4 perennial grasslands (Barnes et al. 2000). Due to a combination of overgrazing and fire suppression, many grassland areas on Freeman Ranch have experienced significant woody encroachment over the last century (Van Auken 2000). The study site is located in a former grassland being invaded with Ashe juniper (*Juniperus ashei,*'juniper' hereafter) and Honey mesquite (*Prosopis glandulosa*, 'mesquite' hereafter). Historical aerial pictures show that the trees at the site were 25-30 years old in 2006, and at that time, represented ~50% total site land cover (González 2010). The grassland vegetation is indicative of heavy grazing and is dominated by the invasive grass King Ranch bluestem *(Bothriochloa ischaemum,* a C4 grass*).* The mean annual temperature is 19.6°C and the mean annual precipitation is 913.3 mm, with a high intra-annual variability in precipitation. Summers are hot and dry with sporadic rainfall, while winters are cool with frequent rainfall.

2.2. PLANT AND SOIL CHARACTERISTICS

In Central Texas, the most common woody encroaching species is Ashe juniper (*Juniperus ashei* Buchholz), a drought-tolerant evergreen tree, native to northeastern Mexico and the south-central United States. Ashe juniper is predominantly shallow-rooted with an expansive

fibrous root system confined to thin soils (Hall 1952). Ashe juniper is not different from other conifers, in that it has low leaf nitrogen levels and low photosynthetic capacities (Chapter 1). Mesquite is a common encroacher in other ecosystems, but is thought to be excluded from most of the Edwards Plateau due to the shallow soil depths common in this region (Eggemeyer and Schwinning 2009), but appears occasionally where deeper soils prevail. Mesquite trees are winter-deciduous, drought avoiding phreatophytes, and are generally considered deep-rooted, although more shallow lateral roots have been documented (Ansley et al. 1991).

The soil at the site is Upland Rumple gravelly clay loam (Clayey-skeletal, mixed, active, thermic Typic Argiustolls) with weathered limestone (Bk horizon) at depths of ~1-2 m. The A horizon is ~20 cm thick and overlies a ~40 cm thick Bt1 horizon containing a high percentage of chert fragments. Below that is a Bt2 horizon containing few rock fragments (Barnes et al. 2000). Excavations showed the presence of tree roots throughout A and Bt horizons but limited penetration of tree roots into the Bk horizon (pers. comm. Susan Schwinning).

2.3. SOIL ORGANIC CARBON POOLS

In the spring of 2005, we laid out four transects per encroaching species, extending from the tree trunk into the grassland. Tree canopies of both species extended 1.5-2 m from the tree trunks, and each transect was 3.5 m in length. Previous studies indicate that woody plants do influence SOC pools under the canopy, but that the influence is spatially variable along the bole to dripline (Throop and Archer 2008, Cable et al. 2012). We sampled mineral soils every 50 cm along each transect at two depths (0-10 cm and 10-20 cm) after removal of the litter layer. Soil samples were dried and sieved over 2 mm in the lab. We quantified bulk soil organic carbon (SOC), total nitrogen (TN), C/N ratio and carbon isotopic signatures for all soil samples. Total particulate organic matter (POM) was determined on the 0-10 cm depth samples by physical

separation of the 53µm-2mm soil fraction by wet sieving. POM is a biologically and chemically active part of the bulk soil organic matter pool that has been shown to be sensitive to land-use change (Cambardella and Elliott 1992). Organic C, total N and carbon isotopic ratios were determined on all bulk soil samples and POM fractions. Leaf material of trees and grassland species was dried to constant weight at 70 °C, weighed and ground for determination of specific leaf area and elemental and carbon isotopic composition (%C, %N, C/N, $\delta^{13}C$, University of Wyoming Stable Isotope Facility). The fraction of the different soil organic carbon pools derived from C3 sources, was calculated using a simple mixing model (Boutton et al. 1998) with isotopic signature of KR bluestem grass leaves as C4 end-member and C3 tree leaves of the respective tree species as C3 end-member.

2.4. SOIL RESPIRATION MEASUREMENTS

We measured soil respiration rates over pre-installed 6" diameter PVC collars under each vegetation type (n=5 for grassland, juniper, mesquite) monthly from December 2004-December 2006, and again in February 2007 and July, 2007 to expand the range of microclimatic conditions encountered. The collars were installed in the summer of 2004 in the primary fetch of the AmeriFlux tower site FR-2 where energy, water and CO_2 fluxes are being measured using eddy covariance (Litvak et al. 2011). They were inserted into the soil to 4 cm, with 2 cm above the soil surface. The litter on the soil surface was left in place and plants were clipped when they had emerged before a measurement.

Soil respiration measurements were made using a CO_2 flux chamber (Li6400-09, LI-COR, Lincoln, Nebraska, USA) connected to a portable infrared gas analyzer (LI-6200, LI-COR, Lincoln, Nebraska, USA). The soil temperature at 2, 5 and 10 cm was taken using a handheld thermometer (HH506A, Omega Engineering, Inc., Stamford, Connecticut, USA) and a soil

sample was taken between 0 and 10 cm to determine the water content gravimetrically in the lab. An average bulk density of 1.37 g/cm^3 was determined and used to convert the gravimetric water content into volumetric water content. There are 3 soil pits present at the study site, located under the three vegetation types (grassland, juniper, mesquite), which are equipped with thermocouples at 2, 5 and 10 cm, as well as volumetric water content probes (ECH$_2$O probe, Decagon Devices, Inc., Pullman, WA, USA) at 0-10 cm and 10-20 cm that are measured continuously. Soil data 30-minute means were recorded using a data logger (CR5000, Campbell Scientific, Logan, UT, USA). These data series were used as model inputs to estimate the annual sums of soil respiration.

2.5. MODELS OF SOIL RESPIRATION

Different models of soil respiration have extensively been used in the literature (Conant et al. 2004, Webster et al. 2009) and they differ in how and which driving parameters are incorporated to explain the observed variation in soil respiration. Soil respiration in arid and semi-arid ecosystems largely depends on the interaction of soil moisture and temperature (Conant et al. 2004, Correia et al. 2012), therefore we limited ourselves to models that only use soil temperature and soil moisture as explaining variables (Table 1).

We modeled the effect of soil temperature as either a fixed temperature sensitivity as in the Q_{10} model, the power model or the exponential model (respectively T1, T2, and T3), or as a variable temperature sensitivity in the Lloyd and Taylor model (T4) and the logistic model (T5) (see references in Table 1). The variable temperature sensitivity allows for the temperature response to decline with increasing temperature, e.g. a 10 degree increase has a stronger effect on the rates if the increase is from 5-15 degrees, instead from 25-35 degrees. The T5 model modulates the effect of temperature through a logistic function, and also allows for smaller

increases in soil respiration at higher temperatures, and is comparable to a variable temperature sensitivity model.

In many models, soil moisture is incorporated as a positive linear function (Epron et al. 1999), while others allow for a decline in soil respiration when the soil moisture exceeds the range of optimal conditions (Mielnick and Dugas 2000, Tang and Baldocchi 2005). We chose to only use a positive linear function, as there was no evidence for decreased soil respiration at higher soil moisture contents in our dataset.

Soil respiration processes are also strongly regulated by substrate quantity and quality, composition of the decomposer community, supply of root exudates and overall photosynthetic activity of the vegetation cover (Raich and Tufekcioglu 2000, Reichstein et al. 2003, Fierer et al. 2005, Tang et al. 2005). To investigate whether the observed differences in soil respiration rates between the different vegetation types stems solely from differences in micro-climatic conditions or whether there are other intrinsic factors at play, we quantified the residuals of the different soil respiration models.

2.6. DATA ANALYSIS

A nonlinear curve fitting procedure, NLINFIT in Matlab (MathWorks Inc., Natick, MA, USA) was used to parameterize the soil respiration models with observed data, using soil respiration rate, soil temperature at 5 cm and volumetric water content (0-10 cm). This was done for all vegetation covers separately and combined. R^2, RSS and the Akaike's Information Criterion (AIC) were calculated to compare model performance. The AIC approach for model ranking favors models with fewer parameters.

We used SAS software (SAS Institute, Cary, NC, USA) PROC MIXED to evaluate (1) differences in soil organic carbon pools; (2) differences in microclimatic conditions and soil respiration rates; and (3) differences in model residuals.

For the soil organic carbon pools, effects of species and distance along the transect were investigated per carbon pool, for soil organic carbon content, total nitrogen, C/N ratio and carbon isotopic signature. Separately, differences between pools (SOC 0-10 cm, SOC 10-20 cm, POM 0-10 cm) were investigated per species.

For the soil respiration measurements, soil respiration, soil moisture and soil temperature were investigated for differences between vegetation type and over time. The residuals of the TM4 and TM5 models were calculated with a general parameterization of the model (three vegetation types combined) and residuals were tested for differences between vegetation type and time. This step was taken to investigate whether the differences in measured soil respiration rates were due to different soil microclimatic factors only, which would be explained by the respiration model, or whether there were other intrinsic factors at play.

3. Results

3.1. CLIMATE

The climate at the study site is characterized by mild, humid winters and hot, dry summers, with periods of dry heat, punctured by pulse rain events. In 2005 and 2006, the mean annual air temperatures, were, respectively, 19.9 and 20.6ºC, slightly above the 40-year climate normal for the site, 19.6 ºC. Minimum daily average air temperatures were 1.7 and 0.3 ºC, with recorded air temperatures as low as -4.6 and -3.4 ºC. Maximum daily averages were 31.1 and

30.7 ºC (in September and August respectively), with record midday air temperatures of 39.3 and 37.1 ºC.

The precipitation in 2005 and 2006 was 738 and 815 mm, respectively. In 2005, the summer was characterized by several substantial rainstorm events and accompanying dry-downs. The summer of 2006 was characterized by a 60-day period without rain in July-August, which was only alleviated with rains in September.

3.2. PLANT AND SOIL CHARACTERISTICS

The two tree species, juniper and mesquite, both had high carbon contents in their leaves, but differed significantly in N content resulting in C/N ratios of 38.9 and 17.2, respectively (Table 2). The C4 grass KR bluestem had low carbon and intermediate nitrogen, resulting in mid-range C/N ratios (23.9-25.4). King Ranch bluestem had a low $\delta^{13}C$ ratio of -13.8 ‰, as expected for a C4 species. The C3 species had $\delta^{13}C$ values in line with their expected water use efficiency, with a low value for the drought avoiding mesquite of -27.3‰ and a relatively high value for the drought tolerant juniper of -25.6‰ (Table 2).

The bulk soil organic carbon pool under juniper showed a significantly higher carbon concentration in the first two sampling points closest to the tree bole, compared to the rest of the transect. This effect was significant for the two soil depths (0-10 cm and 10-20 cm) (Figure 1). Integrated over the upper 20 cm of the soil profile, juniper had on average 10.9 g C kg^{-1} and 2.3 g C kg^{-1} more soil organic carbon in the first two sampling points closest to the bole, compared to the transect outside of the tree canopy (sampling points 5-7).

Bulk density of the soil was on average 1.37 g cm^{-3}, but varied widely and was difficult to assess due to the many rocks in the soil. Therefore, we report SOC results in

concentrations of carbon [g kg^{-1} soil], rather than density of carbon [g m^{-2}]. The average bulk density can be used to convert to carbon density to compare our sites to other study sites.

The bulk soil organic carbon pools along the mesquite transects had higher variability along the transect and therefore showed fewer significant differences. The carbon concentration (SOC) was significantly different between the first two sampling points for the 0-10 cm layer, but no significant differences were found further along the transect. Total nitrogen was only significantly higher on the first sampling point on the mesquite transect, compared to sampling points 3-4-5. The C/N ratio of the bulk soil organic carbon did not show significant differences along the transect, and the isotopic signatures of the bulk SOC were inconsistent (Figures 1 & 2). Of the two tree species, only juniper had a significantly larger concentration of carbon in the particulate organic matter (POM) fraction in the 0-10 cm layer, with 10 g/kg more POM-C in the first sampling point, compared to transect outside the tree canopy. The C/N ratios of the POM fraction were higher than the C/N fraction of the bulk soil, indicating that the POM fraction is derived from recent inputs of plant material, and is less decomposed and processed than the bulk soil organic carbon. The two encroaching species showed significant differences in the C/N ratio of the POM fractions (Figure 3), with lower values for mesquite. For juniper, the isotopic signature of the POM fraction was significantly lower, closer to the tree bole, compared to the rest of the transect, while there were no significant differences along the mesquite transect. A simple isotopic mixing model was used to assess the relative contributions of C3 and C4 sources to the POM fraction (Figure 3c). The C3-derived portion of the POM fraction did not differ significantly along the transect, and only a marginally significant difference ($p=0.039$) was found between the species.

3.3. SOIL MICROCLIMATE UNDER DIFFERENT VEGETATION TYPES

Soil temperature, as well as the daily amplitude in soil temperature was generally higher under the grassland vegetation. Minimum soil temperature at 5 cm soil depth under grass, juniper and mesquite cover were, respectively, 6.01, 6.54 and 6.55 ºC in 2005 and -1.4, 6.6, and 6.5 in 2006. Maximum temperatures under these three vegetation types are 41.3, 27.9 and 30.8 ºC in 2005 and 48.8, 29.3 and 30.1 in 2006. In our manual measurements, lower soil temperatures were consistently observed under juniper and mesquite than in grassland. Two 10-day time sequences of the soil temperature recorded continuously at 5 cm soil depth under the three vegetation types, representative for summer and winter periods (Figure 4), illustrate the seasonality and differences in soil microclimate under the three vegetation types we observed.

Volumetric soil water content ranged between 3-36 %, 2-40% and 4-39% under grassland, juniper and mesquite, respectively, in 2005 and from <0.5-31.5%, <0.5-37.9%, <0.5-32.8% in 2006. In our manual measurements, soil moisture was often higher under woody plants, except during winter months when there was no photosynthetic activity in the grassland and hence no water uptake (Dec ’04, Jan, Mar ’05, Feb’06).

3.4. SOIL RESPIRATION IN RELATION TO MICROCLIMATE UNDER DIFFERENT VEGETATION TYPES

Soil respiration rates showed a pronounced seasonal trend under all three vegetation types, but small differences in rates were observed (Figure 5, Table 4). Soil respiration rates were higher for the grassland compared to under juniper for most of the year, with a marked reversal during the winter months (Dec ’04, Jan, Feb, Dec 05, Feb 06).

The seasonal trend in soil respiration under all vegetation types did not only reflect seasonal changes in soil temperature, but also a strong dependence on soil moisture (Figure 5). Average values of soil respiration per date across vegetation types ranged from 0.27 to 7.47 umol

$m^{-2}s^{-1}$. Generally rates were low either at low temperatures (e.g. Feb and Dec in 2005; Jan, Nov, Dec in 2006), or when soil temperatures were high, but soil moisture conditions were low during summer drought conditions (e.g., Jun in 2005, Jul and Aug 2006) (Figures 5 a-b).

3.5. PARAMETERIZATION MODELS

Models with soil temperature as the only microclimatic variable performed poorly, with only 13-42 % of the variation in soil respiration rates explained (Table 5). Incorporating soil moisture as an explaining variable improved the variation explained to 60-75 % (Table 5).

For the general parameterization (all vegetation types combined), as well as for the parameterizations for the specific vegetation type, the logistical model TM5 performed best, based on AIC values, followed by the power model TM2, and the extensively used TM4 model. The simpler Q_{10} (TM1) model, which is functionally equivalent to the exponential model (TM3), showed the poorest agreement with the observations.

The temperature response of models TM2, TM4 and TM5, for soil water contents of 10, 20, and 30% is visualized in Figure 6. Although the overall pattern is the same, with higher temperatures and higher soil water contents giving rise to higher soil respiration rates, the differences between the models also became more expressed at higher temperatures and soil water contents. The logistic TM5 model had an effectively dampened temperature response at higher temperatures, while the Lloyd & Taylor model TM4, with a variable temperature response, achieved the highest rates at high temperatures (Figure 6). Based on their performance, we only used models TM2, TM4 and TM5 to examine the model residuals and compare different model estimates over a wide range of soil temperature and water content.

The residuals of the models were generally more positive in 2005 and negative in 2006, pointing out that the models, which were parameterized using data from both years,

underestimated soil respiration rates in the relatively wet year of 2005 and overestimated them in the dry year of 2006. The residuals were higher in the grassland soil than in the wooded areas during the summer of 2005 (Jul, Aug, Sept 2005), which suggests that the generally parameterized models underestimated soil respiration more under grassland cover during these time periods. In Dec 2004 and Sept 2006, the residuals were higher under juniper. The unexpected low soil respiration under grassland in Sept 2006 can be explained by the lack of recovery of the grassland canopy after the severe two-month summer drought.

Based on the vegetation-specific model parameterizations (Table 5), soils under both encroaching trees have a higher base respiration and a lower temperature response compared to grassland in all models, except model TM5. The Q_{10} values of the TM1 model range between 2.13 for the juniper cover and 2.78 for the grassland cover. The TM5 model, which is a logistic function, has a higher maximum rate and a higher inflection point ($T'_{1/2max}$) in the grassland soils, compared to the soils under the encroaching trees (Table 5, Figure 8).

The soil moisture sensitivity of soil respiration was modeled through a linear function (Tables 1&5), and was also dependent on soil temperature (Figure 9). At lower temperatures, soil respiration under the encroaching trees was more sensitive to soil moisture than in grassland soils for all three models TM2, TM4 and TM5. At higher temperatures, the grassland soil was much more sensitive to soil moisture than the soils under the encroaching trees.

To visualize the differences in model estimates for the parameterization per vegetation type, we plotted the difference of the models as a function of soil temperature and soil moisture in a 2D plot (Figure 10). The vegetation-specific parameterizations (Table 5, Figures 8 & 9) resulted in large differences in modeled SR rates between grassland and both tree species, with rates up to 5 µmol CO_2 m^{-2} s^{-1} higher in the grassland for the high soil temperature – high

soil moisture combination. For lower temperatures, the models produce slightly higher SR rates for juniper and mesquite than for the grassland. Small differences in parameterization between the juniper and mesquite models resulted in differences of only up to 0.4 μmol CO_2 m^{-2} s^{-1} in both the TM4 and TM5 models, with higher rates under juniper for low-medium temperatures and wet conditions. The parameterizations of soil respiration for both encroaching trees, as well as the climatic sensitivities resulting from these parameterizations, are remarkably small. The parameterization for different vegetation types provide soil respiration rates consistent with observed real-life differences between vegetation types. Higher soil respiration in grassland in summer, non-drought conditions, and relatively higher under juniper under winter conditions.

3.6. Annual soil respiration

Annual sums were calculated using the continuous measurements of soil moisture and soil temperature under the three vegetation types, based on the vegetation-specific model parameterizations. Annual soil respiration (Table 6) ranged between 447-611 g C m^{-2} yr^{-1}, with lower values for the drier year of 2006. Differences among the models were small, with more variation for the grassland and a tendency for the TM4 model to estimate higher annual soil respiration than the TM2 or TM5 models. The annual estimates indicate that as juniper and mesquite cover increased in these grasslands, annual respiration rates decreased by 9-12% and 14-16%, respectively (Table 6).

4. Discussion

4.1. Soil organic carbon pools

We found significantly more soil organic carbon under juniper trees compared to grassland. The increase under juniper was largely due to an increase in the soil POM fraction. A recent meta-analysis reported a range of values for changes in soil organic carbon pools due to

woody encroachment – from losses of 6200 g C m^{-2} to gains of 2700 g C m^{-2}, with an average accumulation of 385 g C m^{-2} (Barger et al. 2011). Reported changes in SOC specifically in juniper encroached systems are similarly variable, and have either decreased (Jackson et al. 2002), increased (Jessup et al. 2003, Neff et al. 2009), or remained unchanged (Smith and Johnson 2003) following encroachment. The 10.9 g kg^{-1} increase reported here translates to an increase of 2986 g C m^{-2} or 149 g C m^{-2} cm^{-1} depth. This increase in SOC is large compared to the range reported by Barger et al (2011), but is much smaller than reported differences between encroaching woodland and grassland (see Table 7) (Jessup et al. 2003, Neff et al. 2009).

We found no significant increases of the SOC pool, nor POM fraction, under mesquite at our study site. Reported values of changes in SOC in the literature following mesquite encroachment also span from losses (Jackson et al. 2002, McCulley and Jackson 2012) to large increases (Liao et al. 2006). The largest increases in SOC are reported for mesquite encroachment across a 120 year chronosequence in the Rio Grande Plains of Texas (Liao et al. 2006) where increases up to five times the background were measured. In mesquite tree clusters, the landscape element most closely resembling our ecosystem, an average rate of increase of 0.08 g C kg^{-1} yr^{-1} against a low background SOC value of 7.4 g C kg^{-1} in the remnant grasslands was found (Liao et al. 2006). For a more recently encroached area, such as our study site, this translates into an increase of 2.4 g C kg^{-1} after 30 years of encroachment. An increase this small might not be detected against a larger background of grassland SOC, especially given the large variability in the SOC pools on the mesquite transects. We conclude that mesquite trees at our study site are likely too young to show a significant increase in SOC pools.

4.2. SOIL RESPIRATION RATES

Overall, soil temperature and soil moisture are the key drivers of soil respiration in this ecosystem, as in other dry ecosystems (Conant et al. 2004). However, small differences in soil respiration rates between the different vegetation covers were observed, with lower respiration rates under the encroaching trees for most of the year. The observed differences between grasslands and trees are in line with the current understanding that soil respiration largely stems from recent photosynthate (Hogberg et al. 2001, Ryan and Law 2005). In this context, both the phenological differences between the species and the concurrent flux of assimilates to roots help to explain observed trends in soil respiration rates. Higher rates observed in the grassland during the summer are expected given the higher temperatures, but also because this is when the photosynthetic effort of the C4 grasses is concentrated provided there is sufficient moisture (Figure 5).

In contrast to grassland and mesquite trees, junipers photosynthesize year round and soil respiration rates under juniper were relatively higher during the winter, although only significantly higher than the other vegetation types in January 2005. This effect is contrary to what is expected based on solely temperature, given that the sheltering effect of thick juniper canopy results in reduced soil temperatures during the winter months (Figure 5). In previous studies, decreased respiration rates with juniper encroachment were attributed solely to altered microclimate (Smith and Johnson 2004). In our study, although soil temperature under juniper is most always lower than in grassland soils, and soil moisture often higher, we found three lines of evidence to support that the lower rates of soil respiration rates measured under juniper do not stem solely from differences in microclimatic conditions. First, we showed juniper alters the soil conditions by increasing organic carbon storage in the bulk soil, and the POM fraction (Figure 1). This result is consistent with measured soil respiration rates and microclimatic variables. The

SOC pool can build up through input of quantitatively more carbon from the plants, or qualitatively poorer carbon inputs while lower soil temperature can lead to lower microbial activity, lower respiration rates and increased carbon pools in the soil. Microbial communities can play a role in variation of soil carbon pools and fluxes, and there were small differences between grassland and juniper soils in substrate-induced respiration on 18 carbon sources and fungal community structure based on RFLP analysis, but not in bacteria RFLPs (Christine Hawkes, unpublished data). Second, after accounting for the differences in microclimatic conditions through the use of a common parameterized soil respiration model, we still found significant differences in the residuals of the respiration rates between the vegetation types. Third, the different parameterizations for different vegetation types, gives meaningful differences in modeled rates, with higher respiration rates in the grassland during periods of high soil temperature, and higher respiration rates for juniper at colder temperatures. The meaningful differences in parameterization suggest that, not just the microclimatic conditions, but the actual soil respiration process under juniper is altered compared to the grassland community.

Contrary to our predictions, soil respiration under mesquite was not larger than the soil respiration rates we measured in the open grassland. Previous studies suggest that mesquite, with its nitrogen fixing capability, is often the catalyst of change in community and ecosystem ecology (Hibbard et al. 2001) and higher respiration rates in response to mesquite encroachment are attributed to a fertile island effect (Hibbard et al. 2001, McCulley et al. 2004, Cable et al. 2012). This ‘fertile island effect’ results from higher quality inputs of litter (lower C/N ratios) and improved climatic factors under mesquite canopy. In other sites, these improved conditions harbor the growth of other understory species and mesquite clusters, and in turn, increase soil

organic carbon content and soil respiration rates (McCulley et al. 2004). Our study serves as an example that these changes do not always occur.

Mesquite is not a common encroacher in the ecoregion of this study, and most commonly has been cited not to be successful in the region because a lack of soil depth (Eggemeyer and Schwinning 2009). Mesquite does encroach at our study site, but has not formed clusters or understory during the last 25 years of encroachment, in contrast to other mesquite encroached ecosystems. Soil respiration rates were often significantly higher in the grassland, compared to mesquite, when temperatures were high and soil moisture sufficient (Aug '05, Sep'05, Jul '07). However, our measurements indicated that soils under mesquite experienced slightly higher soil respiration rates than juniper, which can be explained by a number of factors. First, the less dense canopy structure, compared to juniper, allows for higher temperatures and higher heterotrophic respiration rates. Second, the assumed higher availability of nitrogen might stimulate microbial activity and accelerate decomposition rates and carbon loss from recent, as well as older soil organic carbon – a phenomenon known as priming (Kuzyakov et al. 2000, Fontaine et al. 2004). And lastly, the litter of mesquite trees might be less recalcitrant than the litter of juniper trees.

Our results for mesquite are still somewhat unexpected, since other studies have shown a strong potential of mesquite to increase SOC pools and soil respiration rates. In studies performed in south Texas, the duration of encroachment has a large impact on the soil organic carbon pool (Liao et al. 2006). In semi-arid riparian areas in Arizona, medium mesquite trees did have lower soil respiration rates than large mesquite trees and grassland areas, which was attributed to a low carbon use efficiency of the soil microbes, low litter and low root biomass

(Cable et al. 2012). None of these variables have been quantified here, but similar conditions might be responsible for the observed lower soil respiration under mesquite at our site.

4.3. MODEL EVALUATION

We evaluated different soil respiration models with three objectives in mind. First, we evaluated what parameters were important and what model function best represented our measurements. Second, we compared the characteristics of the soil respiration processes under the three vegetation types, independent of the microclimatic conditions. And third, in order to scale the measurements in time, we evaluated the different model functions and their effect on annual respiration sums.

For the general parameterization, as well as for all vegetation types separately, the logistical model (TM5) performed best, based on Aikake criterion, followed by the power model (TM2), and the extensively used Lloyd & Taylor model (TM4). The simpler Q_{10} (TM1) model, which is functionally equivalent to the exponential model (TM3), showed the poorest agreement with the observations. Incorporating soil moisture as an explaining variable improved the variation explained to 60-75 %, up from 13-42% when only soil temperature was used as an explaining variable (Table 5). Soil respiration goes up with moisture availability, because it enhances autotrophic respiration, and it allows for a larger availability of substrates and microbial mass turnover to the microbial community. The better performance of TM4 compared to TM3 (Table 5), shows that the use of a variable temperature sensitivity is warranted as well. The TM5 model, which accounts for temperature effect through a logistic function, also allows for smaller increases in soil respiration at higher temperatures, and is comparable to a variable temperature sensitivity.

4.4. PREDICTIONS OF MODELS

The sensitivity of soil respiration to climatic drivers, such as soil temperature and soil moisture, are important factors in making predictions for the carbon balance of ecosystems under climate change scenarios. Our data show a lower temperature sensitivity of soil respiration under both encroaching trees (e.g. lower Q_{10} in model TM1) compared to the grassland soil, meaning that encroached areas will lose relatively less carbon to the atmosphere when soil temperatures rise. One caveat is that the Q_{10} value is inferred from measurements over several seasons which might confound Q_{10} values with other seasonal processes, such as phenology (Yuste et al. 2004, Davidson et al. 2006). We want to turn this argument around and claim that this seasonal Q_{10} still has value in local modeling exercises, just because the Q_{10} is based on seasonal measurements, and factors in the direct effect of phenology and photosynthetic activity on soil respiration, while lab/controlled environment derived Q_{10} values cannot account for this. The soil respiration models also show a lower sensitivity to soil moisture under the encroaching trees at high temperatures. We predicted this, based on the lower dependence of photosynthetic carbon uptake in trees on soil moisture, as opposed to grasses.

The model choice does not have a large effect on the annual sums of soil respiration, although the TM4 model has slightly higher annual sums in the year 2005 for all vegetation types, and also for the grassland in the year 2006. TM4 did produce the largest soil respiration rates at high temperatures, despite its variable temperature sensitivity. The logistic model, TM5, is a more effective model function to allow for lower temperature sensitivity at higher temperatures.

For the two years studied, the annual sums of soil respiration were smaller by 3.5-20.5% and 9.8-22.7% under juniper and mesquite cover than in grassland areas. The dry year of 2006 showed a stronger reduction in soil respiration under the encroaching trees, which might

seem counterintuitive because the grassland is more sensitive to soil moisture at high temperatures. Beside the sensitivities to climate, the microclimate itself is also altered.

5. Conclusion

Land cover change alters the biogeochemistry of ecosystems in different ways. We show that woody encroachment by two species in a central Texas savanna ecosystem, lowers soil respiration rates, and alters the sensitivity of the soil respiration process to climatic drivers. The sensitivity of soil respiration to temperature decreased under both encroaching species, and the response of soil respiration to soil moisture was less pronounced under the encroaching species at higher temperatures.

Based on our results, soil respiration processes following woody encroachment are altered through both direct and indirect effects, and these effects do not differ greatly depending on the encroaching species. The increased SOC storage under juniper, as well as the decreased soil respiration and lower sensitivity to climatic factors under both encroachers, suggest that the reduction in respiration we measured will contribute to the carbon sink strength as juniper continues to increase in this particular ecosystem.

6. Figures

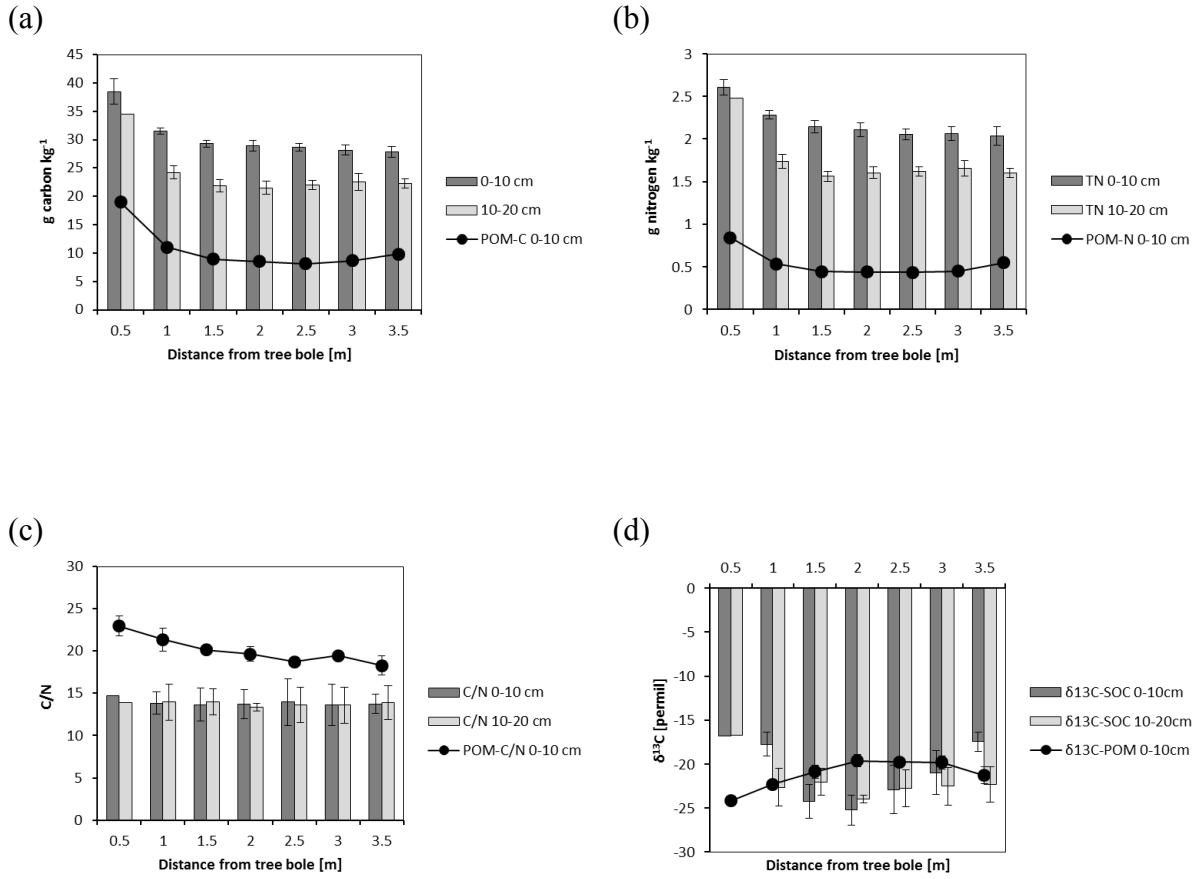

Figure 2.1: Soil characteristics for transects extending from juniper tree boles into grassland areas (4 transects) (a) Soil organic carbon concentration (SOC) and carbon concentration in particulate organic matter per kg soil (POM-C); (b) Soil total nitrogen (TN) and nitrogen density in particulate organic matter per kg soil (POM-N); (c) C to N ratio of bulk soil (C/N) and particulate organic matter (POM-C/N); (d) carbon isotopic composition of bulk soil (SOC-$\delta^{13}C$) and particulate organic matter (POM-$\delta^{13}C$).

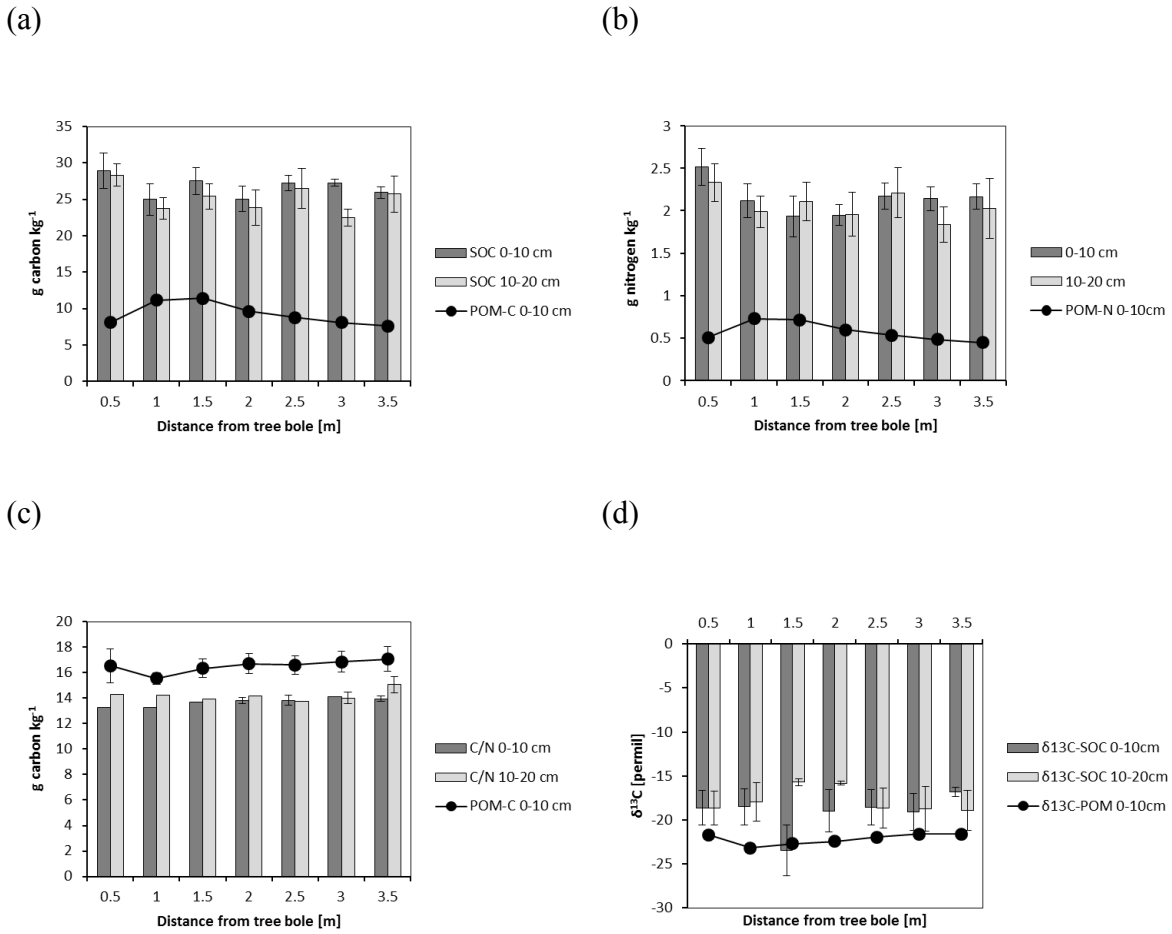

Figure 2.2: Soil characteristics for transects extending from mesquite tree boles into grassland areas (4 transects) (a) Soil organic carbon concentration (SOC) and carbon concentration in particulate organic matter per kg soil (POM-C); (b) Soil total nitrogen (TN) and nitrogen density in particulate organic matter per kg soil (POM-N); (c) C to N ratio of bulk soil (C/N) and particulate organic matter (POM-C/N); (d) carbon isotopic composition of bulk soil (SOC-$\delta^{13}C$) and particulate organic matter (POM-$\delta^{13}C$).

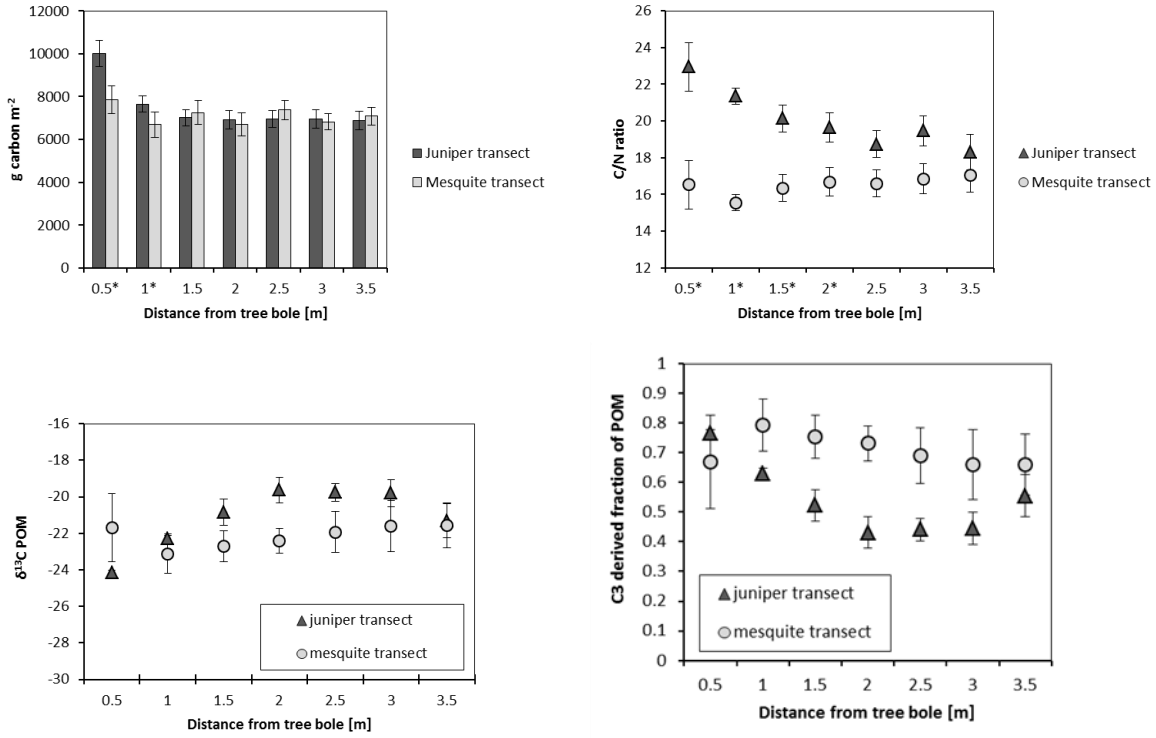

Figure 2.3: Comparison of juniper and mesquite transects for parameters that significantly differed between the two encroaching species: (a) Total soil organic carbon (SOC) in the 0-20cm soil profile; (b) C/N ratio (c) carbon isotopic signatures and (d) fraction of POM-C derived from C3 sources.

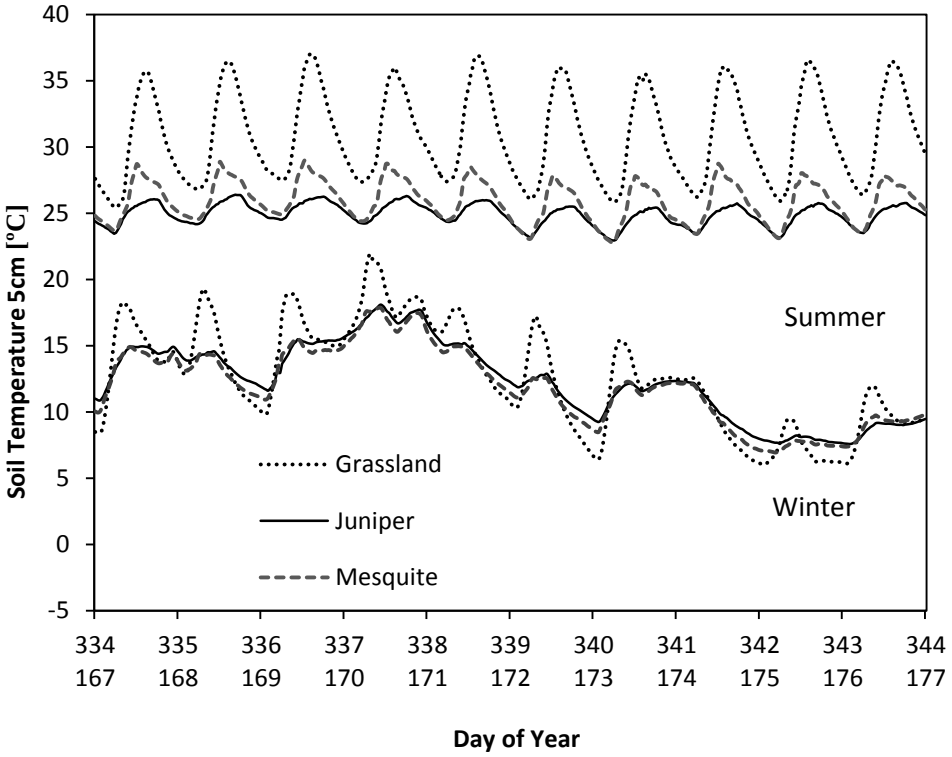

Figure 2.4: Two 10-day traces of soil temperature at 5 cm under the three vegetation covers, representative of summer (DOY 167-177, 2005) and winter (DOY 334-343, 2005).

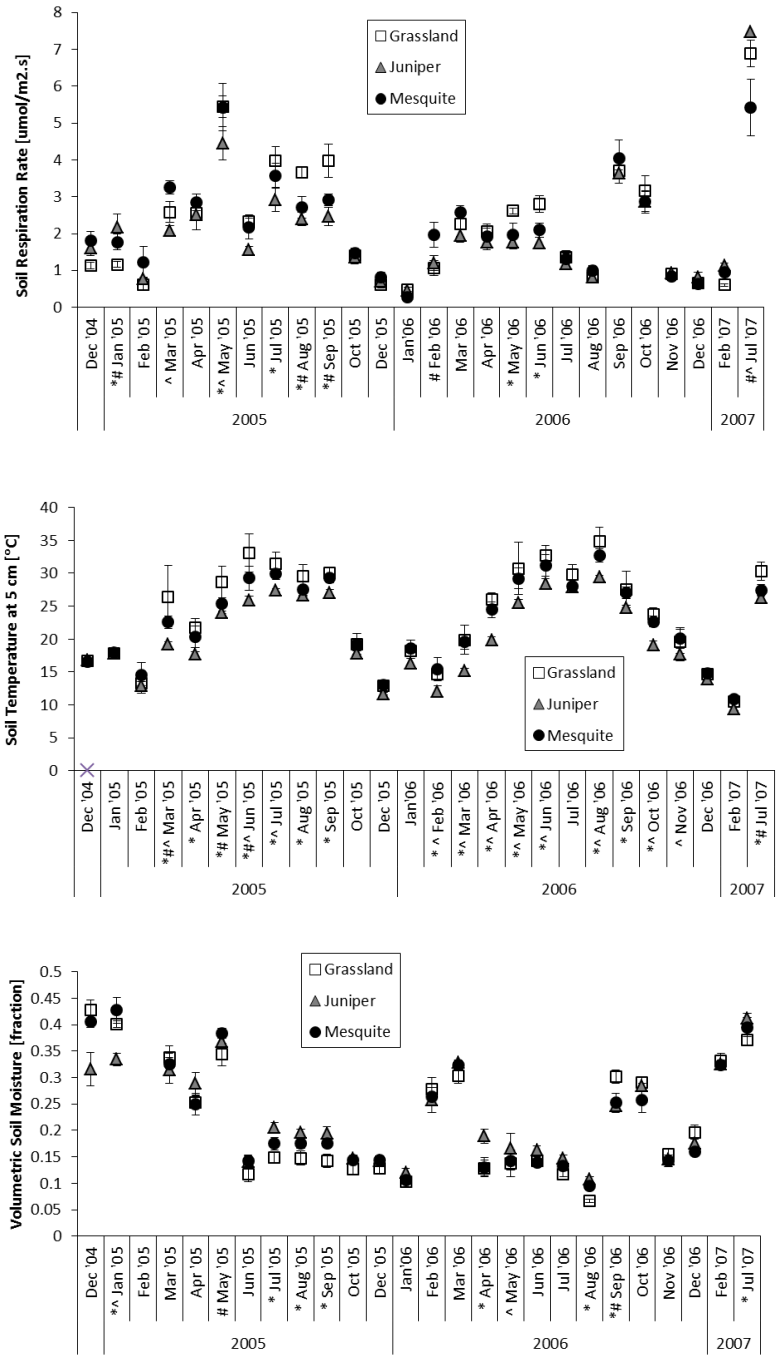

Figure 2.5: Seasonal course of soil variables manually measured in three vegetation covers: grassland, juniper and mesquite. (a) Soil respiration rate, (b) Soil temperature at 5 cm soil depth and (c) Volumetric soil moisture content (mean ± 1 standard error). Significant differences between vegetation types are given next to the month, * # ^ denotes significant differences ($p < 0.05$) between grassland-juniper, grassland-mesquite and juniper-mesquite respectively.

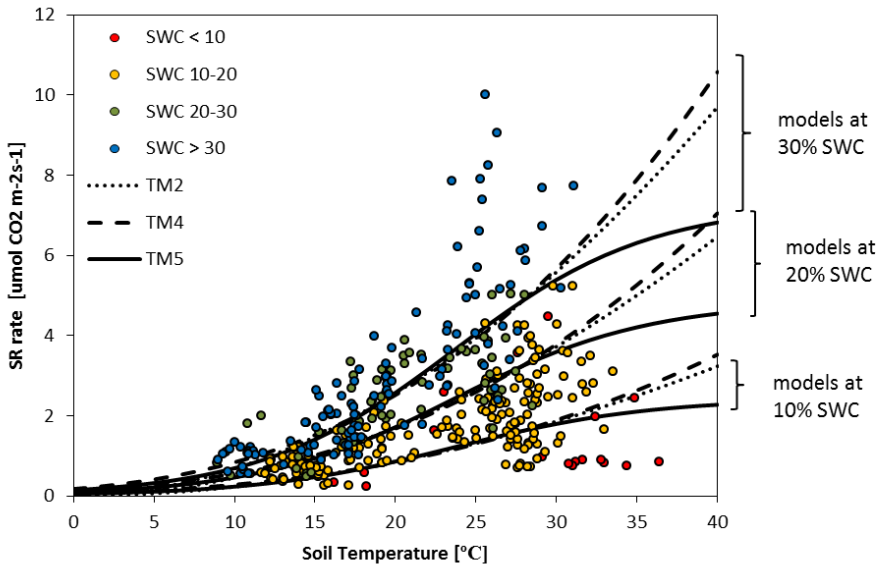

Figure 2.6: Soil respiration in function of soil temperature, according to models TM2, TM4 and TM5 with a common parameterization for all vegetation types. Different model results are given for different levels of soil water content. The measured data are given in color, binned according to soil water contents [<10%, 10-20%, 20-30%, >30%]

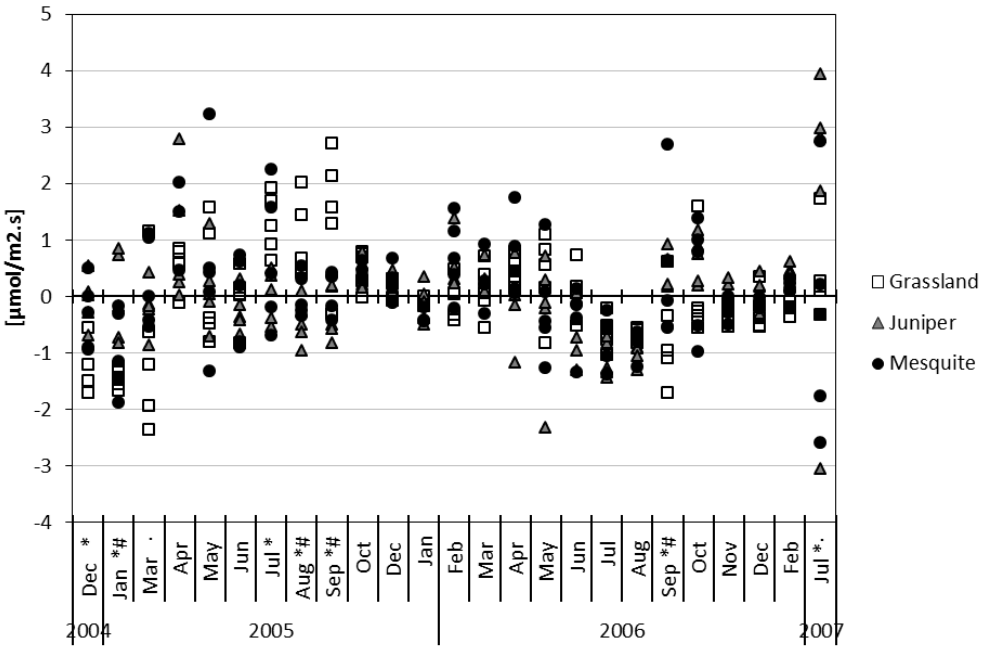

Figure 2.7: Residuals of the general parameterized model TM4. Significant differences in residuals between vegetation types are given next to the month name (* # · denotes significant differences ($p < 0.05$) between grassland-juniper, grassland-mesquite and juniper-mesquite respectively)

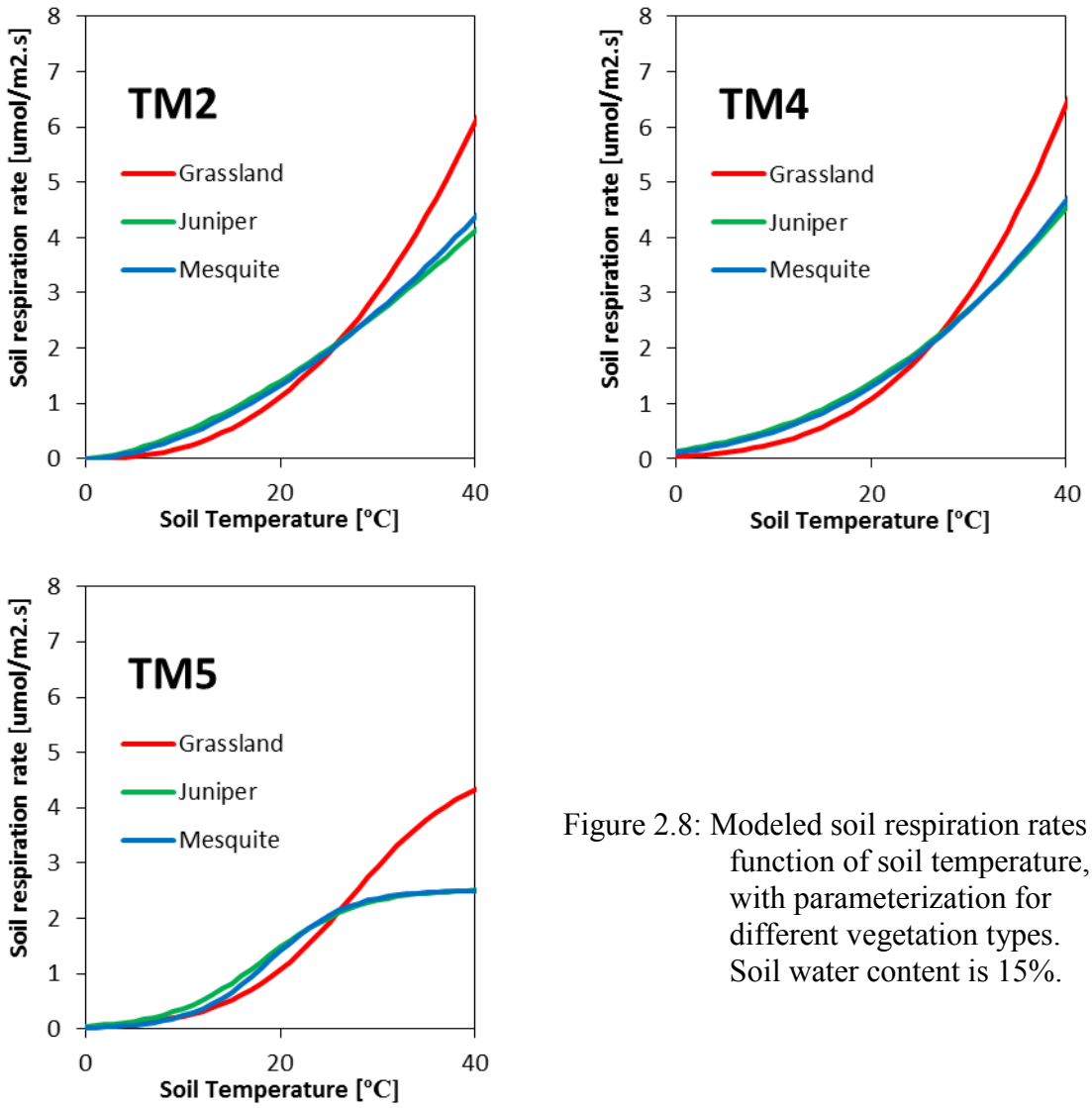

Figure 2.8: Modeled soil respiration rates in function of soil temperature, with parameterization for different vegetation types. Soil water content is 15%.

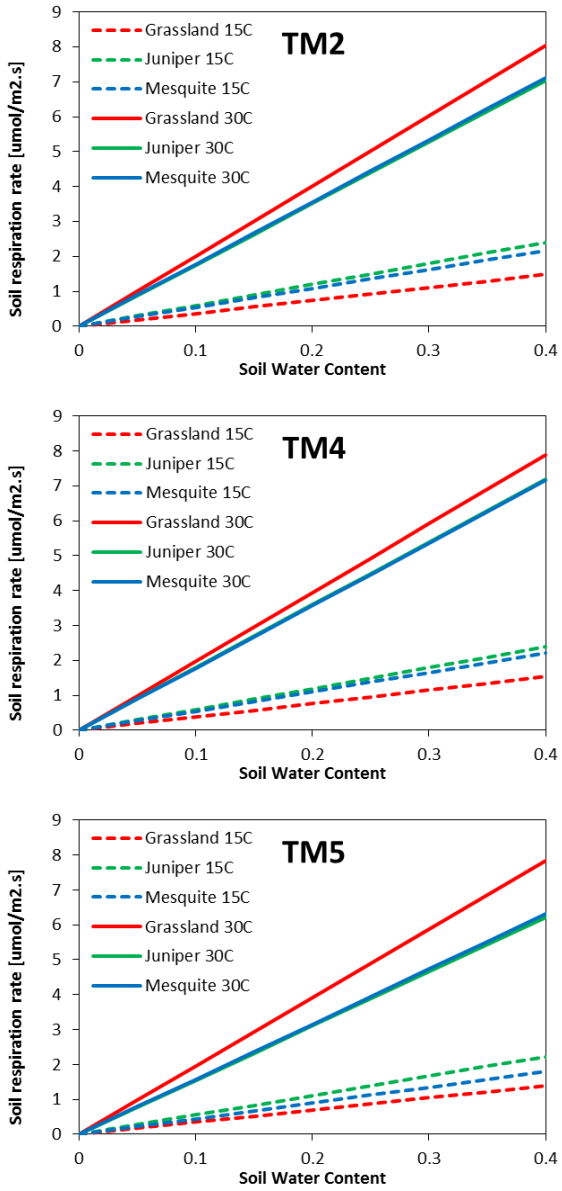

Figure 2.9: Modeled soil respiration rates in function of soil water content, with parameterization for different vegetation types. Soil temperature is 15ºC and 30ºC.

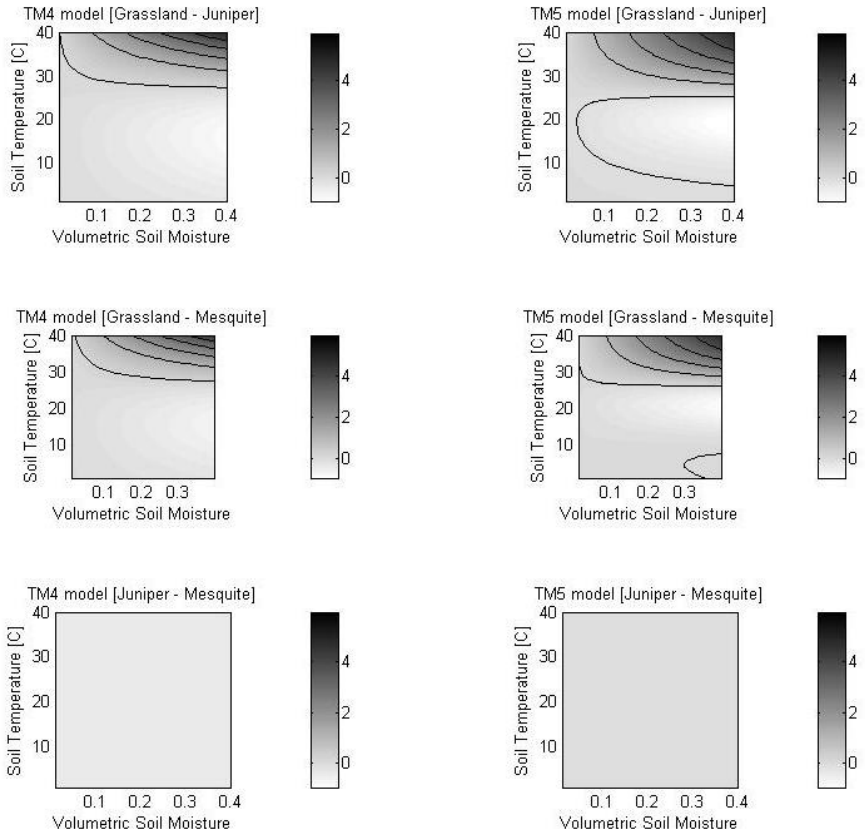

Figure 2.10: Differences between modeled respiration rates for the different vegetation covers parameterizations for models TM4 and TM5. Contour lines represent 1 μmol CO_2 m^{-2} s^{-1} differences.

7. Tables

Table 2.1: Soil respiration model description.

Model Name	Equation	Form	Variables	Reference
T1	$R = R_{10}\, Q_{10}^{\frac{(T-10)}{10}}$	Q_{10}	T	(van't Hoff, 1884)
T2	$R = a_1 T^{a_2}$	Power	T	(Kucera and Kirkham 1971)
T3	$R = b_1 \exp(b_2 T)$	Exponential	T	(van't Hoff, 1884)
T4	$R = \mathrm{R}_{10} \exp\left[E\left(\frac{1}{(283.15 - T_0)} - \frac{1}{(T - T_0)}\right)\right]$	Lloyd & Taylor	T	(Lloyd and Taylor 1994)
T5	$R = \frac{R_{max}}{1 + \exp(c\,\left(T_{1/2max} - T\right))}$	Logistic	T	(Richards 1959)
TM1	$R = R'_{10} M Q'^{\frac{(T-10)}{10}}_{10}$	Q_{10} + Linear	T, M	
TM2	$R = a'_1 M T^{a'_2}$	Power + Linear	T, M	
TM3	$R = b'_1 M \exp(b'_2 T)$	Exponential + Linear	T, M	(Epron et al. 1999)

Table 2.1 (continued): Soil respiration model description.

TM4	$R = \mathrm{R}'_{10}\mathrm{M}\exp\left[E\left(\frac{1}{(283.15 - T_0)} - \frac{1}{(T - T_0)}\right)\right]$	Lloyd & Taylor + Linear	T, M	(Reichstein et al. 2003)
TM5	$R = \frac{MR'_{max}}{1 + \exp(c'\left(T'_{1/2max} - T\right))}$	Logistic + Linear	T, M	

Table 2.2: Leaf characteristics

	N content [%]	**C content** [%]	**C/N** [-]	**δ13C** [‰]	**SLA** [cm2/g]
Ashe juniper	1.27 ± 0.11 (c)	48.0 ± 0.26 (a)	38.9 ± 1.20 (a)	-25.6 ± 0.20 (c)	64.82 ± 1.81 (a)
Honey mesquite	2.95 ± 0.11 (a)	47.9 ± 0.31 (a)	17.2 ± 1.15 (c)	-27.3 ± 0.22 (b)	88.13 ± 4.55 (a)
King Ranch bluestem	1.80 ± 0.12 (b)	44.4 ± 0.34 (b)	25.4 ± 1.27 (b)	-13.8 ± 0.24 (d)	181.78 ± 7.15 (c)
Texas wintergrass	1.95 ± 0.12 (b)	43.8 ± 0.34 (b)	23.9 ± 1.26 (b)	-28.6 ± 0.24 (a)	150.17 ± 4.72 (b)

Values are gives as average ± standard error. Significant differences between species, according to mixed model results, are denoted with different letters.

Table 2.3: Soil organic carbon – mixed model results.

	C content	N content	C:N ratio	$\delta^{13}C$
SOC 0-10 cm				
Species	0.0005	n.s.	n.s.	n.s.
Distance	0.0004	0.0139	n.s.	0.01
Species*Distance	n.s.	n.s.	0.03	n.s.
SOC 10-20 cm				
Species	n.s.	n.s.	n.s.	n.s.
Distance	0.0016	0.066	0.023	n.s.
Species*Distance	n.s.	n.s.	n.s.	n.s.
POM 0-10 cm				
Species	n.s.	n.s.	<0.0001	n.s.
Distance	0.0032	n.s.	n.s.	0.029
Species*Distance	0.0003	0.0124	0.04	0.0347

Table 2.4: Soil temperature, soil moisture and soil respiration: mixed model results.

Main effects	Soil Temperature	Soil Moisture	Soil Respiration	Res TM4	Res TM5
Time	<0.0001	<0.0001	<0.0001	<0.0001	<0.0001
Vegetation	<0.0001	0.3568	0.1741	0.9019	0.9897
Vegetation*Time	<0.0001	<0.0001	<0.0001	<0.0001	<0.0001

Table 2.5: Estimated parameters and model performance of different soil respiration models.

	Vegetation	Parameter Estimates [CI]			R^2	RMSE	AIC
T1	All Types	R_{10}= 1.28 [1.06 - 1.50]	Q_{10}= 1.57 [1.40 - 1.74]		0.194	1.41	264
	Grassland	R_{10}= 1.18 [0.819 - 1.54]	Q_{10}= 1.66 [1.37- 1.94]		0.284	1.42	91
	Juniper	R_{10}= 1.23 [0.822 - 1.64]	Q_{10}=1.60 [1.22 - 1.99]		0.141	1.48	101
	Mesquite	R_{10}= 1.48 [1.06-1.90]	Q_{10}=1.42 [1.16-1.69]		0.132	1.36	78
T2	All Types	a_1= 0.084[0.019 - 0.150]	a_2 = 1.07 [0.825 - 1.31]		0.226	1.39	249
	Grassland	a_1= 0.046 [-0.016 - 0.107]	a_2 = 1.26 [0.851 - 1.67]		0.331	1.372	82
	Juniper	a_1= 0.100 [-0.053 - 0.253]	a_2 = 1.01 [0.518 - 1.50]		0.161	1.46	97.5
	Mesquite	a_1= 0.169 [-0.051 - 0.388]	a_2 = 0.849 [0.439 - 1.26]		0.164	1.34	73
T3	All Types	b_1 = 0.814 [0.591- 1.037]	b_2 = 0.045 [0.034- 0.056]		0.194	1.417	264
	Grassland	b_1 = 0.713 [0.377- 1.049]	b_2 = 0.05 [0.033- 0.068]		0.284	1.42	91
	Juniper	b_1 = 0.767 [0.335- 1.199]	b_2 = 0.047 [0.023- 0.071]		0.141	1.479	101
	Mesquite	b_1 =1.042 [0.561- 1.522]	b_2 = 0.035 [0.017- 0.054]		0.132	1.362	78
T4	All Types	R_{10} = 1.111 [-0.89 - 1.332]	E_0 =224 [-172 - 275]		0.216	1.398	254
	Grassland	R_{10} = 0.973 [0.624- 1.323]	E_0 =259 [174 - 344]		0.317	1.387	85
	Juniper	R_{10} = 1.116 [0.702- 1.531]	E_0 =218 [111 - 325]		0.154	1.467	99
	Mesquite	R_{10} = 1.32 [0.89- 1.749]	E_0 =176 [89 - 264]		0.153	1.346	75
T5	All Types	R_{max} =3.07 [2.79 - 3.35]	c = 0.337 [0.199 - 0.474]	$T_{1/2max}$ =16.4 [15.3- 17.5]	0.284	1.34	222
	Grassland	R_{max} =3.40 [2.95- 3.84]	c = 0.356 [0.146- 0.565]	$T_{1/2max}$ =18.19 [16.46- -19.92]	0.421	1.28	66
	Juniper	R_{max} =2.79 [2.26- 3.32]	c = 0.334 [0.053- 0.615]	$T_{1/2max}$ =15.1 [12.8- 17.3]	0.200	1.43	93
	Mesquite	R_{max} =2.93 [2.52- 3.34]	c = 0.372 [0.099- 0.644]	$T_{1/2max}$ =15.7 [13.9- 17.5]	0.241	1.28	64

Table 2.5 (continued): Estimated parameters and model performance of different soil respiration models.

TM1	All Types	R'_{10} = 3.49 [3.06- 3.91]	Q'_{10} =2.36 [2.17- 2.54]	0.678	0.907	-81
	Grassland	R'_{10} = 2.58 [1.98- 3.18]	Q'_{10} =2.78 [2.42- 3.14]	0.733	0.881	-34
	Juniper	R'_{10} = 4.17 [3.31- 5.03]	Q'_{10} =2.13 [1.82- 2.45]	0.708	0.873	-35
	Mesquite	R'_{10} = 3.95 [3.11- 4.80]	Q'_{10} =2.15 [1.85- 2.46]	0.601	0.932	-18
TM2	All Types	a'_1 = 0.027 [0.011- 0.043]	a'_2 =1.92 [1.74- 2.10]	0.69	0.891	-94
	Grassland	a'_1=0.005 [0.00- 0.010]	a'_2=2.44 [2.11- 2.76]	0.748	0.857	-41
	Juniper	a'_1=0.090 [0.004- 0.175]	a'_2=1.551 [1.25- 1.86]	0.719	0.856	-40
	Mesquite	a'_1=0.053 [-0.001- 0.106]	a'_2=1.71 [1.39- 2.03]	0.624	0.905	-25
TM3	All Types	b'_1 =1.48 [1.19- 1.77]	b'_2 =0.086 [0.078- 0.094]	0.678	0.907	-81
	Grassland	b'_1 =0.928 [0.59- 1.26]	b'_2 =0.102 [0.089- 0.115]	0.733	0.881	-34
	Juniper	b'_1 =1.95 [1.27- 2.64]	b'_2 =0.076 [0.061- 0.091]	0.708	0.873	-35
	Mesquite	b'_1 =1.83 [1.19- 2.48]	b'_2 =0.077 [0.063- 0.091]	0.601	0.932	-18
TM4	All Types	R'_{10} = 2.79 [2.38- 3.20]	E'_0 = 407 [369- 445]	0.688	0.893	-92
	Grassland	R'_{10} = 1.84 [1.33- 2.36]	E'_0=505 [439 - 572]	0.745	0.861	-40
	Juniper	R'_{10} = 3.64 [2.80- 4.49]	E'_0=340 [274- 406]	0.716	0.86	-39
	Mesquite	R'_{10} = 3.25 [2.44- 4.06]	E'_0=363 [296 - 430]	0.617	0.912	-23
TM5	All Types	R'_{max} = 24.2 [17.5- 31.0]	c' =0.165 [0.123- 0.208]	$T'_{1/2max}$ =23.6 [19.8 - 27.4]	0.692	0.89	-96
	Grassland	R'_{max} =32.2 [15.6- 48.9]	c' =0.17 [0.112- 0.228]	$T'_{1/2max}$ =27.4 [21.0- 33.8]	0.750	0.86	-41
	Juniper	R'_{max} =16.9 [11.9- 21.9]	c' =0.209 [0.099- 0.319]	$T'_{1/2max}$ =18.4 [14.8- 22.0]	0.729	0.84	-43
	Mesquite	R'_{max} =16.8 [13.2- 20.3]	c' =0.249 [0.138- 0.359]	$T'_{1/2max}$ =19.04 [16.7- 21.4]	0.644	0.88	-30

Table 2.6: Annual sums of soil and ecosystem respiration

	2005			2006			2 year sum
	TM2	**TM4**	**TM5**	**TM2**	**TM4**	**TM5**	(average of models)
Rs grassland	603	611	593	570	580	550	1169
Rs juniper	580 (-3.8%)	583 (-4.6%)	572 (-3.5%)	462 (-18.9%)	461 (-20.5%)	465 (-15.4%)	1041 (-10.9%)
Rs mesquite	544 (-9.8%)	548 (-10.3%)	534 (-9.9%)	447 (-21.6%)	448 (-22.7%)	448 (-18.5%)	990 (-15.3%)
Rs ecosystem	588	593	579	515	519	506	1100
Reco		672			776		1448
Rs:Reco	0.87	0.88	0.86	0.66	0.66	0.65	0.76

Units are in g carbon m^{-2}, percent difference, compared to the grassland cover, is given between brackets. The site-wide average Rs and Reco are given for comparison, as well as the ratio of these 2 quantities. The site-wide annual average of soil respiration is calculated as the % cover weighted average, with 50% grassland cover, 38% juniper cover and 12% mesquite cover.

Table 2.7: Literature values of changes in SOC pools

			Juniper			
			this study	(Jessup et al, 2003)	(Smith & Johnson, 2004)	(Neff et al, 2009)
Upper layers	Grassland /Intercanopy	[g kg^{-1} soil]	27.5	40.0	36.2	5.0
	Woodland/Tree cluster	[g kg^{-1} soil]	38.5	80.0	38.7	65.0
	change	[g kg^{-1} soil]	**11.0**	**11.0**	**10.98**	**11.0**
Profile	Grassland /Intercanopy	[g kg^{-1} soil]	25.6	29.0	31.0	
	Woodland/Tree cluster	[g kg^{-1} soil]	36.5	48.0	32.6	
	change	[g kg^{-1} soil]	**10.9**	**19.0**		

			Mesquite		
			this study	(Liao et al, 2006)	(Liao et al, 2006)
				upland cluster ~30 yrs	drainage ~120 yrs
Upper layers	Grassland /Intercanopy	[g kg^{-1} soil]	27.5	7.4	6.1
	Woodland/Tree cluster	[g kg^{-1} soil]	28.9	9.8	30.1
	change	[g kg^{-1} soil]	**1.4**	**2.4**	**24.0**
Profile	Grassland /Intercanopy	[g kg^{-1} soil]	25.6		
	Woodland/Tree cluster	[g kg^{-1} soil]	28.6		
	change	[g kg^{-1} soil]	**3.1**		

CHAPTER 3: ABIOTIC CONTROLS ON CARBON EXCHANGE PROCESSES AT AN ENCROACHING SAVANNA SITE IN CENTRAL TEXAS

Abstract

Savanna and grassland ecosystems comprise 28% of the global land surface and account for 37% of the terrestrial NPP. Savannas occur where precipitation is limited and strong links between water availability and carbon uptake exist. The size of the carbon pool that savannas represent, as well as its sensitivity to precipitation, warrant a close examination of carbon fluxes in a savanna ecosystem in relation to climatic drivers, especially in the context of climate change and carbon cycle –climate feedbacks.

We analyzed patterns of ecosystem-atmosphere carbon exchange in a Central Texas savanna undergoing woody encroachment with two main objectives: (1) quantify the carbon balance of the savanna ecosystem during three years of contrasting water availability, and (2) quantify the response of net and gross carbon fluxes (tower-based net ecosystem exchange (NEE) and component fluxes Gross Primary Productivity (GPP) and Ecosystem Respiration (Reco)) to both temperature and water availability.

The savanna was a significant net carbon sink during this period - on average 405 g C m^{-2} yr^{-1}, with large differences between years. The timing of precipitation, and differential sensitivity of gross photosynthesis and respiration to water availability, explained the difference in carbon balance between years. Gross fluxes showed a strong dependence on daily average temperature and on soil water content in the drier years. Increases in daily average temperature when temperature stayed below 20ºC favored Reco more than GPP. Further increases in daily average temperature, in the 20-30ºC range, favored GPP over Reco. Ecosystem respiration was more

sensitive to soil moisture deficits than gross photosynthesis. While the differences between years could be attributed to differences in rainfall distribution, the overall large size of the carbon sink can be explained by the imbalance between uptake and release, brought forth by the encroachment process. Important ecosystem characteristics, such as temperature sensitivity of net carbon exchange, as well as the relative sensitivities of gross carbon fluxes to soil moisture, suggest that the encroachment process not only acts as a large sink to atmospheric CO_2, but that it also renders the ecosystem less sensitive to climatic extremes.

1. Introduction

Savanna and grassland ecosystems make up 28% of the terrestrial land surface and 37% of global NPP (Grace et al. 2006). Savanna ecosystems occur in regions where rainfall is seasonal and productivity is primarily limited by the magnitude and timing of precipitation events (Walker and Noy-Meir 1982, Scholes and Walker 1993, Cook et al. 2002), creating strong links between precipitation, available soil moisture, evapotranspiration, and carbon uptake (Williams and Albertson 2004). Savanna ecosystems are undergoing woody encroachment at a global scale (Archer et al. 1995), with possible large, but uncertain contributions to the overall terrestrial carbon sink (Houghton et al. 1999, Barger et al. 2011, Houghton et al. 2012, King et al. 2012). The size of the biome, the wide-spread structural changes and the vulnerability of these ecosystems to climatic factors, especially rainfall and water availability, makes quantifying the carbon balance of savanna ecosystems important, especially in view of climate change and carbon cycle-climate feedbacks (Ciais et al. 2013).

Climate change is predicted to reduce the capability of ecosystems to sequester carbon from the atmosphere (Friedlingstein et al. 2006), leading to a positive feedback to the climate

system. The carbon balance of an ecosystem results from the difference between carbon uptake (photosynthesis) and release (autotrophic and heterotrophic respiration). Carbon uptake processes are controlled by temperature, water availability, and incoming radiation (Law et al. 2002). Respiration processes are controlled by temperature, water availability, and substrate supply (Raich and Schlesinger 1992, Hogberg et al. 2001, Ryan and Law 2005). The differential sensitivity of carbon uptake and release processes to temperature and soil moisture determines the overall response of site-specific carbon balance to climate.

Temperature is the most important abiotic driver of biological systems across scales, ranging from enzyme kinetics (Farquhar 1989, Bernacchi et al. 2001) to biome distributions and productivity (Raich and Schlesinger 1992, Baldocchi et al. 2001). Photosynthesis depends on temperature, with adaptation and acclimation of individual species to local temperature resulting in different ecosystem level responses (Yuan et al. 2011). Respiration processes are also largely driven by temperature and often modeled by an ever increasing temperature function (Lloyd and Taylor 1994). However, at longer timescales Reco is inherently limited by GPP via the provision of substrates for heterotrophic respiration (Hogberg et al. 2001, Janssens et al. 2001). The relative effect of temperature on photosynthesis and respiration is not known, but often it is assumed that respiration processes are more sensitive to temperature, leading to net decreases in carbon balance at higher temperatures (Kirschbaum 2000, Anderson-Teixeira et al. 2011).

In addition to temperature, both ecosystem production and respiration can be limited by water. Up to 40% of the terrestrial land surface is controlled by water availability (Beer et al. 2010), particularly in mid to low latitudes (Yi et al. 2010). Decreasing soil moisture negatively impacts plant photosynthesis through stomatal closure or altered metabolic processes (Flexas and Medrano 2002). Soil moisture declines also reduce respiration processes, as autotrophic

respiration declines with photosynthesis and heterotrophic respiration becomes limited by substrate availability (Chapter 2). A FluxNet synthesis study has shown that carbon uptake is on average 50% more sensitive than carbon release to decreases in water availability (Schwalm et al. 2010). A corollary is that in water limited ecosystems, wet years are thought to be associated with strong carbon uptake (nets sinks), normal years are slight carbon sinks or carbon neutral, and drought years are associated with net carbon loss (net sources) (Eamus et al. 2001, Hastings et al. 2005, Kurc and Small 2007). Other studies have indicated that the annual net carbon balance of an ecosystem is not always a direct function of annual precipitation and that the distribution pattern of precipitation may play an overriding role (Xu and Baldocchi 2004, Ma et al. 2007).

Our objectives in this study were to (1) quantify the carbon sink strength of a savanna site undergoing woody encroachment, and (2) to determine the climatic controls on this carbon sink. We expected the encroaching savanna site to be a net carbon sink (Barger et al. 2011), and the ecosystem level fluxes to show strong variation with water availability. To address the first objective, we quantified net ecosystem carbon exchange (NEE) of a savanna in central Texas experiencing woody encroachment, and partitioned the net flux in canopy photosynthesis (GPP) and ecosystem respiration (Reco). We calculated the metric Reco/GPP to study relative changes in respiration and photosynthesis at a daily time step. We did this exercise for three years (2005-2007), which spanned a wide range of environmental conditions that allowed us to study the different component fluxes in relation to climatic drivers to address the second objective.

2. Methods

2.1. SITE DESCRIPTION

This research took place on Freeman Ranch, a 4200 ha research area, owned by Texas State University and located on the eastern Edwards Plateau in Central Texas. The Edwards Plateau is a 93,000 km^2 region in central Texas that is both ecologically and geologically unique in the area (Amos and Gehlbach 1988, Johnson 2010). Historically, much of the Edwards Plateau was vegetated by grassland and open savanna dominated by prairie grasses and isolated live oaks (*Quercus virginiana*). Chronic overgrazing by livestock after European settlement resulted in replacement of palatable tall and midgrasses by more grazing resistant shortgrasses, and fire suppression increased populations of unpalatable woody species, predominantly Ashe juniper (*Juniperus ashei*) (Van Auken 2000). Our study site is a former grassland, experiencing woody encroachment by Ashe juniper and Honey mesquite that first appeared in aerial photographs 25 years earlier. The grassland diversity is further suppressed by the invasive grass species King Ranch bluestem (*Bothriochloa ischaemum*).

The climate of the study site is characterized as semi-arid, with cool winters and hot summers, with periods of dry heat interrupted by rain events. The mean annual temperature is 19.6ºC and the mean annual precipitation is 913.3 mm. Texas savannas are subject to highly variable seasonal and annual precipitation regimes. Precipitation is largely bimodal with most of the rainfall occurring in the spring and fall, yet the variability remains high especially in the summer months (National Climate Data Center).

2.2. CARBON FLUXES

Net ecosystem exchange of carbon (NEE) was measured for a period of 3 years, 2005-2007, using open-path eddy covariance techniques following standard AmeriFlux guidelines. For

a detailed description of instrumentation at the site, see Litvak et al. (2011). All fluxes were calculated as 30-min averages. The eddy covariance term was corrected for density fluctuations due to heat and water vapor fluxes using the procedure of Webb et al. (1980). Frequency response corrections were applied using the method of Massman (2000), while the empirical approach of Laubach and McNaughton (1998) was used to correct for sensor separation. A friction velocity (u^*) filter was used to reject data obtained when turbulence was below a threshold of 0.15 m s^{-1} (Hastings et al. 2005). Supporting measurements included air temperature, relative humidity, net radiation, up and down welling global irradiance, and up and down welling photosynthetic photon flux density. Soil moisture, soil temperature and soil heat flux were measured at different depths in three locations: in open grassland, under juniper canopy and under mesquite canopy. Gaps in meteorological data and turbulent fluxes were filled using on-line tools from the Max Planck Institute of Biogeochemistry (Reichstein et al. 2005). Net ecosystem exchange of carbon (NEE) was partitioned into gross primary productivity (GPP) and ecosystem respiration (Reco) by fitting hyperbolic light response curves with a respiration term to daytime NEE data and accounting for both the temperature sensitivity of ecosystem respiration and the vapor pressure deficit limitation of photosynthesis (Lasslop et al. 2010). The daily integral of net and gross carbon fluxes was calculated and Reco/GPP was calculated on a daily time-step. To study how net and gross fluxes, as well as the ratio Reco/ GPP, were affected by climatic drivers, the daily fluxes were binned according to average daily temperature (1ºC increments), and average daily soil water content (1% increments), and average daily fluxes for each bin were calculated.

3. Results

3.1. CLIMATE

In 2005, 2006, and 2007, the mean annual air temperatures were, respectively, 20.0, 20.7 and 19.1 ºC. Total annual precipitation from 2005 to 2007 was 738, 815, and 1514 mm, respectively, representing 19% below, 10% below, and 65% above the long-term average. In 2005, the summer was characterized by three substantial rain events and accompanying dry-downs. Based on the Palmer Z drought Index (PZI), the summer months in 2005 on the Edwards Plateau were categorized from very moist to severe drought (PZI =[-3.44, 2.55], NCDC). The summer of 2006 was characterized by a 60-day long period without rain in July-August, and the summer months were categorized from mid-range to severe drought based on the Palmer Z drought Index (PZI =[-2.29, -0.26], NCDC). In contrast, the summer months of 2007 were categorized as mid-range to extremely moist (PZI = [0.1-8.65], NCDC) with July 2007 being the wettest July month on record.

3.2. ECOSYSTEM-LEVEL CARBON FLUXES

3.2.1. Seasonal trends in NEE

Ecosystem NEE fluxes followed a clear seasonal pattern with effects of precipitation superimposed on the annual temperature regime (Figure 1a). Maximum rates of NEE, GPP and Reco were seen in the summers after recent rainfall events, and reached values of -5.7 g C $m^{-2}day^{-1}$, 10.27 g C $m^{-2}day^{-1}$ and 8.4 g C $m^{-2}day^{-1}$ in 2005, 2006, and 2007, respectively (Figure 1b). On most days, this savanna was a carbon sink, with negative daily NEE in 79% of the three year period. Of the days when the ecosystem was a carbon source, 42% were associated with precipitation events (Figure 2a).

In the three years of study, there were four periods when the ecosystem acted as a source of carbon to the atmosphere for more than seven consecutive days (Figures 2, 3). At the end of the 60-day long drought in the summer of 2006, the ecosystem became a carbon source, which continued for 13 days after the rainfall in September 2006. During this 25-day period, before and after the rain, the overall carbon loss of the ecosystem was 22 g C m^{-2}. The other three periods when the ecosystem acted as a carbon source for seven or more consecutive days were in late fall or winter months. The overall loss of carbon was small each time, respectively 1.28 g C m^{-2}, 4.4 g C m^{-2} and 4.5 g C m^{-2} during 7-day periods in November '05, January '07 and December '07 (Figure 2b). These periods were associated with low temperature, low photosynthetic active radiation, or both. Other periods when the system acted as a carbon source, associated with summer precipitation pulses, lasted only two to four days (June 17th 2006 (DOY 195), July 3rd 2007 (DOY 184), August 17th 2007 (DOY 229)).

3.2.2. Reco, GPP and Reco/GPP

Ecosystem respiration closely followed the precipitation distribution pattern in 2005-2007, with high efflux periods after rainfall events and rapid reduction in Reco during dry-downs. The important role that precipitation pulses play in driving ecosystem fluxes in this savanna, is more clear from a comparison of 100-day summer periods in 2005, 2006 and 2007 (Figure 4). In 2005, the summer season was dominated by three rainfall events, followed by dry-down periods, when both Reco and GPP decreased, but the overall system remained a significant carbon sink. The largest daily net uptake rate of the three years occurred during the second dry-down period in 2005, when there was a net uptake of 5.68 g C m^{-2} day^{-1}on DOY 213. In 2006, the summer was characterized by a 60-day long summer drought, which had a large impact on the carbon exchange processes, with lower gross primary productivity and ecosystem respiration.

By the end of the 2006 summer drought, gross fluxes were reduced to values smaller than 2 g C m^{-2} day^{-1}, and the system became a small carbon source, smaller than 1 g C m^{-2} day^{-1}. In 2007, there were many rainy summer days, leading to a reduced pulse pattern in the fluxes. For example, the large 186 mm rainstorm on July 20th (DOY 201) did not cause any obvious change in the flux pattern, due to rain in the days leading up to it, while the 39 mm rain event on August 16th (DOY 228) followed a short 13 day dry-down and did produce a small pulse pattern.

The fraction of carbon lost as respiration per total carbon gained through photosynthesis (Reco/GPP) typically fell after precipitation pulses (Figure 4), indicating that ecosystem respiration decreased faster than gross primary productivity in the dry-down after rainfall events and therefore that respiration was more responsive to decreases in water availability than GPP (Figure 1b, 2). During the prolonged summer drought of 2006, Reco/GPP initially declined (favoring GPP over Reco), but rose again as the drought wore on and GPP was gradually more impacted.

3.2.3. Cumulative fluxes

Cumulative annual NEE was -508 g C m^{-2} yr^{-1}, -287 g C m^{-2} yr^{-1} and -420 g C m^{-2} yr^{-1} for 2005 through 2007, respectively (Table 1). The year-to-year variability in cumulative ecosystem respiration (Reco) follows variability in precipitation, with the least precipitation and Reco in 2005 (738 mm, 672 g C m^{-2} yr^{-1}), more precipitation and Reco in 2006 (815 mm, 776 g C m^{-2} yr^{-1}), and large quantities of precipitation and Reco in 2007 (1514 mm, 1042 g C m^{-2} yr^{-1}).

Cumulative gross primary productivity, and therefore also NEE, did not follow this same pattern, with relatively more GPP in 2005 than in 2006 (1180 vs 1063 g C m^{-2} yr^{-1}). GPP was larger in 2007 (1463 g C m^{-2} yr^{-1}) than in the two drier years, but because of the large difference between GPP and Reco in 2005, the carbon sink was largest in 2005 (Table 1).

3.3. RELATIONSHIP BETWEEN CLIMATIC DRIVERS AND ECOSYSTEM CARBON FLUXES

Overall, NEE showed a relatively flat response to temperature at lower temperatures (<20 ºC) and an increase in net carbon uptake at temperatures > 20 ºC (Figure 5a). The temperature response of GPP showed maximum daily averages around 26°C. The annual differences in temperature response reflect differences in water status among the three years. In 2007, abundant water allowed for higher gross carbon fluxes at higher temperatures (Figure 5c). Ecosystem respiration rates from this savanna also displayed a temperature optimum of 22-26ºC (Figure 5b). Higher temperatures were observed in the summer, which often coincided with low water availability in 2005 and 2006. Lower Reco values found at the high end of the temperature scale for 2007 also occurred during a relatively dry period in the summer of 2007 (DOY 218-219, 224-227) when there was no rain for 13 days. The ratio of Reco/GPP ratio was highest in all three years at around 18-20°C daily average temperature, suggesting that Reco is more sensitive than GPP to increasing temperatures below 20ºC. As daily average temperature > 20ºC, GPP becomes again more important than Reco in driving this relationship.

Despite the strong response of both photosynthesis and respiration fluxes to precipitation events, the relationship between soil water content and carbon fluxes was less clear than the temperature response. In 2005-2006, Reco and GPP correlated positively with soil water content, but not in 2007 when water was not a limiting factor. High values of GPP and Reco at mid-range soil water content values in 2007 can be explained by water availability in the entire soil profile and a fully developed grassland canopy, while the soil water metric we used only represents the top 10 cm of the soil profile. The ratio of Reco/GPP showed a modest increase with soil water content (Figure 6b), meaning that changes in soil moisture have a relatively stronger effect on

respiration processes than on photosynthesis. For soil water values below 10%, the ratio of Reco/GPP was on average always lower than 1, meaning that the ecosystem stays carbon positive under low water availability. The values of Reco/GPP > 1, as observed at the end of the drought in the summer of 2006 (Figure 4) are binned together with other days of low soil water content in 2006, with an average Reco/GPP < 1. This points to a shortcoming of our approach - the soil water content in the upper 10 cm is not the best indicator of drought duration or intensity.

4. Discussion

4.1. Ecosystem-level carbon fluxes

The encroaching savanna site was an important carbon sink, during the three years of this study, with an average carbon sequestration of 405 g C m^{-2} yr^{-1}. Reported values of carbon balance for forest ecosystems are between ~+100 and -600 g C m^{-2} yr^{-1} (Luyssaert et al. 2007) and from ~+220 to ~-650 g C m^{-2} yr^{-1} when other non-disturbed ecosystems are included (Anderson-Teixeira et al. 2011). Similar to what has been measured in other semi-arid biomes, we observed large variability between years and the precipitation has a strong influence on the carbon fluxes of the ecosystem (Xu and Baldocchi 2004, Kurc and Small 2007, Ma et al. 2007, Yi et al. 2010).

The strongest carbon sink occurred in the year with the least precipitation (-508 g C m^{-2} in 2005), suggesting that the relationship between carbon cycling and rainfall is complex. The distribution pattern of precipitation can explain the difference between the years 2005 and 2006, if considered in the context of a pulse driven ecosystem (Huxman et al. 2004). The relative responses of GPP and Reco to water availability can explain differences between 2005 and 2007.

Litvak et al. (2011) postulated that a carry-over effect of large amounts of precipitation in the fall of 2004, stored in the soil profile, could be responsible for the large net carbon sink in

2005 at our site. An additional explanation might be that the observed precipitation pulses in the summer of 2005 caused a net increased uptake of carbon. The savanna site showed strong pulse responses to rainfall events, as is common in semi-arid and arid ecosystems (Huxman et al. 2004). The pulse response as defined by Huxman et al. (2004) is an instant carbon release following a rainfall event, due to the immediate activation of the soil microbial community, as well as displacement of the CO_2 rich soil air. This is followed by a period where increased water availability benefits vascular plants and increases net uptake of the ecosystem as soil respiration decreases as a result of the drying of the top soil (Huxman et al, 2004). The net effect of the pulse depends on the size of the pulse, and also the initial soil and canopy conditions (Williams et al. 2009).

The three precipitation pulses in the summer of 2005 did trigger large net CO_2 uptake, probably due to the fact that the events were spaced close enough in time, and presumably enough water was available in the dry-down periods for the C4 grassland to maintain its green leaf area, while respiration was reduced. Herbaceous composition from a nearby grassland site shows that the grassland in the summer of 2005 did not go fully dormant as opposed to the summer of 2006 (Kjelgaard et al. 2008). In comparison, 2006 was characterized by one long summer drought, but received ample precipitation in the fall. The summer drought was so severe that the grassland layer became fully dormant, and the ecosystem acted as a small carbon source at the end of the drought and during the following recovery period. Precipitation in September of 2006 did trigger a pulse response which was from a different magnitude than the other pulse responses, because the system acted as a continued source of carbon for 13 days after the rains on September 5th, while other pulse responses during the three years of study only showed periods of two to four days when the ecosystem acted as a carbon source after a precipitation

event. This can be explained by a larger build-up of CO_2 in the soil pore space during the extended droughts, and the needed recovery of the grassland canopy after being fully dormant during the drought period. The coincidence of the prolonged drought with optimal growing temperatures resulted in 2006 having the lowest GPP of the three years of this study.

A comparison between 2005 and 2007 shows larger gross fluxes in 2007 due to the ample water availability, but also a smaller difference between the gross fluxes, resulting in a smaller sink. Ecosystem respiration was 36% lower in 2005 compared to 2007, while gross primary productivity was only 20% lower in 2005 compared to 2007. This serves only for illustrative purposes, because the extremely wet year of 2007 should not be considered the climate norm for the ecosystem under study. The imbalance between gross primary productivity and respiration was thus greater in 2005 than 2007, resulting in a larger carbon sink in 2005.

We conclude that the differences in carbon fluxes among the three years of this study can be explained by the distribution patterns of precipitation. Both comparisons (2005-2006 and 2005-2007) rely on the idea the ecosystem respiration is more sensitive to drier periods than gross primary productivity.

4.2. CLIMATE CONTROL

4.2.1. Water availability

Based on the latitude and the annual temperature of our ecosystem, we expected water availability to have a strong control on carbon fluxes (Yi et al. 2010). We also found that ecosystem respiration was more sensitive to soil water deficits than photosynthesis. Although this has been observed in other ecosystems, this is more the exception than the rule (Schwalm et al. 2010, Anderson-Teixeira et al. 2011).

A global analysis of the sensitivity of GPP and Reco to droughts found that on average GPP is 50% more sensitive to droughts than Reco, which results in a net decline in carbon sink with droughts (Schwalm et al, 2010). Analyis of FluxNet data showed that there was a significant variation among biomes, and the analysis per biome (11) and climatic season (4), showed that in 9 of 44 cases, the reverse was true and Reco was more impacted than GPP by droughts. Those nine cases included all four seasons in woody savannas (represented by eight different tower sites), as well as summer seasons in evergreen needle forest and mixed forests (Schwalm et al, 2010). In grasslands and savanna (as opposed to 'woody savannas') this pattern was not observed, with the difference between savanna and woody savanna, having a woody cover below or over 30%. The presence of (enough) trees seems to be a critical factor in deciding where an ecosystem falls on this dividing line. In Chapter 1, we established that grasses are generally more sensitive to drought than trees, and that the presence of trees with a deeper rooting depth can render the gross primary productivity of an ecosystem less sensitive to droughts. Although the observed pattern holds for most of the 3 year period, the metric Reco/GPP did show an increase near the end of the 2006 summer drought.

4.2.2. Temperature

We expected the temperature response function of the ecosystem to give insights in the climatic control on carbon fluxes in this Central Texas savanna. The response of net ecosystem carbon exchange to temperature is often characterized by two temperatures – a minimum temperature where the system becomes a sink instead of a source, and an optimum temperature where net uptake peaks and after which the net uptake declines (Yuan et al, 2011). Net carbon exchange at our study site did not show such a clear temperature peak response curve. Instead, there is a broad temperature range (0-24°C) which is characterized by a small carbon uptake on

average (0-1.5 g C day^{-1}). The variability in NEE at any given temperature is large compared to other sites (Niu et al. 2012), but in central Texas daily average temperature is not a direct substitute for seasonality or phenology, because daily average temperatures of (e.g.) 24°C can occur in any season, meaning that a clear temperature effect associated with phenology, as seen in other ecosystems, is absent in our data. At temperatures above 24°C, the response differed between years, and the confounding factor of soil moisture became obvious, with the largest average net uptake rates in the wet year of 2007, lower average uptake in 2005, and very low average net uptake in 2006.

The wide range of temperature conditions where the ecosystem acts as carbon sink may be due to the presence of both C3 and C4 species at our site. Niu et al (2004) found that net ecosystem exchange of a C3 and a C4 grassland had optimum temperatures that differed as much as 10°C. Then again, leaf level measurements at our site (Chapter 1) indicated that the C4 grass and the C3 encroacher mesquite both had peak net uptake rates at leaf temperatures of ~32°C, while the dominant encroacher juniper had a relatively flat temperature response over the whole temperature range of leaf-level measurements [11-40°C]. Therefore, the encroaching trees are likely responsible for the broad temperature range over which the ecosystem is carbon positive.

The gross carbon fluxes show a more straightforward optimum function, with temperature optima around 26-27°C. This seems like a low temperature compared to the leaf-level data, but average daily temperature is not a direct substitute for daytime leaf temperature which ultimately controls photosynthetic uptake. We also have to caution here that the decline in GPP at temperature above the optimum is not solely due to the temperature response of photosynthesis. Days with high average daily temperature coincide with hot, dry summer days, when drought effects and stomatal closure due to low relative humidity also reduce photosynthesis (e.g. Reichstein et al. 2002).

We expected the ratio of Reco to GPP to show an increase in response to temperature - meaning that we expected respiration processes to become more important as temperatures rise (Kirschbaum 2000, Anderson-Teixeira et al. 2011). Instead, the ratio of Reco to GPP at the

encroaching site shows a weak temperature optimum around 18ºC. Although we do not expect responses to climatic drivers to be linear (Zhou et al. 2008), we did try to see whether this is possible in a modeling context. We plotted the ratio of the temperature responses of a Lloyd & Taylor soil respiration model parameterized for our site (TM4, Chapter 2, (Reichstein et al. 2003)) and the temperature response of the C3 and C4 model of photosynthesis parameterized for tree species and grass species at our site (Chapter 1, (Collatz et al. 1991, Collatz et al. 1992)).

The C3 model of photosynthesis has increasing rates of photosynthesis with temperature due to the enzymatic reactions showing an exponential increase with temperature. A high temperature stress function is then imposed to decrease C3 photosynthesis at higher temperatures. The C4 model of photosynthesis has both of these features, and in addition has a low temperature stress function which reduces modeled photosynthetic rates at low temperatures (Appendix). This function effectively reduces carboxylation rates to 50% at 15ºC and to 27% at 10ºC. The theoretical response curves of the soil respiration to photosynthesis ratio, showed a very weak optimum around 10ºC and a relative flat response up to 30ºC (Figure 13). Although our simple theoretical consideration does not match up with the ecosystem level physiological curve of Reco/GPP, neither the optimum or flat response characteristic could be obtained when only C3 or C4 photosynthesis was included. We conclude that the presence of both C3 trees and C4 grasses is responsible for the characteristic Reco/GPP temperature response.

4.3. ENCROACHMENT PROCESS

Although the variation in NEE between the three years of study can be explained by differences in precipitation distribution, the overall large size of the carbon sink is not attributable to differences in climate. Luyssaert et al. (2007) argued that on a global scale, GPP in forest ecosystem is controlled by climate, but that net ecosystem productivity (NEP) is

controlled by non-climatic conditions such as successional stage, management, site history, and site disturbance. In this context, woody encroachment is often more likened to a shift from one alternate stable state to another (Scheffer et al. 2001, Knapp et al. 2008) instead of a disturbance-succession process (e.g. Thornton et al. 2002). Regardless of the theoretical framework, the encroachment process fundamentally alters carbon storage in the ecosystem, in the form of wood, stems, deeper roots, long-lasting foliage, litter and soil organic carbon pools. Mean residence times of these 'tree' carbon pools is much longer, and as thus respiration processes have a long lag on the uptake processes. This large imbalance of GPP and Reco explains the large carbon sink we observed for this ecosystem (see Chapter 4). On longer timescales (decennia, centuries), without human or natural disturbances, encroached ecosystems will reach a new equilibrium state in the form of dense climax stand or 'cedar breaks', where respiration and photosynthesis are likely more balanced. Although we have solely focused on carbon, the woody encroachment process will have important consequences for water balance, species diversity, wildlife, rangeland productivity and other ecosystem products and services (Eldridge et al. 2011).

4.4. CLIMATE CHANGE AND WOODY ENCROACHMENT

Climate change and woody encroachment is a two-way interaction. Woody encroachment can have an impact on the climate system by increasing the terrestrial carbon sink strength (Pacala et al. 2001), while climate change also has a direct impact on terrestrial land surfaces (Friedlingstein et al. 2006), and thus on the encroachment process.

Woody encroachment is considered to be a large, although uncertain carbon sink for CO_2 from the atmosphere (0.12 ± 0.2 Pg yr^{-1} in the US, Houghton et al. (2012)), representing about 24% of the US terrestrial carbon sink (0.489 Pg yr^{-1}). The sink partly offsets the increase in CO_2 due to fossil fuel burning. Net changes in the response of an ecosystems net carbon uptake to

climatic factors, act either as a positive or negative feedback to the climate system. In this view, woody encroachment has a direct negative feedback on the climate system though the large carbon sink it represents, as well as an indirect negative feedback through the reduced sensitivity to droughts.

Regional climate change predictions for Central Texas indicate an increase in annual surface temperature of ~3.2ºC by the end of the century, with more warming in the summer than in winter (Jiang and Yang 2012). Predicted changes in precipitation tend to differ. CMIP3 simulations indicated a drying trend for the southwest of the US (Seager et al. 2007), but downscaled versions of CMIP3 indicated a small decrease in precipitation in central Texas, with decreases in winter precipitation, and a small increase in summer precipitation (Jiang and Yang 2012). CMIP5 also does not predict decreased precipitation for North America (Christensen et al. 2013). Nevertheless, the combined effect of higher temperatures, which increase evapotranspiration, and uncertain changes in precipitation, increase the risk of droughts for the 21st century (Dai 2013).

In the three years of this study, the worst future climate predictions were best represented in the year 2006. The year 2006 had the lowest carbon sink strength of the three years of the study, meaning that severe droughts do indeed create a positive feedback to the climate system. The effect of woody encroachment would be to mediate this feedback, as seen in the comparison of our site to another nearby grassland site. Where the encroaching ecosystem under study lost ~22 g C m^{-2} during the 2006 summer drought, the nearby grassland site lost 50-60 g C m^{-2} during this same drought period (Kjelgaard et al. 2008).

Climate change can also have a direct impact on the encroachment process. The competitive advantage of C4 grasses at higher temperatures will likely be reduced under higher atmospheric CO_2 concentrations and a drier climate, indicating further progression of woody encroachment. If temperatures, vapor pressure deficits, and summer droughts further increase, tree mortality might adversely affect woody encroachment (Williams et al. 2013). After the conclusion of our study, a historic drought in 2011 resulted in the mortality of 100-500 million

trees over Texas, with observed mortality rates of 6% for Ashe juniper at a nearby site (Kukowski et al. 2013). If we consider the fate of encroached areas under extreme climatic events, such as a prolonged intense drought, encroached areas might see a reversal back to the original state ('grassland'). In this scenario, the notion "Slow in, Rapid out"- used to describe slow carbon accumulation during succession, followed by a quick release after disturbance - would apply and would constitute a large positive feedback to the climate system.

5. Conclusion

We showed that an encroaching central Texas savanna site acted as an important carbon sink during the three years of study, with an average sink size of 405 g C m^{-2} yr^{-1}. The ecosystem level carbon fluxes showed strong responses to precipitation pulses, which were superimposed on the seasonal temperature trend. The ecosystem had a year-long growing season due to the encroaching trees, which virtually made the ecosystem a year-long carbon sink.

We studied net (NEE) and gross carbon fluxes (GPP and Reco), as well as their ratio (Reco/GPP) in function of two climatic drivers – temperature and soil water content. Ecosystem respiration proved to be more sensitive to decreases in soil water content than gross primary productivity. Since it was shown that tree photosynthesis was less impacted by soil water deficits than photosynthesis by grasses, we ascribed this lower sensitivity of GPP to water deficits, to the presence of trees. The broad temperature range over which the ecosystem was carbon positive was also attributed to the presence of the trees. Overall, we found that the encroachment process resulted in important changes in ecosystem characteristics in relation to climatic drivers, and an important carbon sink.

6. Figures

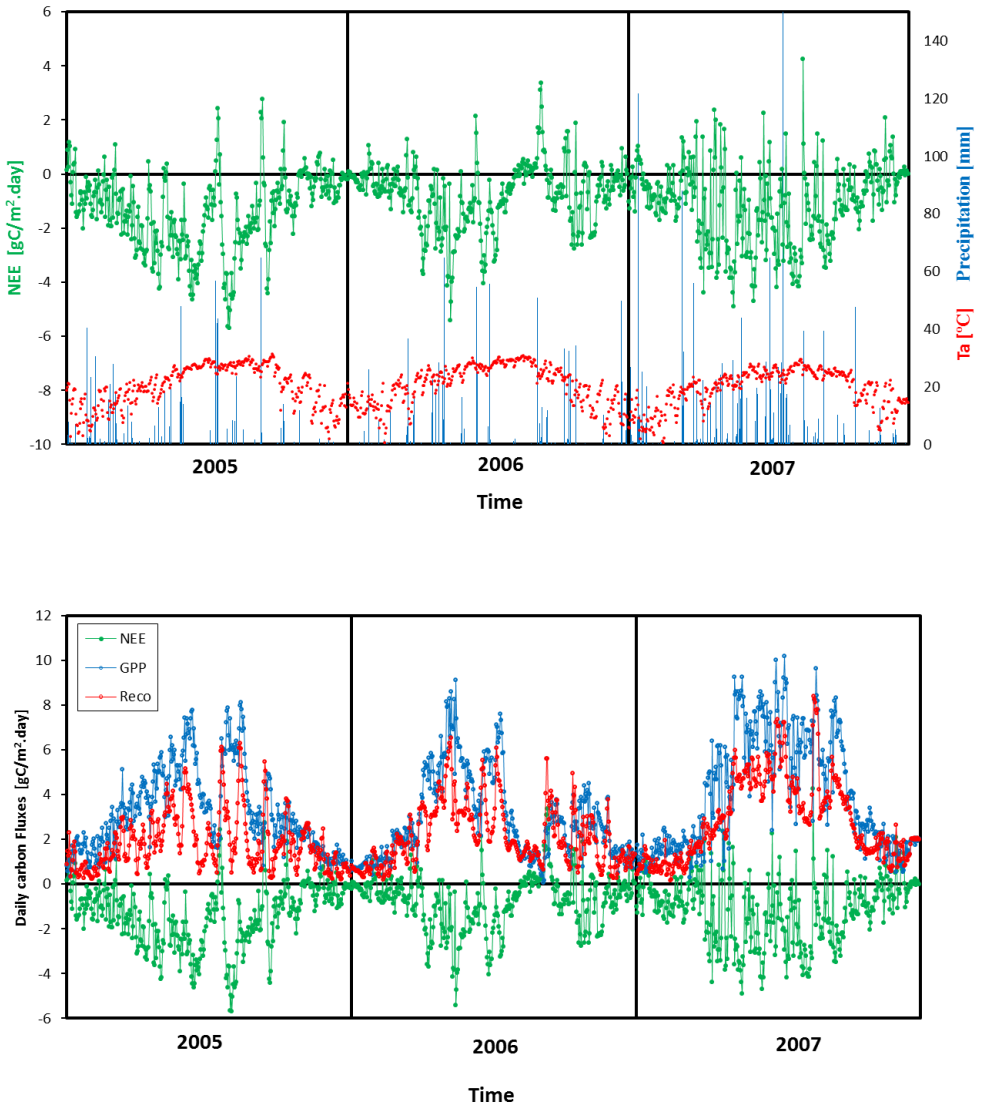

Figure 3.1: (a) Daily values of average temperature, precipitation and net carbon fluxes (NEE) during the three years of study. (b) Daily net and gross carbon fluxes – NEE is partitioned into gross primary productivity (GPP) and ecosystem respiration, according to the algorithm of Lasslop et al (2010).

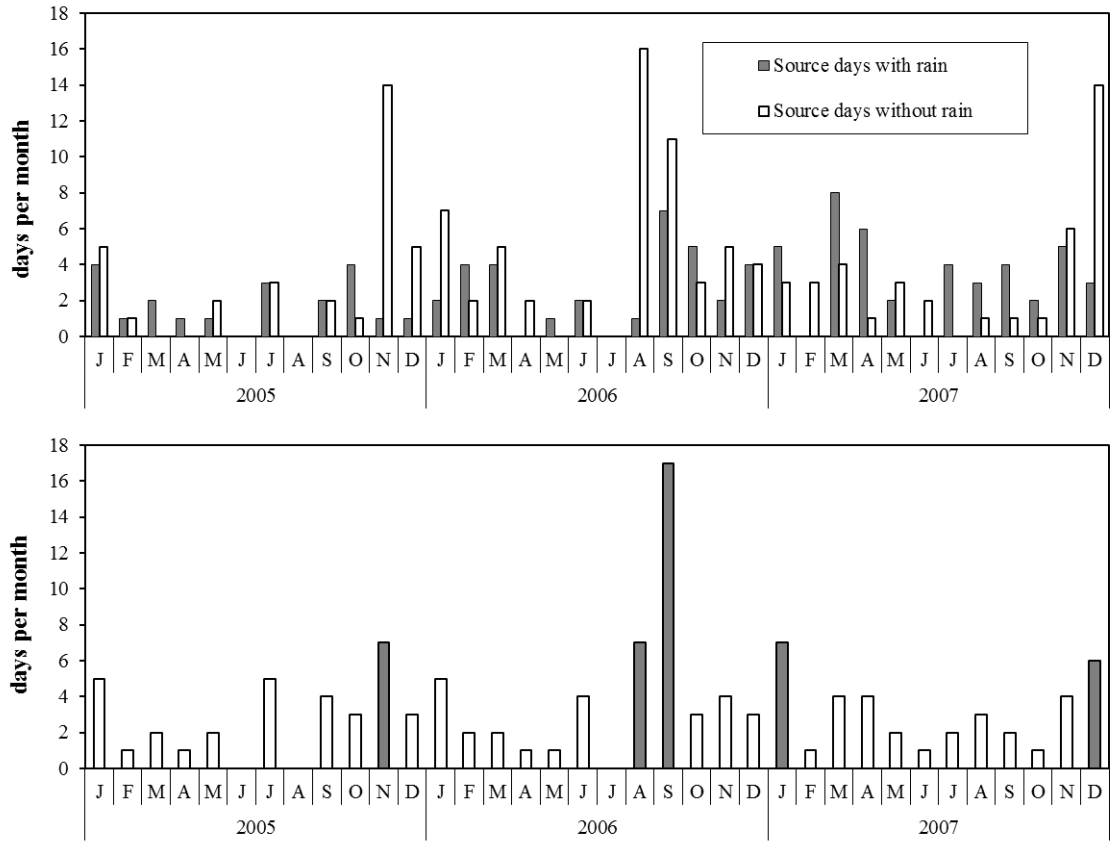

Figure 3.2: Carbon source days: (a) Monthly number of source days with and without precipitation; (b) Number of consecutive source days per month.

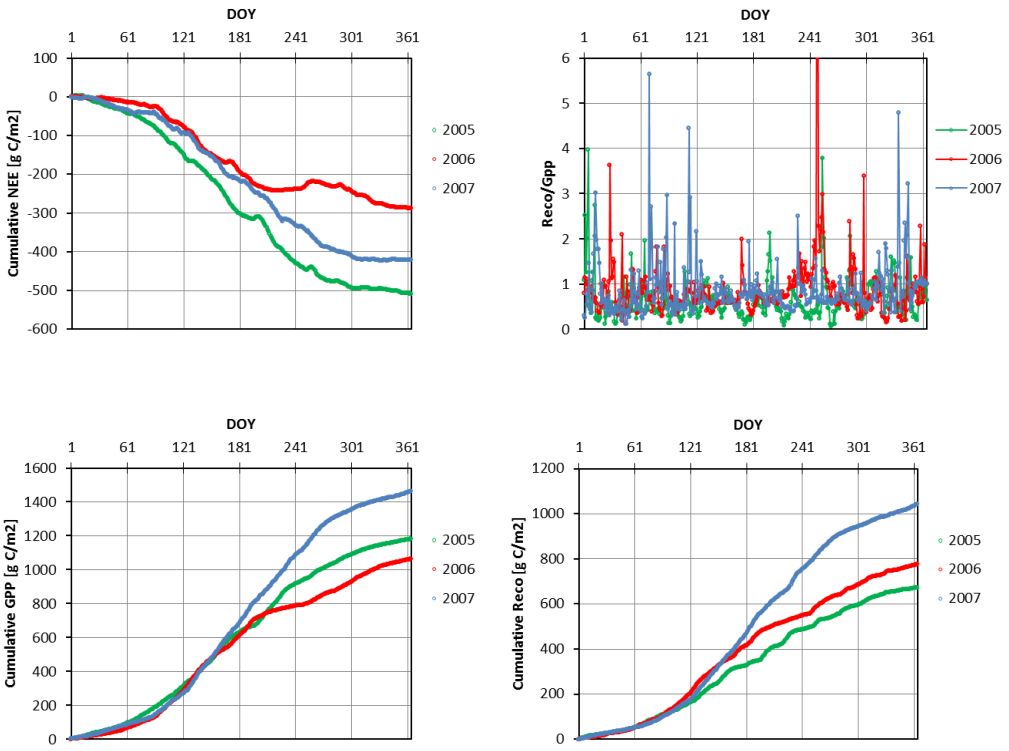

Figure 3.3: Cumulative net and gross carbon fluxes, as well as the ratio Reco/GPP for the three years of the study.

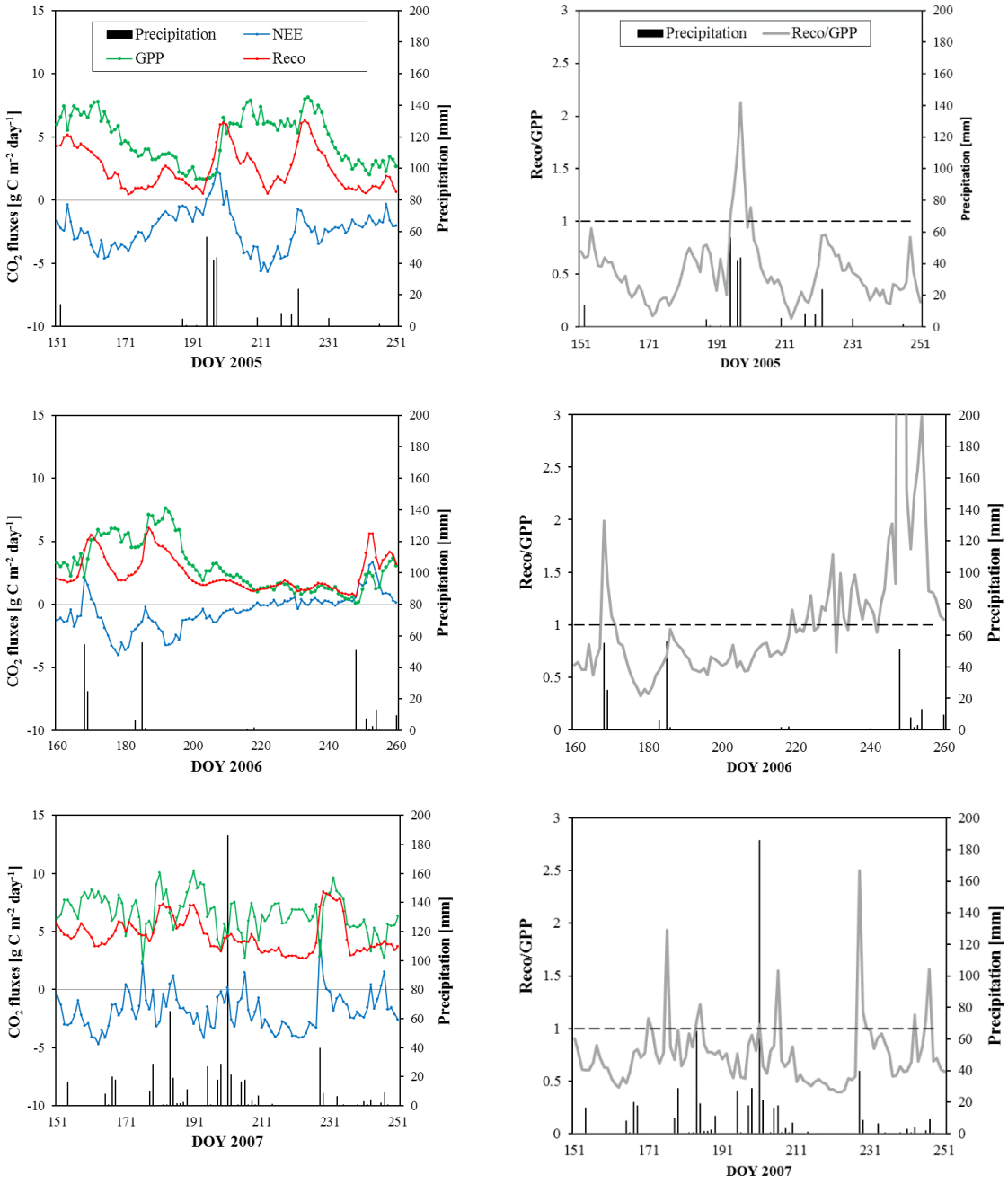

Figure 3.4: Detailed view of net and gross carbon fluxes, and precipitation distribution, during 100-day periods in the summer of 2005, 2006 and 2007. In the left column the net and gross fluxes are portrayed. In the right column, the ratio of Reco to GPP is given.

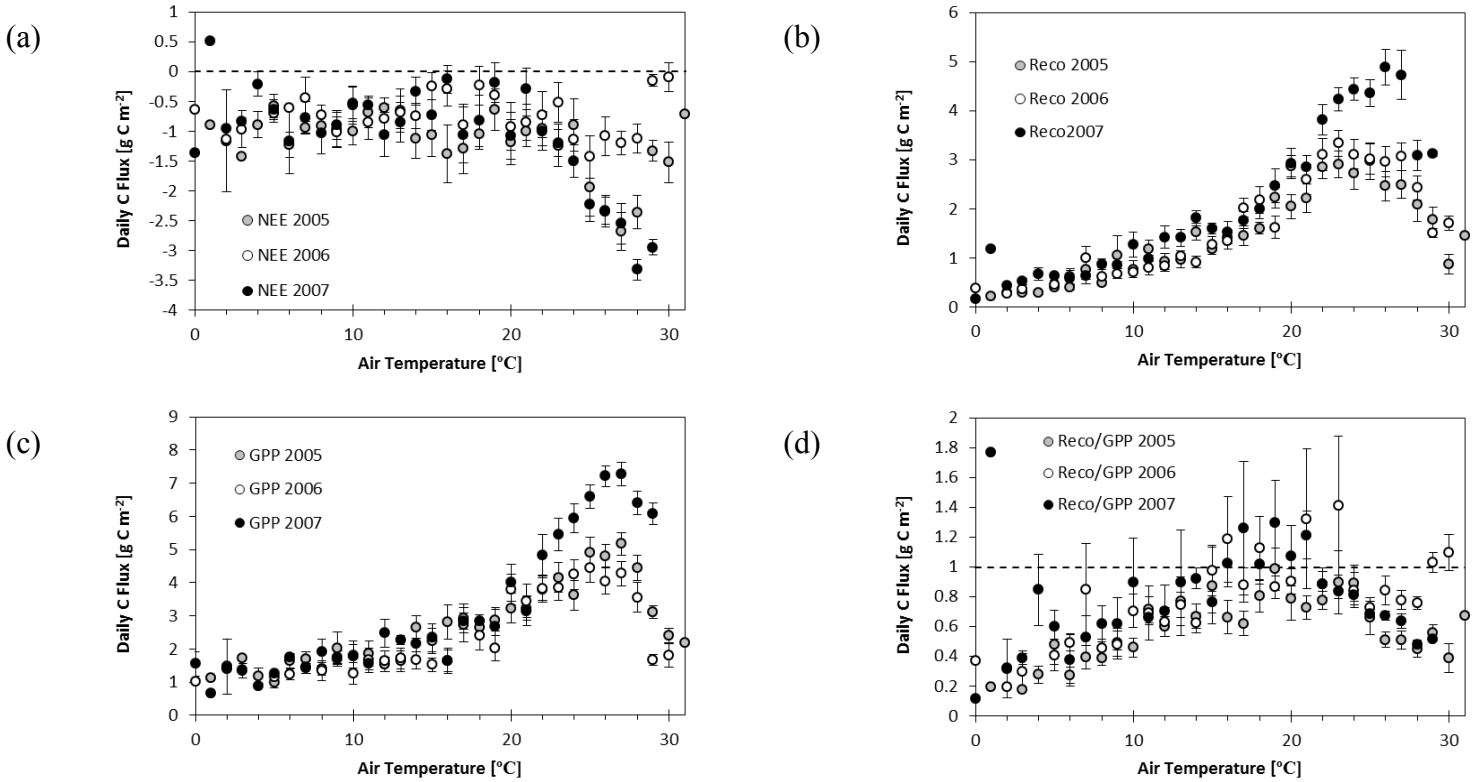

Figure 3.5: Average daily carbon fluxes in function of average daily temperature. Days were binned in 1ºC temperature increments and averages per bin are displayed. (a) Net Ecosystem Exchange; (b) Ecosystem Respiration; (c) Gross Primary Productivity; (d) the ratio Reco/GPP

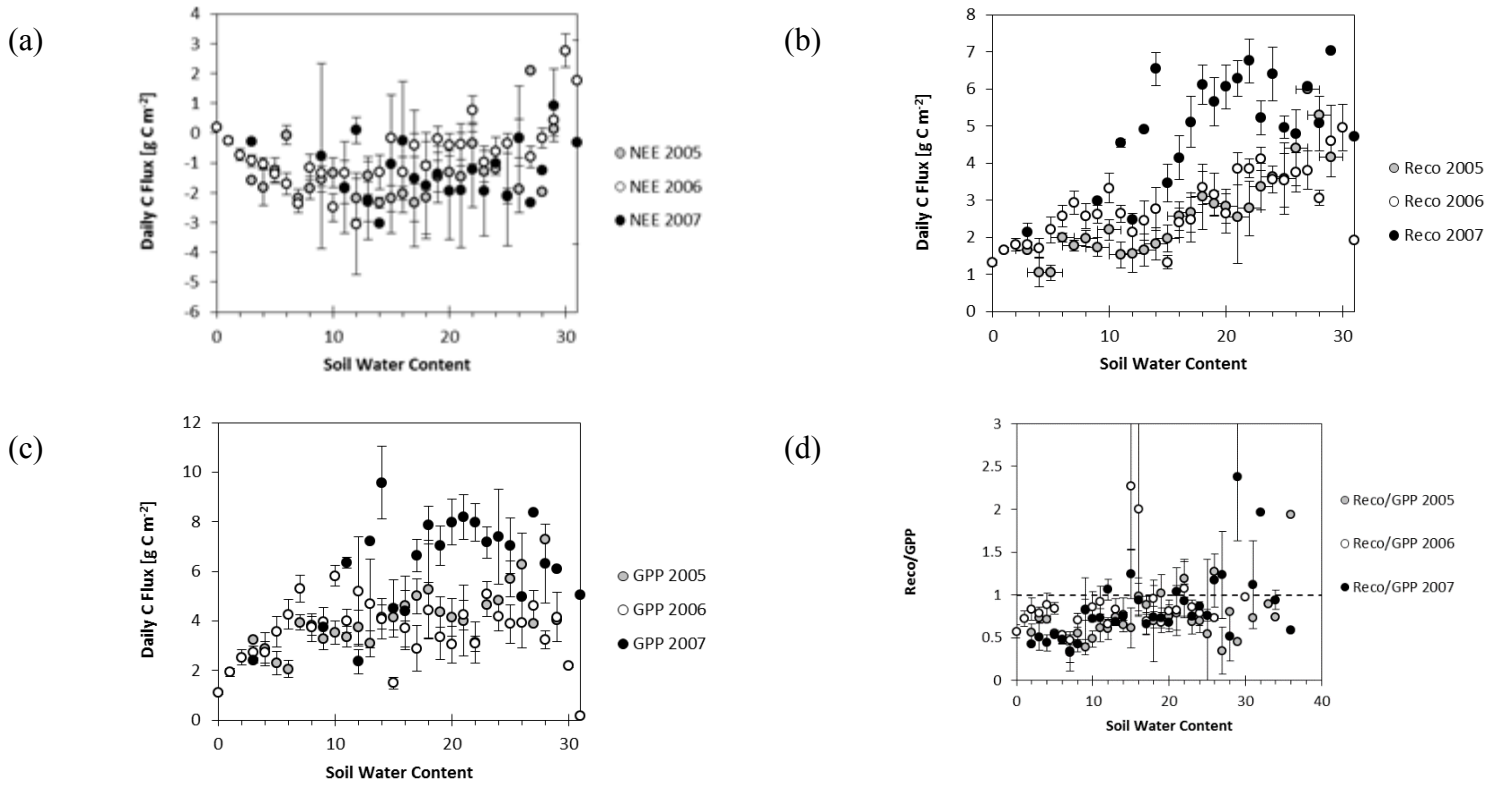

Figure 3.6: Average daily carbon fluxes in function of soil water content. Days were binned in 1 % soil water content increments and averages per bin are displayed. (a) Net Ecosystem Exchange; (b) Ecosystem Respiration; (c) Gross Primary Productivity; (d) the ratio Reco/GPP. To reduce noise, only days with average temperatures above 18°C were used for Figure 6 a-b-c. In Figure 6d, no data was excluded based on temperature.

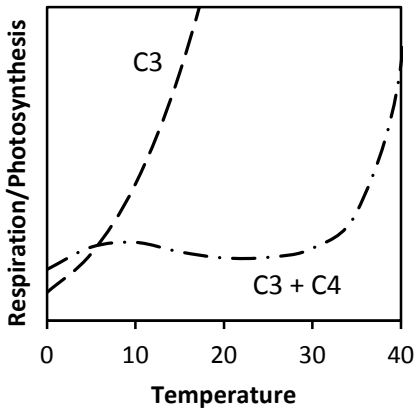

Figure 3.7: Theoretical temperature response of the ratio of soil respiration to photosynthesis. The temperature response of respiration was modeled as a Lloyd & Taylor function (model TM4, Chapter 2). The temperature response of photosynthesis was modeled using Collatz et al. (1991, 1992) for C3 and C4 photosynthesis. To exaggerate differences, photosynthesis was set 4x as high as respiration.

7. Tables

Table 3.1: Annual sums of precipitation and ecosystem level carbon fluxes.

	Units	2005	2006	2007
Precipitation	**[mm]**	738	815	1514
NEP	**[g C m^{-2} $year^{-1}$]**	-508	-287	-420
GPP	**[g C m^{-2} $year^{-1}$]**	1180	1063	1463
Reco	**[g C m^{-2} $year^{-1}$]**	672	776	1042
Reco/GPP	**[-]**	0.569	0.730	0.712

CHAPTER 4: BIOTIC CONTROLS ON CARBON EXCHANGE PROCESSES IN AN ENCROACHING SAVANNA IN CENTRAL TEXAS

Abstract

Woody plant encroachment in grassland and savanna ecosystems is a global phenomenon. The change in biogeochemical characteristics of the ecosystem accompanying this shift in vegetation structure are manifold, and the net consequences for the carbon balance cannot be generalized over climate, soil or encroaching species. To come to a process-based understanding of the carbon dynamics in a Central Texas encroaching savanna, we analyzed patterns of carbon exchange during three years of contrasting water availability. We hypothesized that the overall imbalance between carbon uptake and release (photosynthesis and respiration) we observed was due primarily to the increased photosynthetic uptake of encroaching woody species. We scaled species-specific models of photosynthesis, to estimate contributions of two encroaching tree species, as well as the dominant C4 grassland species, to ecosystem level gross primary productivity (tower-based GPP). We also scaled cover-specific models of soil respiration to estimate tree/grass contributions of soil respiration to ecosystem respiration (tower-based Reco). We further made direct comparisons of chamber-based soil respiration and grassland NEE to tower-based instantaneous ecosystem respiration (Reco) and net ecosystem exchange (NEE).

We found that the ecosystem as a whole was a significant carbon sink of -405 g C m^{-2} yr^{-1} on average. The encroaching trees increased canopy photosynthesis by 180% and decreased soil respiration by 14%, compared to the C4 grassland, resulting in a strong carbon sink due to the encroachment process. As expected, the changes in carbon uptake were more important than changes in carbon loss, but both processes contributed to the significant carbon sink strength of this ecosystem. The encroaching process also altered the ecosystem carbon dynamics in relation to climatic drivers. Ashe juniper was largely responsible for ecosystem GPP during the winter months (December-February) and allowed the ecosystem to remain a small carbon sink during this period, effectively lengthening the growing season and widening the temperature range over which the ecosystem acts as a carbon sink. Encroaching trees were also found to be more drought resistant, reducing the ecosystems sensitivity to droughts.

We conclude that woody encroachment acts as an important carbon sink primarily by increasing the carbon inputs in the ecosystem. Woody encroachment also reduces the sensitivity of GPP to climatic drivers. These two effects constitute a direct effect, as well as negative feedback to the coupled carbon-climate system.

1. Introduction

Atmospheric CO_2 has increased from 278 ppm in pre-industrial times to an average annual value of 396 ppm in 2013 (NOAA, Mauna Loa) resulting from anthropogenic activities such as fossil fuel burning and changes in land use and cover (Le Quéré et al. 2014). In 2014, monthly means exceeded the threshold of 400 ppm for three consecutive months (April – June) for the first time in human history. The increase in atmospheric CO_2 is partly counterbalanced by natural processes – uptake in oceans, vegetation, and soils (Le Quéré et al. 2014). These processes are themselves subject to climate change, effectively creating a coupling between the global carbon cycle and the climate system.

Globally, savannas are a classic example of an ecosystem undergoing structural and functional change, in this case resulting from woody encroachment, with possible large, but uncertain contributions to the overall terrestrial carbon sink (Houghton et al. 1999, Pacala et al. 2001). Savannas comprise 18% of the terrestrial land surface worldwide and are responsible for 29% of the global net primary productivity of the terrestrial biosphere (Grace et al. 2006). In the US, the estimated carbon sink associated with woody encroachment is 0.1 Pg C yr^{-1} (~20% total land sink) and the associated error is 0.2 Pg C yr^{-1} (Houghton et al. 2012). This makes it the largest unknown in the US carbon balance and one of the key uncertainties that demands a more detailed understanding of how woody encroachment impacts carbon cycling (King et al. 2007).

The uncertainty associated with woody encroachment stems from three different sources. First, it is not clear how widespread woody encroachment is. Second, the possible carbon sink due to woody encroachment can be reversed by human and natural disturbance processes that cause tree mortality, such as land management, fire, and severe

droughts. The third uncertainty is related to whether or not woody encroachment constitutes a carbon sink to begin with, as increases in aboveground biomass might be offset by decreases in belowground carbon pools, especially at sites with high mean annual precipitation (Jackson et al. 2002). Over large environmental gradients, it has been shown that woody encroachment can drastically increase carbon uptake processes (Knapp et al. 2008b) with the observed increases in aboveground production related to mean annual precipitation (Barger et al. 2011). Changes in soil organic carbon pools, on the other hand, have not been found to be directly dependent on MAP, but more related to clay content and bulk density of the soil (Barger et al. 2011).

Here, we examined how woody encroachment by two different tree species affected carbon fluxes in a central Texas savanna ecosystem. Based on the MAP of the region, and soils high in clay content, we expect central Texas savannas to be an important woody encroachment carbon sink. Luyssaert et al. (2007) found that on a global scale, gross carbon fluxes are controlled by climatic drivers, but that net ecosystem productivity (NEP) might be controlled by non-climatic conditions such as successional stage, management, site history, and site disturbance. In this context, woody encroachment is often more likened to a shift from one alternate stable state to another (Scheffer et al. 2001, Knapp et al. 2008a) instead of a disturbance-succession process (Thornton et al. 2002). Regardless of the theoretical framework, the encroachment process can fundamentally alter carbon storage in the ecosystem, in the form of wood, stems, deeper roots, long-lasting foliage, litter and soil organic carbon pools. Mean residence times of these 'tree' carbon pools is much longer, and as thus respiration processes have a long lag on the uptake processes. We therefore hypothesize that the encroachment process causes a large imbalance of carbon uptake and carbon release processes for the tree component of an encroaching savanna.

Our first objective was to examine how the structural make-up of a savanna controls canopy photosynthesis and respiration. We predicted that trees have a significantly higher carbon uptake potential, through time-integrated and spatially integrated photosynthetic carbon fluxes, and that this change in carbon uptake largely outweighs changes in respiration processes, rendering this ecosystem an important carbon sink. Our second objective was to examine how the shift from grassland to trees alters the climatic sensitivities of the ecosystem. Trees have longer growing seasons and are less prone to droughts, altering the relationship between gross carbon fluxes and climatic drivers.

To address our first objective, we assessed the structural make-up of the site, and scaled models of photosynthesis and soil respiration to construct cover-specific carbon balances and assessed contributions of different cover types to the overall ecosystem carbon fluxes. We also directly measured grassland net ecosystem exchange, assessed possible tree-grass interactions, and compared direct measurements of grassland NEE to tower-based NEE fluxes. By doing this scaling exercise over time, we inferred changes in the climate sensitivity of carbon dynamics for this site.

2. Methods

2.1. SITE DESCRIPTION

This research took place on Freeman Ranch, a 4200 ha research area, owned by Texas State University, located on the eastern Edwards Plateau in Central Texas. The Edwards Plateau is a 93,000 km^2 distinct region in south and west central Texas that supports a diversity of plant and animal species, including a number of endemic and endangered species. Historically, much of the Edwards Plateau was vegetated by

grassland or open savanna dominated by prairie grasses and isolated live oaks (*Quercus virginiana*).

Chronic overgrazing by livestock after European settlement resulted in replacement of palatable tall and midgrasses by more grazing resistant shortgrasses, and fire suppression increased populations of unpalatable woody species, predominantly Ashe juniper (*Juniperus ashei*) (Van Auken 2000). A second encroaching species at our study site is Honey mesquite *(Prosopis glandulosa)*, a common encroacher in other parts of Texas, while its distribution on the Edwards Plateau is restricted to the deeper soils of the plateau (Eggemeyer and Schwinning 2009).

The climate of the site is characterized as semi-arid, with cool winters and hot summers. The mean annual temperature is 19.6ºC and the mean annual precipitation is 913.3 mm. However, Texas savannas are subject to highly variable seasonal and annual precipitation regimes. Precipitation is largely bimodal with most of the rainfall occurring in the spring and fall, yet the variability remains high especially in the summer months (National Climate Data Center).

2.2. VEGETATION

Most of Freeman Ranch is occupied by upland habitats, which consist of savanna parkland of Plateau Live Oak (*Quercus virginiana var. fusiformis*) - Ashe juniper (*Juniperus ashei*) clusters interspersed in perennial grasslands. Our study site is a former grassland, experiencing woody encroachment by Ashe juniper and Honey mesquite that first appeared in aerial photos 25 years earlier. The grassland diversity is suppressed by

the invasive species King Ranch bluestem (*Bothriochloa ischaemum*). The two encroaching species at the site are physiologically very different and categorized as a drought tolerating conifer and a deciduous drought avoiding phreatophyte (Chapter 1).

To calculate percent tree cover and the fraction of grassland area in direct proximity of tree cover (1m buffer), we used high-resolution airborne LiDAR (Light detection And Ranging) characterization of Freeman Ranch (Center for Space Research, UT Austin). Further field ground truthing allowed us to estimate the cover of both encroaching species.

An allometric relationship for Ashe juniper (Hicks and Dugas 1998) was checked against juniper trees at our site, and was used to calculate LAI for Ashe juniper based on tree height and tree cover. Honey mesquite's LAI was determined using destructive sampling, following a protocol outlined by Ansley et al (1998). A seasonal function was applied to the site-wide LAI for Honey Mesquite, based on observed changes in mesquite phenology at the site.

The grassland biomass was clipped in nine $0.25m^2$ plots, concurrent with chamber based NEE measurements. Biomass was separated into live and dead, C3, C4 and forb fractions to capture phenological cycles in the composition of the herbaceous layer. Biomass was dried and weighed. Specific leaf area and leaf-stem ratio was determined for the different species and green and total LAI was calculated.

2.3. TOWER-BASED CARBON FLUXES

Net ecosystem exchange of carbon (NEE) was measured for a period of three years, 2005-2007, using open-path eddy covariance techniques following standard AmeriFlux guidelines. For a detailed description of instrumentation at the site, see Litvak et al (2011). Supporting measurements included air temperature, relative humidity, net radiation, up and down welling global irradiance, and up and down welling photosynthetic photon flux density. Soil moisture, soil temperature and soil heat flux were measured at different depths in three locations: in open grassland, under juniper canopy and under mesquite canopy. Gaps in meteorological data and turbulent fluxes were filled using on-line tools from the Max Planck Institute of Biogeochemistry (Reichstein et al. 2005). Net ecosystem exchange of carbon (NEE) was partitioned into gross primary productivity (GPP) and ecosystem respiration (Reco), by fitting hyperbolic light response curves with a respiration term, to daytime NEE data and accounting for the temperature sensitivity of ecosystem respiration and the vapor pressure deficit limitation of photosynthesis (Lasslop et al. 2010). The daily integral of net and gross carbon fluxes was calculated on a daily time-step.

2.4. SMALL SCALE MEASUREMENTS

Grassland NEE and soil respiration were measured monthly during 2006-2007, using a portable 75-cm diameter chamber connected to the LI-6400 photosynthesis system reconfigured as a closed path system (Li-6400, Li-Cor, Inc., Lincoln, NE, USA). To investigate possible tree-grass interactions, NEE chamber bases were placed in open grassland, on the north side and on the south side of juniper clusters. Two fans were

installed in the chamber to provide adequate mixing of the air. NEE was calculated from the change in CO_2 inside the chamber during a 10 second time span. Air temperature, relative humidity and PAR were measured concurrently. Immediately following the NEE measurement, soil respiration and soil temperature were measured in the same plot, and soil moisture content was determined gravimetrically in the lab. All NEE measurements were taken in full sun between 10 AM and 2 PM local time. SAS software (SAS Institute, Cary, NC, USA) PROC MIXED was used to evaluate differences in measured grassland NEE, soil respiration, soil moisture, soil temperature and PAR between the different grassland locations (open, north of trees, south of trees). Least square means were used for the pairwise comparison of the different variables between the grassland locations per time period.

Other small-scale gas exchange measurements, including leaf-level photosynthesis measurements (2006-2007) and soil respiration measurements under different vegetation types (2005-2006) were made and data is reported elsewhere (Chapter 1 & 2). The C3 and C4 biochemical models of photosynthesis and the Ball-Berry model of stomatal conductance were parameterized based on leaf-level measurements for three dominant species at the site. Drought response was incorporated into the models by including a species specific dependence of Rubisco activity on soil moisture content (Chapter 1). For scaling of soil respiration, a model with a Lloyd & Taylor temperature dependence, and a linear dependence on soil water content, was parameterized for the different vegetation covers (model TM4, Chapter 2), (Reichstein et al. 2003) and scaled in time.

2.5. SCALING APPROACH

Two approaches were used: (1) direct measurements of chamber-based grassland NEE and soil respiration were directly compared to ecosystem level fluxes, and (2) models of photosynthesis (2006-2007) and respiration (2005-2006) were scaled to the ecosystem level.

Coupled conductance-photosynthesis models of C3 and C4 photosynthesis (Collatz et al. 1991, Collatz et al. 1992) were used to calculate net photosynthesis values for the three dominant species at the site for each half hour period of 2006-2007. The following meteorological data from the EC tower were used as inputs: air temperature, relative humidity, photosynthetic active radiation (PAR), CO_2 concentration and soil water content. An energy balance approach was attempted to estimate leaf temperature, but proved unsuccessful, therefore air temperature was substituted for leaf temperature. Physiological parameters for the photosynthesis models were estimated in Chapter 1. A linear dependence of maximum carboxylation rate ($V_{c,max}$) activity on soil water content <15%, was used for all three species (Chapter 1, model C), although this meant a constant value for mesquite (Chapter 1).

Leaf level photosynthesis was scaled to the canopy level using a big leaf approach (Sellers et al. 1992, Sellers et al. 1996a, Sellers et al. 1996b), in which leaf level photosynthesis is multiplied by a canopy PAR use parameter, Π, to estimate canopy photosynthesis:

$$A_{canopy} = A_{leaf} . \Pi$$

$$\Pi = \frac{V\ N\left(1 - \ exp(-k\ L_T/N)\right)}{k}$$

In the equation of the PAR use parameter, the numerator represents the fraction of PAR absorbed by the green canopy and the denominator k is the mean radiation weighted extinction coefficient. Lt is the total LAI, and V is the greenness fraction. N is a clumping factor which allows for more beam penetration into the canopy due to the clumping of leaves. The mean radiation weighted extinction coefficient k, was calculated for each day per species, assuming a spherical leaf angle distribution (Campbell and Norman 1998), and was based on zenith angle of the sun, PAR data and leaf optical properties. Optical properties from Sellers et al. (1996a) for needleleaf evergreen trees, deciduous broadleaf trees and grassland were used for Ashe juniper, Honey mesquite and King Ranch bluestem, respectively. Green fraction of the trees was assumed to be one. Green fraction of the grassland varied according to grassland composition analysis. The clumping factors used were from a globally derived dataset of clumping factors for different vegetation types, and were set to 1/0.78, 1/0.62 and 1/0.74 respectively for Ashe juniper, Honey mesquite and King Ranch bluestem (Chen et al. 2005). Larger clumping factors here mean more clumping and more light penetration through the canopy. A sensitivity analysis of the PAR use parameter (Π) to LAI, clumping factor and greenness fraction was performed. The scaling was performed for the three vegetation covers separately, and area averaged, making the assumption that there was no shading influence from the trees on grassland canopy photosynthesis (see discussion). Gapfilling of the

modeled canopy photosynthesis was done for 10% of the data, due to missing PAR data and the inability of the photosynthesis model to produce reasonable photosynthetic rates. When less than 50% of data per day was missing, half hourly rates were gapfilled based on a relation between zenith angle and modeled rates in a 3-day moving window. When more than 50% of daily data was missing, half hourly rates were not gapfilled, but daily sums were taken as the average of adjoining days.

2.6. OVERVIEW OF MEASURED AND MODELED DATA – SOME CONSIDERATIONS

Photosynthetic models were parameterized based on leaf-level measurements in 2006-2007 (Chapter 1). Soil respiration models were parameterized based on measured soil respiration rates in 2005-2006 (Chapter 2). Tower fluxes were measured from 2005-2007 (Chapter 3). Chamber-based NEE measurements, as well as measurements of grassland composition and phenology, were made in 2006-2007 (this chapter).

In 2007, soil respiration measurements were made in the grassland patches, concurrent with the chamber-based NEE measurements. However, the previously parameterized soil respiration models severely underestimated the 2007 soil respiration rates, probably due to the overall wetness of the ecosystem in 2007. For this reason, we did not extend the scaling of soil respiration to 2007 and strongly caution against the use of the parameterized soil respiration model outside the soil moisture range for which it was parameterized.

The scaling procedure for the photosynthesis model relies on structural vegetation data. Due to the lack of grassland structural data in 2005, we did not scale the photosynthesis models for 2005. We used scaled photosynthetic uptake, to estimate contributions of species to overall canopy photosynthesis, and scaled respiration

measurements to estimate contributions to overall soil respiration, to construct (incomplete) carbon balances per species/cover type.

3. Results

3.1. CLIMATE

In 2005, 2006, and 2007, the mean annual air temperatures were, respectively, 20.0, 20.7 and 19.1 ºC. The precipitation amounts in 2005 and 2006 were 738 and 815 mm respectively, 19 and 10% below the average. In contrast, the following year 2007, was extremely wet with 1514 mm of precipitation, 65% above the average. Details are given in Chapter 3.

3.2. VEGETATION

There was 50% tree cover in an 80-m radius around the AmeriFlux tower based on available LiDAR data. Fractional cover of juniper and mesquite trees were estimated as 0.38 and 0.12, respectively. Plot-based LAI was on average 2.44 and 1.29 for juniper and mesquite, respectively. Grassland LAI was determined monthly during 2006-2007 and plot-level green LAI varied from 0 in winter to a maximum of 1.12 during the summer of 2007 (Figure 1b). The summer drought of 2006 reduced the green C4 grass LAI to near zero.

3.3. COMPARISON OF INSTANTANEOUS FLUX RATES

3.3.1. Chamber-based grassland NEE and tower-based ecosystem NEE

Chamber-based instantaneous grassland NEE fluxes ranged from +1.95 µmol CO_2 m^{-2} s^{-1} to -8.95 µmol CO_2 m^{-2} s^{-1} over the two years of chamber-based measurements (Figure 2). The average instantaneous tower-based NEE at the same times ranged from -1.16 µmol CO_2 m^{-2} s^{-1} to -17.3 µmol CO_2 m^{-2} s^{-1} (Figure 2), while the daily integral of tower-based NEE on days of measurement ranged from +0.49 g C m^{-2} day^{-1} to -3.031 g C m^{-2} day^{-1} (data not shown). Net uptake rates in open grassland patches were highest in the spring of 2006 and 2007, as well as in the summer of 2007. Although direct comparison between chamber-based fluxes and tower-based fluxes are not straightforward due to comparison of different scales (Vourlitis et al. 1993, Norman et al. 1997), the 2-3 times larger net fluxes at the ecosystem level, hint that the tree-component of the ecosystem was accumulating carbon at a much faster pace. Based on fractional cover and differences in flux magnitude, we estimated that the tree component of the ecosystem was accumulating carbon at rates ranging from -3 to -30 µmol CO_2 m^{-2} s^{-1} during times of NEE-chamber measurement (Figure 3). Our scaling analysis, reported in the next section, showed that maximum instantaneous net photosynthetic rates for the tree canopies was -31 µmol CO_2 m^{-2} s^{-1} and -33 µmol CO_2 m^{-2} s^{-1} for Ashe juniper and Honey mesquite respectively, while it was -25 µmol CO_2 m^{-2} s^{-1} for the grassland canopy.

Chamber-based open grassland NEE and tower-based ecosystem NEE fluxes showed an opposite sign during three measurement periods (Jan 06, Aug 06, Sep 06), and very low net uptake at other times (Figure 2), suggesting that at these times the grassland

was carbon neutral or losing carbon to the atmosphere while the savanna as a whole was accumulating carbon. Note that positive instantaneous rates can be interpreted as times when the grassland acted as a source of carbon to the atmosphere. Negative instantaneous flux rates do not directly convey that the system was acting as a carbon sink, because chamber-based measurements were only made between 10 AM and 2PM, when uptake rates are usually highest of the day. An integration over time is needed to qualify as a carbon source or sink on a daily basis. Inspection of the daily integrals showed that during two of these periods the savanna as a whole also acted as a carbon source (Jan 06 and Aug 06), a winter period and a long drought period. In September 2006, the grassland and ecosystem did indeed show an opposite sign in NEE. The grassland was still recovering from the prolonged drought, and was still acting as a carbon source, while the system as a whole was already accumulating carbon again.

Comparison of chamber-based NEE from different grassland areas showed only significant differences between open grass and north side of the juniper during time periods with overall high uptake rates (May-June 2006, May & Sep 2007). An analysis of grassland soil respiration, soil temperature, soil moisture and PAR level inside the chamber showed that PAR was the only explaining variable that significantly differed between open grassland and 'north of tree' patches at these times, and is likely the main reason for NEE to be higher (less uptake) in grassland patches north of tree clusters (data not shown).

3.3.2. Chamber-based soil respiration and tower-based ecosystem respiration

Instantaneous chamber-based measurements of soil respiration, averaged according to cover type, ranged from 0.42 to 5.1 µmol CO_2 m^{-2} s^{-1} in the period 2005-2006 (Chapter 2). Instantaneous soil respiration rates showed a very similar seasonal pattern as instantaneous ecosystem respiration (Figure 4). Area-averaged instantaneous soil respiration sometimes exceeded ecosystem respiration rates during measurement periods in some of the cooler months (Figure 4). While soil respiration is thought be the most important contributor to ecosystem respiration, it is not the only component of ecosystem respiration. This inconsistency is likely due to the problem of directly comparing two very different scales – soil respiration is measured at a scale of ~100 cm^2, while ecosystem respiration is measured at the scale of ~1 ha, a scale difference of six orders of magnitude.

3.4. SCALING APPROACH

3.4.1. Scaling models of photosynthesis

Modeled canopy net photosynthesis explained 62% of the variation in daily tower-based GPP (Figure 5a). It is important to note here that no attempts were made to 'fit' or 'tweak' the model to observed GPP fluxes, and the model was solely based on (1) the parameterized photosynthesis models from physiological work for species at our site (Chapter 1); (2) climatic variables measured at the site; and (3) vegetation structural data, as described earlier.

The modeled canopy photosynthesis rates overestimated annual GPP in 2006 (1186 vs 1063 g C m^{-2}) and underestimated annual GPP in 2007 (1215 vs 1463 g C m^{-2}, Table 1). The seasonality of tower-based GPP was well represented, but some seasonal

characteristics were not captured by the model. In particular, modeled rates did not reflect the severity of drought and recovery period of 2006 (Figure 6), when modeled canopy photosynthesis overestimated GPP; and the late summer of 2007, when modeled canopy photosynthesis underestimated GPP. These three summer months (Aug '06, Aug '07 and Sep '07) accounted for 38% of the error in the 24 month timespan.

The C4 grassland, which covers 50% of the study site, was responsible for 26% of net photosynthetic uptake over the two year period, with lower values in 2006 than 2007, respectively 1186 and 1251 g C m^{-2} yr^{-1} on a grass cover basis (see Table 1 for values on ecosystem m^2 basis and cover type m^2 basis, respectively). According to the model, the C4 grassland contributes up to 45% of the net photosynthesis during favorable conditions in the summer of 2007, but had minimal contributions during the 2006 summer drought (15% in August 2006,) and winter months (down to <3%, Figure 7b).

In reality, the C4 grassland was completely dormant on August 24th, 2006, based on personal observations and NEE chamber measurements. In the modeled estimates, grassland canopy photosynthesis was not reduced to zero, likely due to two reasons. First, the dependence of maximum carboxylation rate on soil water content greatly reduced $V_{c,max}$, but not to zero (Chapter 1, regression model C). Second, the C4 grassland LAI had a direct effect on the scaling factor, and might be responsible for errors. The grassland LAI values were linearly interpolated between measurement dates, and therefore might not represent the dynamics of the grassland cover in the best way. Consider for instance the summer period of 2006. Site-wide grassland green LAI was measured as 0.63, 0.01 and 0.15 on respectively July 18th, August 24th and October 26th of 2006. The grassland

was however already stressed on July 18th, based on the NEE chamber measurements, and might have gone dormant soon afterward, until it recovered after the rain storm on September 5th. The linear interpolation likely overestimated the green grassland LAI and grassland canopy photosynthesis during the summer drought of 2006. Conversely, the modeled values of grass canopy photosynthesis showed an abrupt decline in the late summer of 2007, due to a sharp decline in green grassland LAI between August 23rd and September 19th, 2007. In this case, the interpolated LAI and grass canopy net photosynthesis might have been too low, and the grassland probably stayed active and relatively green to at least half September, 2007.

The encroaching Ashe juniper, which covers 38% of the study site, had a wide range of conditions under which it photosynthesizes and was responsible for 53% of net photosynthetic uptake over the two year period, with higher relative and absolute values in 2006 than 2007 (56% and 1760 g C m^{-2} yr^{-1} in 2006, 51 % and 1637 g C m^{-2} yr^{-1} in 2007). The absolute difference between the two years stemmed from small differences in months with low uptake rates (Jan-Mar, Oct-Dec), while net photosynthesis for Ashe juniper was higher in the summer of 2007, compared to the summer of 2006, as was also true for the two other species. In winter, Ashe juniper had lower uptake rates due to lower temperatures, but net photosynthesis by Ashe juniper in the months of Jan-Mar and Nov-Dec constituted 12% of annual canopy photosynthesis. This lengthening of the ecosystems growing season, combined with the lower ecosystem respiration rates due to lower temperatures in the winter, was responsible for the ecosystem being a carbon sink in the winter.

Mesquite has high photosynthetic uptake rates and is the species least impacted by drought events (Chapter 1). Despite its low canopy cover (12%), Honey mesquite contributes on average 20% of the yearly canopy photosynthesis (Table 1). In Chapter 1, we found that maximum carboxylation rates in Honey mesquite were minimally impacted by soil water content, and also that it has a high stomatal slope. We argued that Honey mesquite is an isohydric species and that it closes its stomates to high evaporative demand, thereby also reducing its photosynthetic uptake in dry atmospheric conditions. While this is obvious in the modeled instantaneous rates of mesquite photosynthesis, and mesquite canopy photosynthesis, the high contribution of mesquite to canopy photosynthesis in August 2006, points to the fact that it is too weak of a control on photosynthesis to effectively reduce mesquite photosynthesis in a modeling context during prolonged drought. We therefore attribute the large error in canopy photosynthesis during August 2006 to (1) insufficient reduction of photosynthesis of all three species in response to drought; and (2) interpolation errors in the LAI of the grassland canopy.

3.4.2. Scaling models of ecosystem respiration

Ecosystem respiration is the sum of all above and belowground respiration processes. All belowground respiration processes (autotrophic and heterotrophic) were measured and modeled here as soil respiration (Chapter 2). Soil respiration represented on average 77% of ecosystem respiration in 2005-2006, with annual fluxes of 593 and 519 g C m^{-2} yr^{-1} in respectively 2005 and 2006. Based on comparison of the daily respiration fluxes (Figures 5b and 6b), soil respiration was smaller than ecosystem respiration 72% of the time. The reverse case, where soil respiration was larger than

ecosystem respiration, was only observed on winter days when overall respiration was low, and on days associated with precipitation pulses during the summer months. This was also obvious from the monthly sums - soil respiration exceeded ecosystem respiration in August and September 2005, and September 2006 (Figure 8a). These three months were associated with strong precipitation pulses. Analysis of the dry-down patterns did not show a specific trend, meaning that sometimes modeled soil respiration declined more rapidly, and sometimes ecosystem respiration declined more rapidly.The dynamics of these pulse patterns are hard to model correctly with a simple soil respiration model (Williams et al. 2009).

The models of soil respiration produced smaller yearly sums in 2006 than in 2005 for all cover types, although ecosystem respiration was larger in 2006 compared to 2005 (Table 1). The difference between the two years in modeled respiration was largely due to the drought in the summer months (July and August 2006) when low soil moisture content gave rise to lower modeled soil respiration rates.

Monthly sums per cover type showed little seasonal variation in the contributions of the different cover types (Figure 8b). Annual sums of soil respiration were smaller under trees than grassland (Table 1), with an average decrease of 14% under trees compared to grassland (Chapter 2).

3.5. CARBON BALANCE PER COVER TYPE

Net photosynthesis on a specific cover basis was 213% larger for Ashe juniper than for the C4 grassland (Table 1), due to the broad seasonal amplitude of Ashe juniper (Figure 9) as well as its relatively high LAI. Honey mesquite had 251% more carbon uptake than the grassland on a specific cover basis, which was expected from its leaf-

level measurements. Soil respiration was reduced by 22% under juniper and 24% under mesquite, compared to the grassland in 2006 (Table 1). This resulted in a carbon balance of -1299 g C m^{-2} for juniper, compared to + 19 g C m^{-2} for the grassland, and a carbon balance of 1527 g C m^{-2} for mesquite.

4. Discussion

We found that the difference between photosynthetic carbon uptake and respiratory carbon losses was much larger for the encroaching species than for the grassland canopy, and that the encroaching trees were responsible for the large net carbon uptake of the whole ecosystem. Through our scaling exercise, we also found that trees alter the sensitivity to climatic factors in important ways.

4.1. CARBON BALANCE

By modeling the two largest carbon fluxes – canopy photosynthesis and soil respiration – we were able to construct incomplete carbon balances for the grassland, encroaching juniper, and encroaching mesquite cover types for the year 2006. In our calculations, net photosynthesis is the difference between gross photosynthesis and leaf respiration. Soil respiration measurements included autotrophic root respiration and heterotrophic respiration. The only major missing component is aboveground respiration associated with stems and wood, which normally only contributes a small percentage of all respiration processes.

Analysis of our model results against tower-based carbon fluxes indicated several shortcomings of the model and our approach. First, the carbon balances per cover type do not add up to the carbon sink we measured at the site. In 2006, canopy photosynthesis was overestimated by 123 g C m^{-2}, and soil respiration presented only 67% of ecosystem respiration. The numbers of the grassland balance compare more favorable to a nearby C3/C4 grassland site at 2.5 km distance, close enough to experience similar climatic conditions as the savanna site. This grassland site was a strong carbon source during the summer drought of 2006 (~50-60 g C m^{-2}), but overall acted as a small carbon sink in 2006. The gross fluxes of the nearby grassland site are in good agreement with our modeled data for the grassland (Figure 10)(Kjelgaard et al. 2008). If we add both incongruities (overestimation of GPP, missing respiration flux) to the overall carbon balance of the trees, meaning that we reduce canopy photosynthesis by 123 g C m^{-2} and increase overall respiration processes by 257 g C m^{-2}, for the tree component of the ecosystem, the outcome does not change our findings, and the results still indicate a much larger net carbon balance for trees compared to grasses.

In our approach we systematically area-average the contributions of the three land covers to the ecosystem flux. However, savanna ecosystem functioning is not just the sum of trees and herbaceous cover (House et al. 2003) because significant positive (facilitation) and negative (competition) tree-grass interactions take place (Scholes and Archer 1997). The uptake of carbon by both woody species and herbaceous vegetation can vary non-linearly with woody cover (Asner et al. 1998, Reich et al. 2001). In this respect, we found that the carbon balance of grassland in direct proximity of the encroaching juniper trees can be affected. Specifically grassland patches north of juniper tree had significantly lower net uptake rates than open grassland areas, but only during periods of highest carbon uptake measured at the ecosystem level. If we consider this in

the overall balance of the ecosystem, this means a further reduction of the grassland contribution to net carbon uptake, which does not alter the overall conclusion that the encroaching trees are responsible for the carbon sink.

We show through our scaling efforts that large changes in aboveground carbon uptake by the encroaching trees are responsible for the large carbon sink. Even if we account for uncertainties, our findings are robust: canopy photosynthesis for the encroaching trees far outweighs that of the grassland canopy. Increases in ANPP due to woody encroachment have been observed in other ecosystems (Knapp et al. 2008b). However, our scaling exercise allowed us to confirm that both encroaching trees increased GPP, despite their differing physiologies. For Ashe juniper, its low photosynthetic rates is more than compensated for by the high LAI and year-round photosynthetic activity. Aboveground processes don't paint the whole picture. The decreased soil respiration under juniper due to its altered microclimate and reduced sensitivity to environmental drivers also contributes to the C sink strength of this savanna. Honey mesquite is thought to be a less important player in this ecosystem due to its lower cover fraction, but its high leaf-level photosynthetic rate also translated into large canopy uptake rates.

4.2. MODELING CONSIDERATIONS

We used a big leaf approach to scale photosynthetic models in space and time. One possible improvement to the photosynthesis model component is the addition of a soil water balance model. In addition, the scaling component might be more accurate given better resolution of site structure and radiation scheme.

The treatment of water stress in the photosynthetic model was based on (i) stomatal closure in response to high evaporative demand – a key feature of the coupled stomatal-photosynthesis model; and (ii) observations of how maximum carboxylation rate was influenced by soil water content for the three different species. This approach did not sufficiently reduce photosynthetic uptake during the summer drought of 2006. Other metrics besides soil water content that were easily accessible, such as evaporative fraction, did not improve results, suggesting that a soil water balance model is needed. However, soil water availability in a karst landscape is particularly difficult to understand or model (Schwinning 2008, Heilman et al. 2009, Schwinning 2010). Since our study, TDR probes and rhizotrons have been installed at the site which should help improve our understanding of soil water storage and rooting depth, and their effect on canopy processes. Further improvements to the photosynthesis model could be made with better estimates of leaf temperatures using an energy balance approach, and parameterization of the mesophyll conductance for the different species (Sun et al. 2014).

The scaling component could be improved by including a more realistic radiative transfer scheme, e.g., the LiDAR data of our site could be used to derive a better clumping factor and a 3D radiative transfer scheme (Chen et al. 2008, Kobayashi et al. 2012). The use of a footprint model for the tower fluxes (Vesala et al. 2008) together with the LiDAR data would allow us to assess the dynamic fractional cover of the three cover types that the flux tower represents, instead of the static ratio of 0.5, 0.38 and 0.12 we used to represent grassland, juniper and mesquite cover.

4.3. CLIMATIC VARIABLES REVISITED

Woody encroachment altered the response of the ecosystem to climatic factor is three important ways. First, the temperature range under which the ecosystem is a carbon sink was broadened by the encroaching juniper, which kept the ecosystem accumulating carbon during winter months. Second, carbon dynamics in the ecosystem became less sensitive to drought, because the encroaching trees were less sensitive to moisture than grasses. Finally, because the trees are not drought deciduous, they might be better positioned to take advantage of precipitation pulses, as evidenced by the gap between grassland and whole-savanna carbon uptake responses after rain pulses following a long drought. These three characteristics all make the ecosystem carbon balance less susceptible to future climate change.

For four months out of the year (November-February), the encroaching juniper is the only dominant species that is photosynthetically active and keeps the ecosystem carbon positive throughout this cooler period, effectively lengthening the growing season and widening the ecosystems temperature range under which it accumulates carbon.

In Chapter 3 we found that ecosystem respiration in the savanna ecosystem is more sensitive to decreases in soil water content than GPP (Schwalm et al, 2010). From a visual inspection of Figure 7(a&b), we can see that carbon release processes are much more pulse driven than carbon uptake processes, with more rapid declines when water becomes limiting. In our modeling context, this difference was built in, not purposefully, but rather as a result of observations in the field. Soil respiration responds linearly to soil water over the whole range of soil water contents, while an effect of water stress on photosynthesis is only implemented at water contents below 15%. This effect was very limited for the two encroaching trees compared to the grassland species (Chapter 1),

indicating that the trees made the ecosystem GPP less susceptible to decreases in soil water content.

In this context, it is also interesting to look at photosynthetic recovery after a precipitation pulse (Volder et al. 2010). Our small scale measurements were on average taken every month, which did not allow studying fast precipitation pulse dynamics. Inspection of the GPP flux in 2005 and 2006 (Figure 2b) shows that GPP actually rose for several days after a precipitation pulse – this lag can be explained by the time it takes to rebuild the grassland canopy (Williams and Albertson 2004, 2005). Grassland NEE chamber measurements after the long 2006 summer drought indicated that the grassland was still a net source of carbon in September 2006, while the ecosystem as a whole was acting as a carbon sink again. This might indicate that the trees are better positioned to take advantage of pulsed water resources.

4.4. WOODY ENCROACHMENT AS CARBON SINK

Woody encroachment is considered an uncertain carbon sink of 0.12 ± 0.2 Pg C yr^{-1} in the US alone (Houghton et al. 2012), which is both a large portion of the terrestrial carbon balance and an even larger uncertainty of it. Where it was once considered an important part of the North American carbon balance (Houghton et al. 1999, Pacala et al. 2001), it is now not included in estimates of land use change or in estimates of the residual land carbon sink (Houghton et al. 2012, Le Quéré et al. 2014). The uncertainty of the sink stems from (i) the unknown extent of woody encroachment, (ii) the uncertainty of the effect of woody encroachment on the carbon balance (Jackson et al. 2002) and (iii) possible reversals of the carbon sink due to land management, invasion of perennial grass species, or tree mortality due to droughts (Bradley et al. 2006, Houghton et al. 2012).

Regarding the second uncertainty, there is an opinion, that woody encroachment initially leads to rapid losses in the soil carbon pools, especially at sites with high MAP (Jackson et al. 2002), which offsets the later increases in aboveground carbon storage. This has not been generally accepted, because there are also large reported increases in SOC with woody encroachment (Liao et al. 2006). On the other hand, high grazing pressure in grasslands and pastures, pre-dating the woody encroachment process, can decrease soil organic carbon storage (Archer et al. 2001), while also reducing competitiveness of the grasses and leading the way to woody encroachment. As such, decreased SOC storage is not the result of woody encroachment per se, but is a factor associated with overgrazing, itself one of the leading causes of woody encroachment. To reduce uncertainties regarding the role of woody encroachment in the carbon cycle, it would be beneficial to address the two processes separately – first to account for the losses of SOC due to grazing pressure in the context of land use change and land degradation (Guo and Gifford 2002), and second to account for increases in carbon storage due to woody encroachment in either the context of land cover change or the residual land carbon sink. If we then consider woody encroachment as either disturbance of an evolution to an alternate stable state (Scheffer et al. 2001, Knapp et al. 2008b), the increases in carbon storage will level off as the ecosystem reaches a new balance between photosynthesis and respiration, and multiple stages of woody encroachment will need to be assessed to study the relative course of increases of photosynthesis and respiration processes over time.

5. Conclusion

We showed that a central Texas savanna site acts as a large carbon sink. Woody encroachment has a dramatic influence of ecosystem functioning, foremost by increasing the carbon uptake, as well as decreasing soil respiration, resulting in a large carbon sink. We showed that woody encroachment also fundamentally alters the seasonality of carbon exchange, and therefore also the relation of ecosystem level carbon fluxes to climatic drivers.

6. Figures

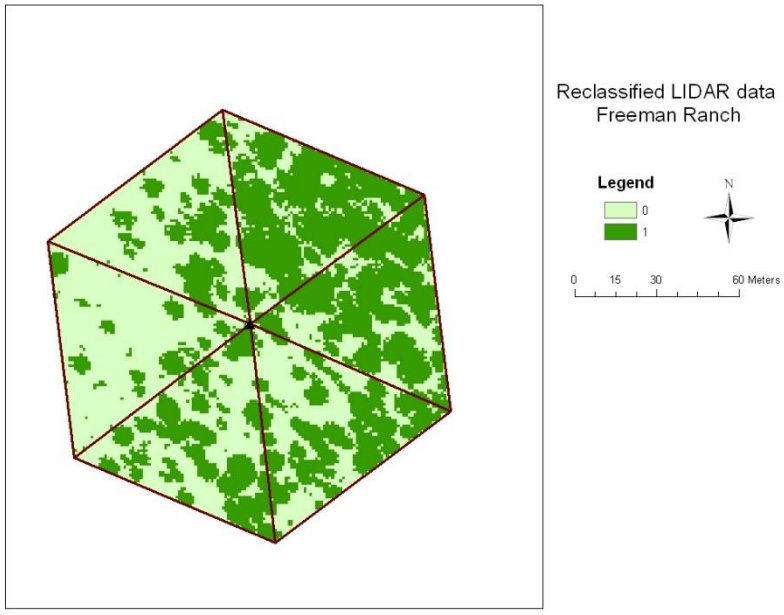

(a)

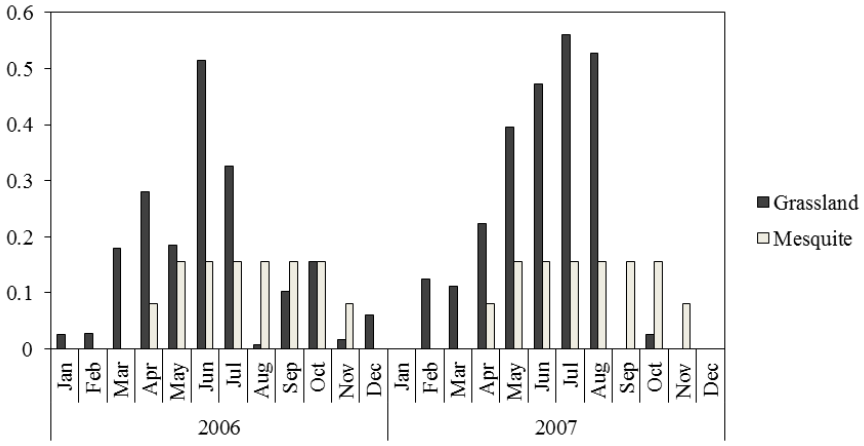

(b)

Figure 4.1: (a) Tree cover map derived from small footprint LiDAR data; (b) Site-wide LAI estimates for C4 grassland and Honey mesquite during 2006-2007.

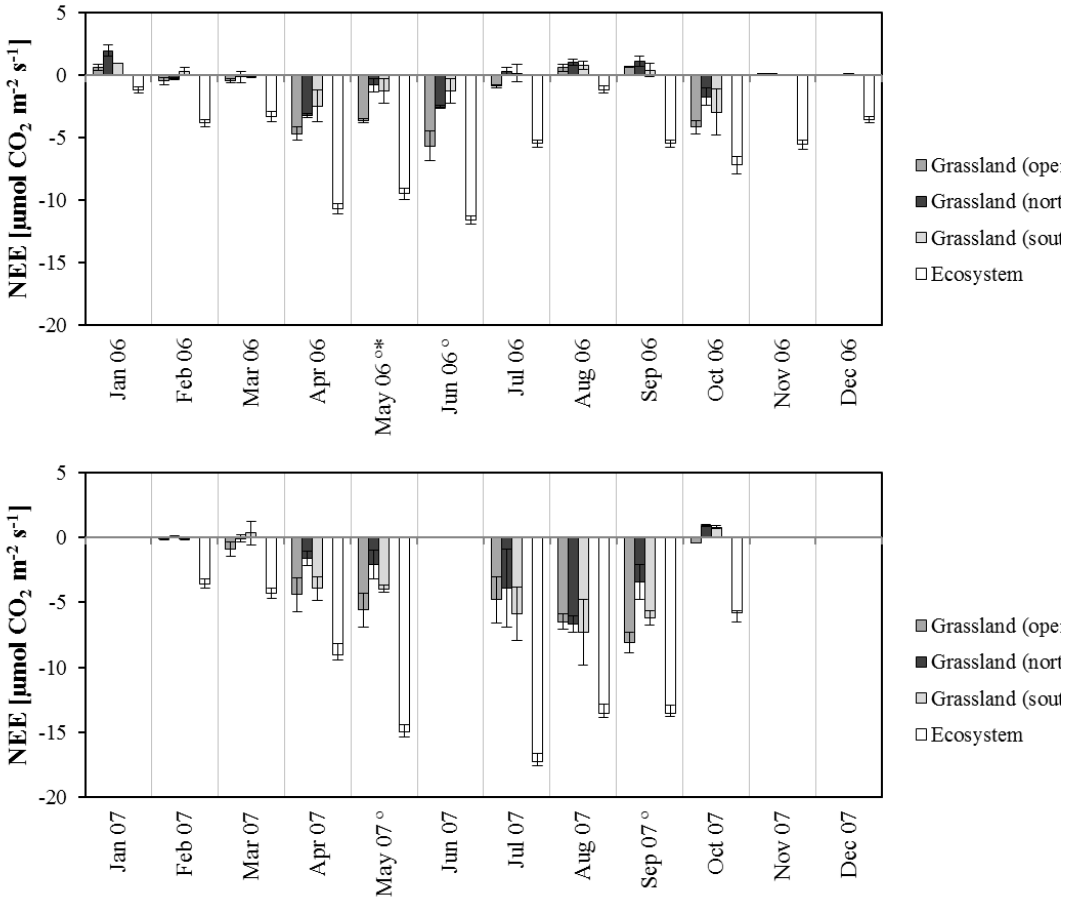

Figure 4.2: Grassland chamber-based NEE for open grassland, and grassland patches north and south of tree clusters. Ecosystem level NEE fluxes are given as comparison. The ecosystem NEE values are the running average of 5 days of midday (10AM-2PM) fluxes, centered on the day of the NEE chamber measurement. Significant differences in chamber-based NEE between locations per month are noted next to the months name (º denotes a significant difference between open grassland and grassland north of tree cluster, while * denotes a significant difference between open grassland and grassland south of tree cluster).

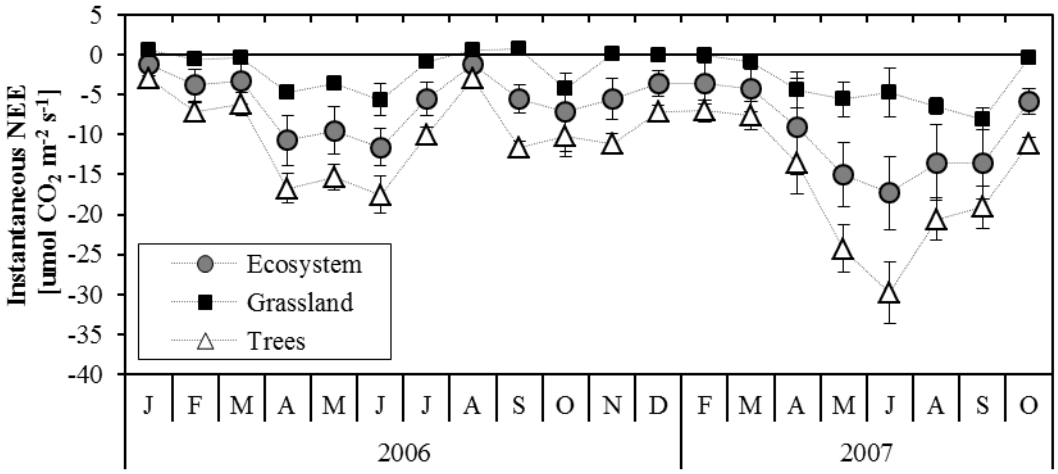

Figure 4.3: Instantaneous NEE rates for savanna ecosystem (tower-based), open grassland component (chamber-based) and trees (average ± stdev). Average NEE for the tree component is estimated based on the difference of cover-weighted grassland NEE and ecosystem NEE. Standard deviation for the tree component is based on the sum of squared grassland and ecosystem standard deviation. Grassland and estimated tree NEE is given per m^2 cover type.

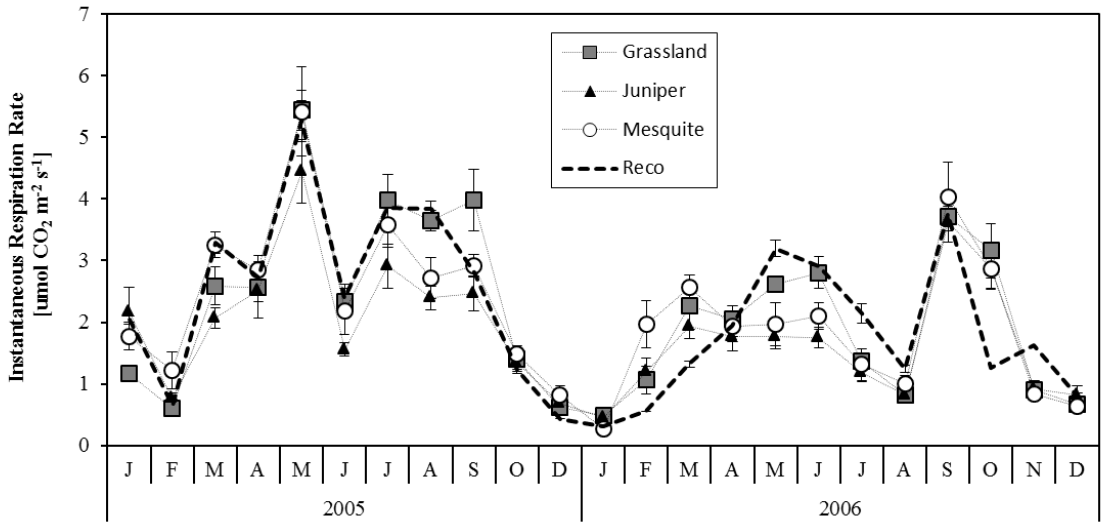

Figure 4.4: Instantaneous (chamber-based) soil respiration rates for grassland, juniper and mesquite cover. Instantaneous Reco rates for savanna ecosystem (tower-based) are given as comparison (average ± stdev).

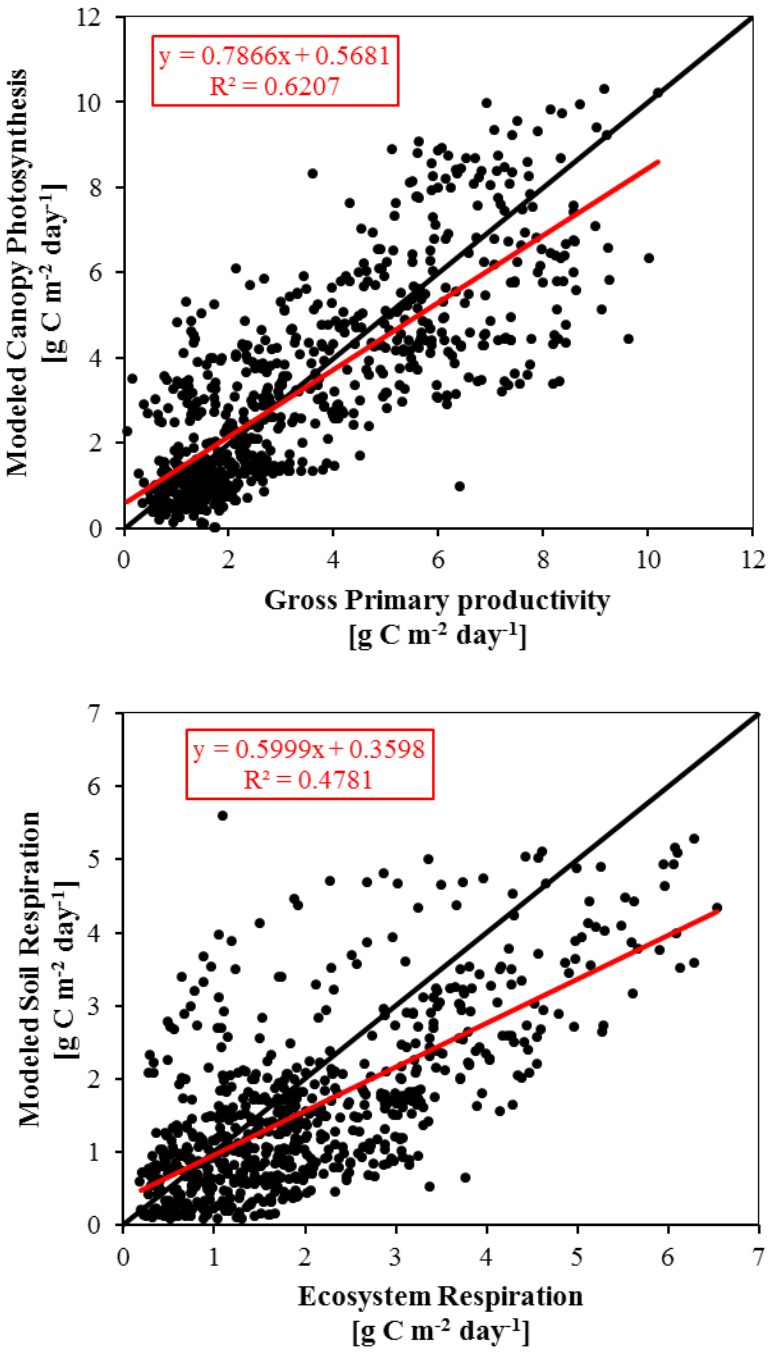

Figure 4.5: (a) Modeled canopy photosynthesis versus tower-based GPP for the period 2006-2007; (b) Modeled soil respiration versus tower-based ecosystem Respiration for the period 2005-2006.

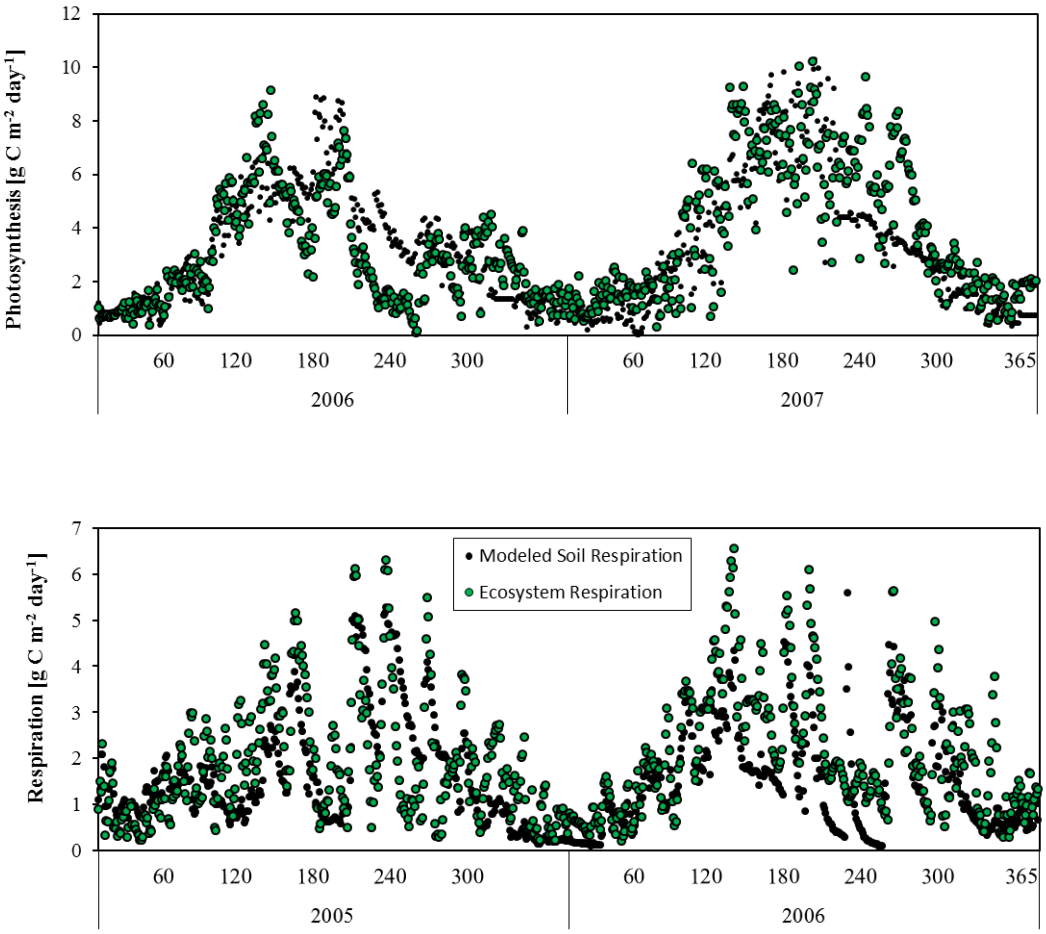

Figure 4.6: (a) Seasonal course of tower-based GPP and modeled canopy photosynthesis for the period 2006-2007; (b) Seasonal course of tower-based Reco and modeled soil respiration for the period 2005-2006.

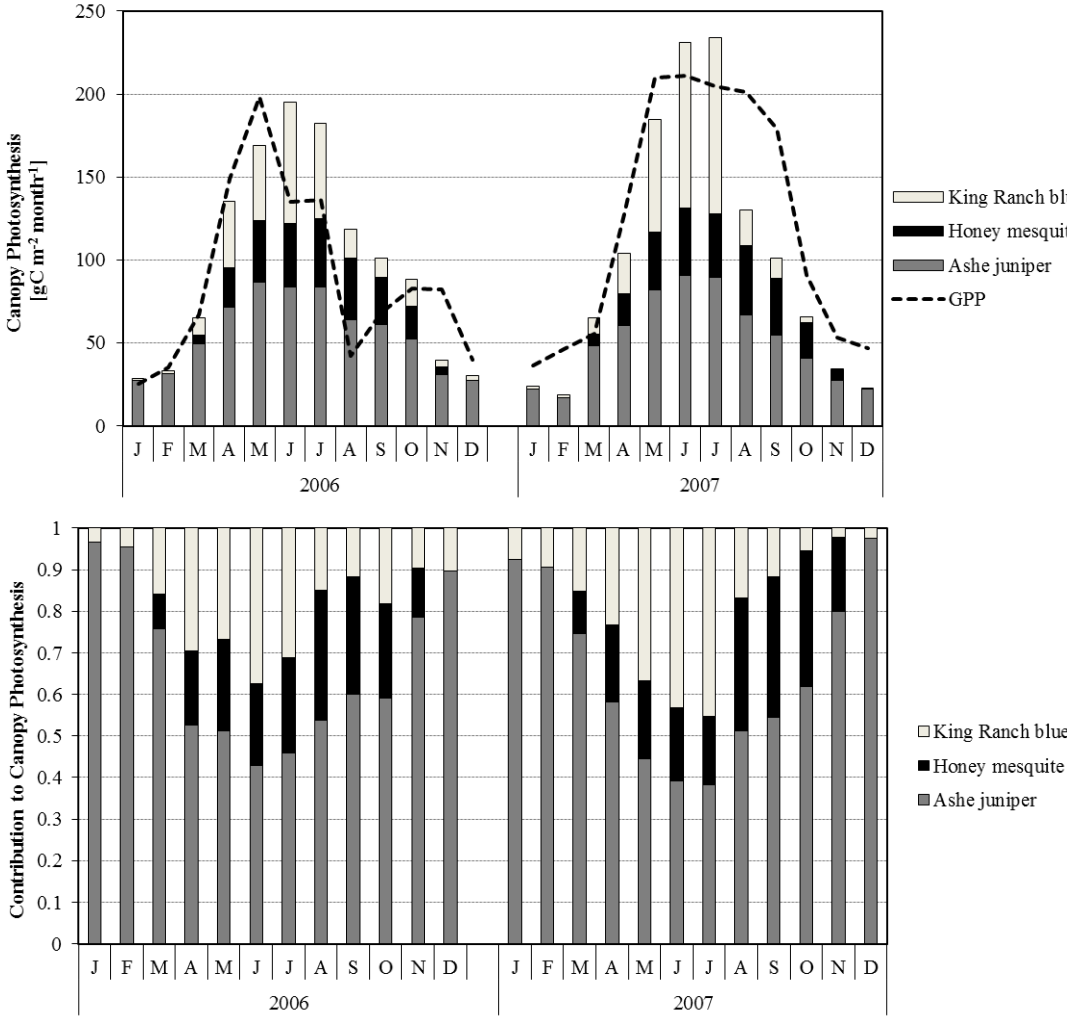

Figure 4.7: (a) Monthly sums of canopy photosynthesis for Ashe juniper, Honey mesquite and King Ranch bluestem given on a per m^2 ecosystem basis. Monthly ecosystem GPP is given for comparison. (b) Contributions of Ashe juniper, Honey mesquite and King Ranch bluestem to modeled canopy photosynthesis.

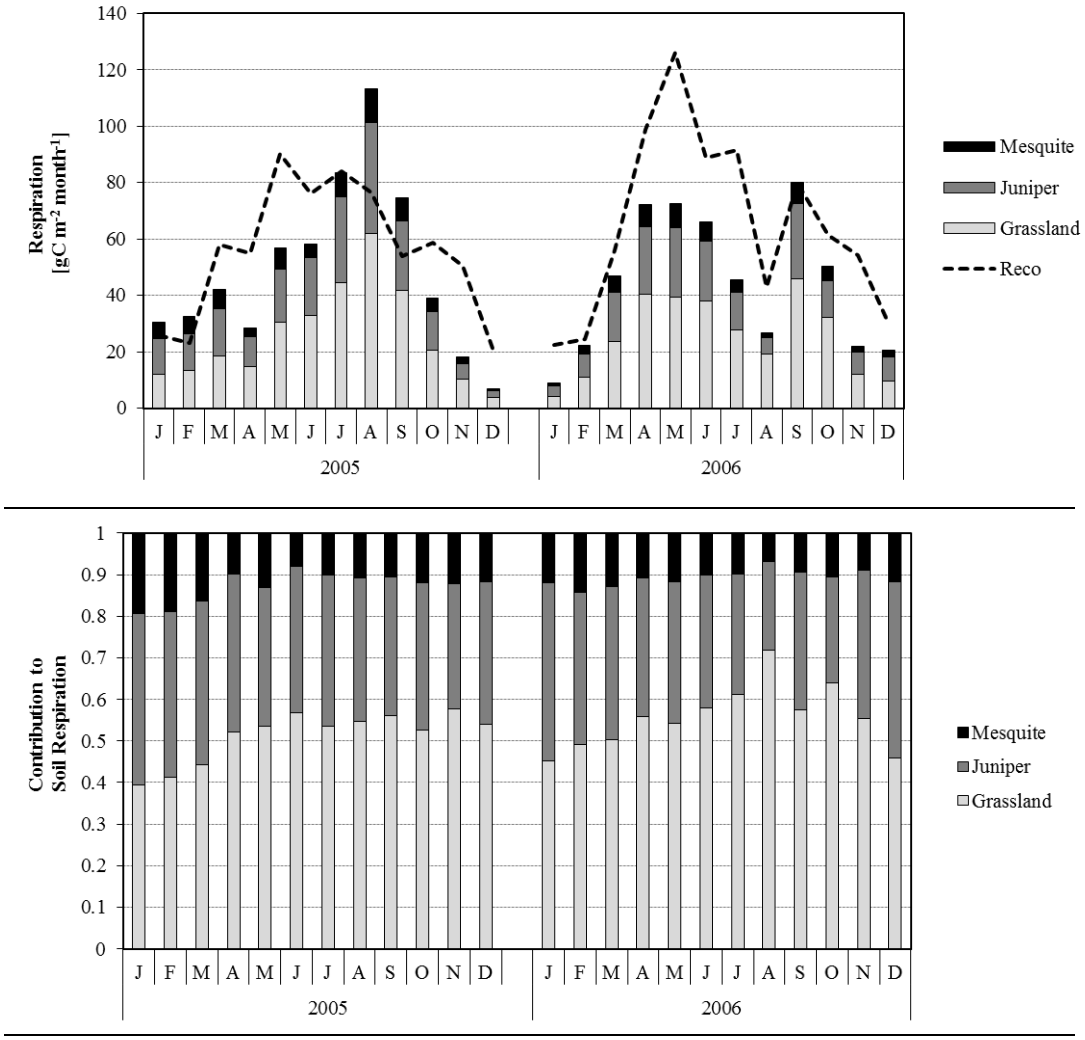

Figure 4.8: (a) Monthly sums of soil respiration for three different land covers, given on a per m^2 ecosystem basis. Monthly ecosystem respiration is given as comparison. (b) Contributions of grassland, juniper and mesquite cover to modeled soil respiration.

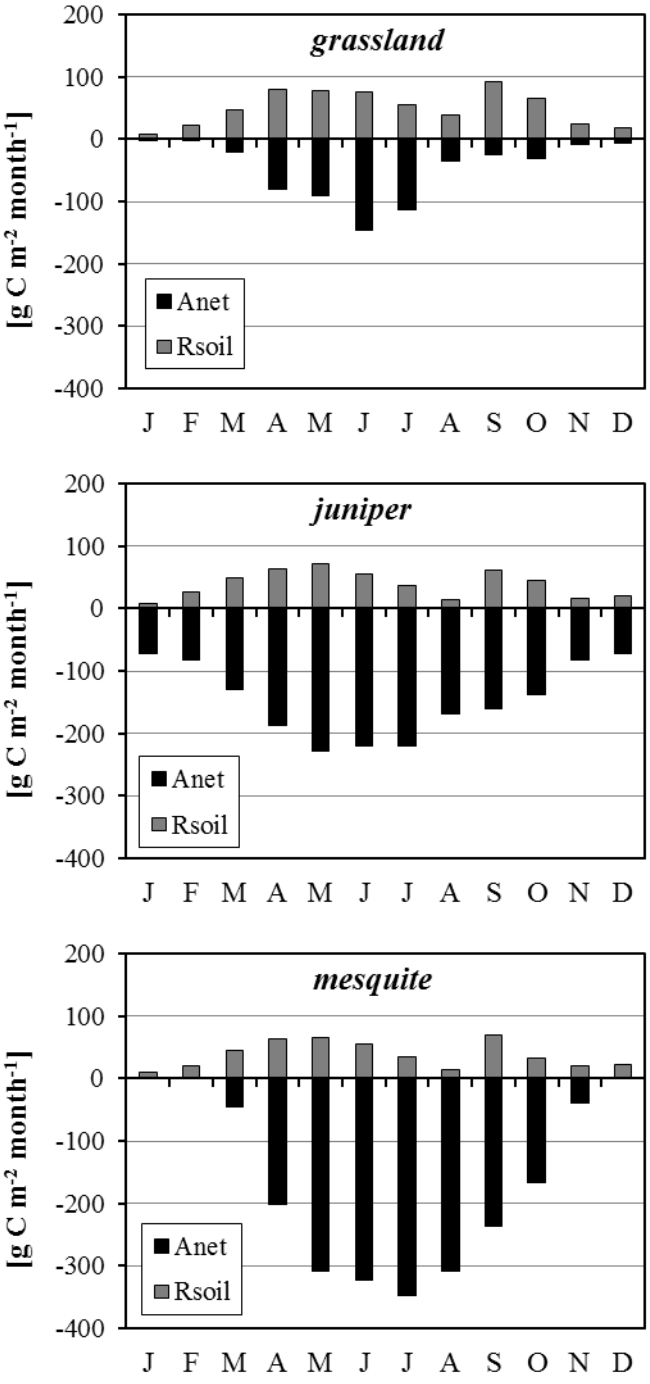

Figure 4.9: Monthly modeled values for canopy net photosynthesis and soil respiration for three cover types, in 2006. Negative values are net photosynthetic uptake, positive values are soil respiration. Values are given on a m^2 cover type basis.

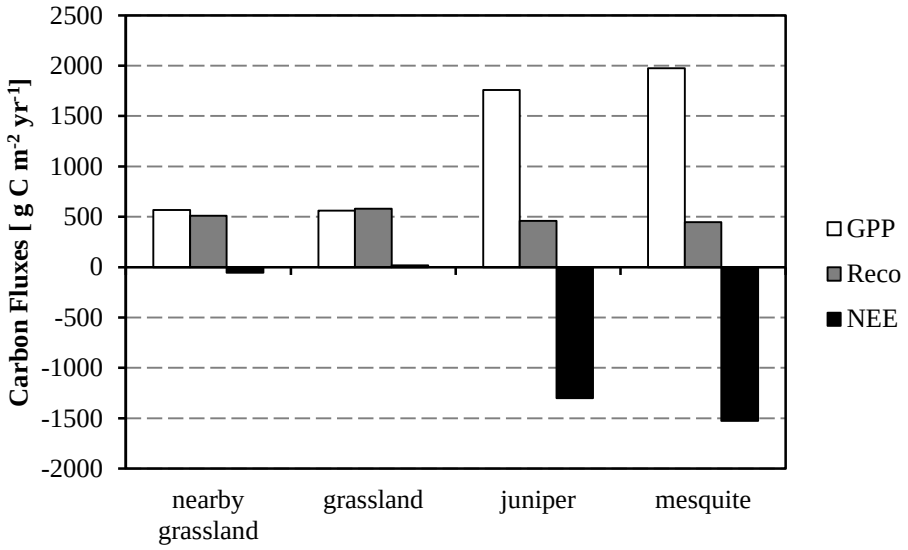

Figure 4.10: Overview of differences between vegetation types in modeled carbon fluxes for the year 2006. Data from a nearby grassland site is given as comparison (Kjelgaard et al, 2008).

7. Tables

Table 4.1: Annual sums of precipitation and ecosystem level carbon fluxes.

	Units	**2005**	**2006**	**2007**
Precipitation	[mm]	738	815	1514
NEE	[g C m^{-2} $year^{-1}$]	-508	-287	-420
GPP	[g C m^{-2} $year^{-1}$]	1180	1063	1463
Reco	[g C m^{-2} year-1]	672	776	1042
Reco/GPP	[-]	0.57	0.73	0.71
Canopy photosynthesis	*[g C m^{-2} year-1]*	-	*1186*	*1215*
Anet grassland	*[g C m^{-2} $year^{-1}$]*	-	*280 (561)*	*350 (701)*
Anet juniper	*[g C m^{-2} $year^{-1}$]*	-	*668 (1760)*	*622 (1637)*
Anet mesquite	*[g C m^{-2} $year^{-1}$]*	-	*237 (1975)*	*242 (2021)*
Soil Respiration	*[g C m^{-2} $year^{-1}$]*	*593*	*519*	-
Rsoil grassland	*[g C m^{-2} $year^{-1}$]*	*305 (611)*	*290 (580)*	-
Rsoil juniper	*[g C m^{-2} $year^{-1}$]*	*222 (583)*	*175 (461)*	-
Rsoil mesquite	*[g C m^{-2} $year^{-1}$]*	*65 (548)*	*53 (448)*	-
Rsoil/Canopy photosynthesis	*[-]*	-	*0.44*	-

Notes: NEP, GPP and Reco are tower-based fluxes. Modeled values are in italic. Land cover specific contributions are given in m^2 ecosystem, and per m^2 specific cover type in brackets. Fractional cover is 0.5, 0.38 and 0.12 for respectively grassland, juniper and mesquite cover.

CONCLUSION AND FURTHER RESEARCH

Woody encroachment of grassland and savanna ecosystems is a global phenomenon, with important consequences for ecosystem functioning and services (Eldridge et al. 2011). Woody encroachment is considered an uncertain carbon sink of 0.12 ± 0.2 Pg C yr^{-1} in the US alone (Houghton et al. 2012), which is both a large portion of the terrestrial carbon sink and an even larger uncertainty of it. Where it was once considered an important part of the North American carbon balance (Houghton et al. 1999, Pacala et al. 2001), it is now not included in estimates of land use change or in estimates of the residual land carbon sink (Houghton et al. 2012, Le Quéré et al. 2014). The uncertainty of the sink stems from (i) the unknown extent of woody encroachment, (ii) the uncertainty of the effect of woody encroachment on the carbon balance at local scales (Jackson et al. 2002), and (iii) possible reversals of the carbon sink by different means, such as land management, invasion of exotic perennial grass species after fire, or tree mortality due to droughts (Bradley et al. 2006, Houghton et al. 2012).

Regarding the first uncertainty, state of the art remote sensing technology is at a stage that a synergy of different products and platforms can be used to accurately determine structural characteristics of savanna ecosystems (Asner et al. 2011, Lucas et al. 2011). This combined with a time-series approach can provide information about the extent of woody encroachment, as well as its progression and reversals through land management and natural causes.

Concerning the second uncertainty, I showed that a central Texas ecosystem which had been undergoing woody encroachment for ~ 30 years, acted as a large carbon sink (Chapter 3). I also showed that regardless of climatic conditions in the three years of study, which ranged from very dry to very moist, the ecosystem remained a carbon sink

at most times, and that climatic variables by themselves were not able to explain the size of the carbon sink. I further showed through the scaling of soil respiration and photosynthetic models that the encroaching trees are responsible for the sink of this savanna ecosystem, both through large increases in photosynthetic uptake and modest decreases in soil respiration carbon losses. I also showed that the encroachment process altered the response of carbon dynamics to climatic drivers. First, the lengthening of the growing season due to encroachment of the evergreen Ashe juniper allowed the ecosystem to stay a year-round carbon sink. Second, the drought tolerance of the encroaching trees made the ecosystem more drought resistant.

Our results fit the overall results of Barger et al. (2011), who found that changes in aboveground net productivity (ANPP) due to woody encroachment, increase with mean annual precipitation (MAP), while changes in belowground carbon storage do not mirror aboveground changes (Barger et al. 2011). Widely differing responses of the soil organic carbon pool have been correlated with soil characteristics, such as clay content and bulk density. I found increased storage of soil organic carbon only under one of the encroaching species, Ashe juniper, while no significant changes were found for Honey mesquite.

There is a persistent notion that increases in aboveground carbon storage might be offset by belowground losses of carbon (Jackson et al. 2002, Houghton et al. 2012), and that woody encroachment initially leads to a rapid loss in the soil carbon pools (SOC), especially at sites with high MAP (Jackson et al. 2002). The observed decreases in soil organic carbon pools, which can offset later increases in aboveground carbon storage, were found when SOC pools under encroaching trees in grazed pasture lands were compared to SOC pools in ungrazed lands. To resolve the large uncertainty that surrounds the carbon sink potential of woody encroachment, I argue to consider the two

different processes, grazing and woody encroachment, separately. High grazing pressure in grasslands and pastures, pre-dating or co-occurring with woody encroachment, has the potential to decrease soil organic carbon storage (Archer et al. 2001), while also reducing competitiveness of the grasses and leading the way to woody encroachment. As such, decreases in SOC storage might not be the result of woody encroachment per se, but can be a factor associated with grazing pressure, itself one of the leading causes of woody encroachment. It would be instructive to first account for possible losses of SOC due to grazing pressure in the context of land use change and land degradation (Guo and Gifford 2002), and second to account for increases in carbon storage due to woody encroachment in either the context of land cover change or the residual land carbon sink. If we then consider woody encroachment either as a disturbance process, or an evolution to an alternate stable state (Scheffer et al. 2001, Knapp et al. 2008), the increases in carbon storage will level off as the ecosystem reaches a new equilibrium between photosynthesis and respiration. As such, a ~100 year mesquite encroached ecosystem in Arizona has acted as a carbon source for five consecutive years during drier than normal conditions (Scott et al. 2009). To come to a full understanding of the impact of woody encroachment on the carbon balance, multiple stages of woody encroachment, over large gradients of mean annual precipitation, need to be assessed to study the relative course of changes in photosynthesis and respiration processes over time.

The reverse process of woody encroachment, either through brush management or tree die-off, also needs further attention, not only to reduce the third uncertainty surrounding the carbon sink potential, but also to address other changes in ecosystem properties (Archer and Predick 2014). Brush management is a general term for several land management practices that reverse the process of woody encroachment by mechanical or chemical means. It is often practiced in the US where woody

encroachment is perceived to reduce forage and livestock production (Anadon et al. 2014), as well as negatively impact streamflow and groundwater recharge in regions where water availability is becoming more critical as the climate changes and population numbers grow (Wilcox 2002, Huxman et al. 2005). Although brush management will likely reduce aboveground carbon storage, its effect on other ecosystem properties, processes and services remains unclear as ecosystems do not automatically revert back to their original grassland state (Archer and Predick 2014).

In this dissertation I specifically studied the impact of woody encroachment on carbon cycling, however effects extend much further than the carbon balance and woody encroachment also carries consequences for biodiversity, conservation, water cycling, and forage and livestock production. All of these consequences might carry (perceived?) larger societal impacts and require further research as well as continued efforts to educate people of their far-reaching impacts on natural ecosystems.

Appendix

Models of C3 and C4 photosynthesis and a stomatal conductance model (Ball et al. 1987) were used in chapters 1 and 4. The used equations, parameters and constants were as follows, and are adapted form texts of Collatz et al. (1991), Collatz et al.(1992) and Campbell and Norman (1998).

C3 PHOTOSYNTHESIS

C3 gross photosynthesis in units of μmol CO_2 m^{-2} s^{-1} is modeled as the minimum of three rate limiting steps:

$$A = \ min\{J_c, J_e, J_s\}$$

where J_c is the Rubisco-limited rate, J_e the light-limited rate and J_s the rate imposed by sucrose synthesis. The Rubisco-limited rate is calculated as

$$J_e = \frac{V_m(C_i - \Gamma^*)}{C_i + K_c\left(1 + {}^{C_{oa}}/_{K_o}\right)}$$

where V_m is the maximum Rubisco capacity per unit leaf area, C_i is the intercellular CO_2 concentration, Γ^* is the compensation CO_2 concentration at which assimilation is zero and is computed from

$$\Gamma^* = \frac{C_{oa}}{2\tau}$$

where C_{oa} is the oxygen concentration in the air and τ is a ratio describing the partitioning of RuBP to the carboxylase or oxygenase reactions of Rubisco. K_c is the Michaelis constant for CO_2, and K_o is the Michaelis constant for oxygen inhibition.

The light-limited rate J_e is calculated as:

$$J_e = \frac{\alpha_P \, e_m Q_p (C_i - \Gamma^*)}{C_i + 2\Gamma^*}$$

where α_p is the absorptivity of the leaf for PAR, e_m is the maximum quantum efficiency, Q_p is the PAR photon flux density (μmol m^{-2} s^{-1}), C_{ci} and Γ^* are as above. The third limiting rate, J_s, is the constraint imposed by the export and use of products of photosynthesis, and is assumed to be:

$$J_s = V_m/2$$

There is a transition from one rate-limiting process to another, with co-limitation as two rates are almost equal. This co-limitation is modeled using quadratic functions:

$$J_p = \frac{J_e + J_c - \sqrt{(J_e + J_c)^2 - 4\theta J_e J_c}}{2\theta}$$

and

$$A_{gross} = \frac{J_p + J_s - \sqrt{(J_p + J_s)^2 - 4\beta J_p J_s}}{2\beta}$$

with coupling coefficients θ and β of 0.95 and 0.98. Leaf respiration is modeled as a constant fraction of Rubisco capacity, and net photosynthesis as the difference between gross photosynthesis and

$$R_d = Resp \, V_m$$

$$A_{net} = A_{gross} - R_d$$

Five model parameters (K_c, K_o, τ, V_m, R_d) are temperature dependent and need a temperature adjustment. The first three parameters are exponentially dependent on leaf temperature:

$$K_c \, (T_L) = K_{c,25} \, exp[0.074(T_L - 25)]$$

$$K_o\ (T_L) = \ K_{o,25}\ exp[0.018(T_L - 25)]$$

$$\tau\ (T_L) = \ \tau_{25}\ exp[-0.056(T_L - 25)]$$

While Vm and Rd also have a high temperature stress function in the denominator which reduces values of Vm and Rd when temperatures become too high:

$$V_m(T_L) = \frac{V_{m,25}\ exp[0.088(T_L - 25)]}{1 + exp[0.29(T_L - htti)]}$$

$$R_d(T_L) = \frac{R_{d,25}\ exp[0.069(T_L - 25)]}{1 + exp[1.3(T_L - 55)]}$$

C4 PHOTOSYNTHESIS

C4 gross photosynthesis in units of μmol CO_2 m^{-2} s^{-1} is also modeled as the minimum of three rate limiting steps:

$$A = \ min\ \{J_c, J_i, J_e\}$$

where J_c is the CO_2 limited rate, J_i is the light limited rate and J_e is the Rubisco limited rate. The CO_2 limited rate is calculated as

$$J_c = k\ C_i$$

where k is the initial slope of the CO_2 response curve and C_i is the intercellular CO_2 concentration.

The light limited rate is calculated as

$$J_i = \alpha\ 0.067\ Q_p$$

where α is the absorptivity of the leaf for PAR, Q_p is the PAR photon flux density (μmol m^{-2} s^{-1}), and 0.067 is a constant combining light use efficiency and fraction of photons used for C3 reactions. If light and CO_2 concentrations are not limiting, C4 photosynthesis becomes limited by Rubisco:

$$J_e = V_m$$

As in the C3 model, there is a transition from one rate-limiting process to another, with co-limitation as two rates are almost equal.

$$J_p = \frac{J_i + J_c - \sqrt{(J_i + J_c)^2 - 4\theta J_i J_c}}{2\theta}$$

and

$$A_{gross} = \frac{J_p + J_e - \sqrt{(J_p + J_e)^2 - 4\beta J_p J_e}}{2\beta}$$

with coupling coefficients θ and β of 0.83 and 0.93. Leaf respiration is modeled as a constant fraction of Rubisco capacity, and net photosynthesis as the difference between gross photosynthesis and leaf respiration:

$$R_d = Resp\ V_m$$

$$A_{net} = A_{gross} - R_d$$

Three model parameters (k, V_m, R_d) are temperature dependent and need a temperature adjustment:

$$k(T_L) = k_{25} 1.8^{((T_L - 25)/10)}$$

Temperature dependence of V_m and R_d includes a high temperature stress function, and V_m also has a low temperature stress function in the denominator which reduces values of V_m and R_d when temperatures become too high (and too low for V_m):

$$R_d(T_L) = \frac{R_{d,25}\ 1.8^{((T_L-25)/10)}}{1 + exp[1.3(T_L - 55)]}$$

$$V_m(T_L) = \frac{V_{m,25}\ 2.1^{((T_L-25)/10)}}{(1 + exp[0.2(15 - T_L)])(1 + exp[0.3(T_L - htti)])}$$

STOMATAL CONDUCTANCE

The Ball-Berry model relates stomatal conductance (G_s) to net photosynthesis:

$$G_s = m\ \frac{A_{net} h_s}{C_s} + b$$

where m and be are respectively the stomatal slope and intercept of the Ball-Berry model, and h_s is the relative humidity at the leaf surface. C_s is the CO_2 concentration at the leaf surface:

$$C_s = C_a - 1.6\ A_{net}/G_b$$

where G_b is the boundary layer conductance. Fick's law is then used to calculate the intercellular CO_2 concentration:

$$C_i = C_s - 1.6\ A_{net}/G_s$$

To come to an overall solution, C_i, A_{net} and G_s are calculated iteratively.

Table A1: Constants for coupled stomatal-photosynthesis models

Symbol	*Value*	*Units*	*Description*
b	see Table 1.5	mol m^{-2} s^{-1}	Intercept Ball-Berry model
m	see Table 1.5	-	Slope Ball-Berry model
$\mathbf{V_m}$	see Table 1.5	µmol m^{-2} s^{-1}	Rubisco capacity
Resp	see Table 1.5	-	Leaf respiration coefficient
htti	see Table 1.5	° C or K	High temperature stress parameter
$\mathbf{e_m}$	0.08	mol/mol	Maximum quantum efficiency C3
$\mathbf{K_c}$	300	µmol/mol	Michaelis constant for CO_2
$\mathbf{K_o}$	300	mmol/mol	Michaelis constant for O_2
$\mathbf{C_{oa}}$	210	mmol/mol	O_2 concentration
α	0.8		Leaf absorptivity for PAR
τ	2.6	mmol/µmol	Specificity ratio CO_2 / O_2

References

Ainsworth, E. A., P. A. Davey, C. J. Bernacchi, O. C. Dermody, E. A. Heaton, D. J. Moore, P. B. Morgan, S. L. Naidu, H. S. Y. Ra, X. G. Zhu, P. S. Curtis, and S. P. Long. 2002. A meta-analysis of elevated CO2 effects on soybean (*Glycine max*) physiology, growth and yield. Global Change Biology **8**:695-709.

Amos, B. B. and F. R. Gehlbach. 1988. Edwards Plateau vegetation: plant ecological studies in central Texas. Baylor University Press, Waco, Texas.

Anadon, J. D., O. E. Sala, B. L. Turner, and E. M. Bennett. 2014. Effect of woody-plant encroachment on livestock production in North and South America. Proceedings of the National Academy of Sciences of the United States of America **111**:12948-12953.

Anderson-Teixeira, K. J., J. P. Delong, A. M. Fox, D. A. Brese, and M. E. Litvak. 2011. Differential responses of production and respiration to temperature and moisture drive the carbon balance across a climatic gradient in New Mexico. Global Change Biology **17**:410-424.

Ansley, R. J., X. Ben Wu, and B. A. Kramp. 2001. Observation: Long-term increases in mesquite canopy cover in a North Texas savanna. Journal of Range Management **54**:171-176.

Archer, S. 1990. Development and stability of grass woody mosaics in a subtropical savanna parkland, Texas, USA. Journal of Biogeography **17**:453-462.

Archer, S., T. W. Boutton, and K. A. Hibbard. 2001. Trees in grasslands: biogeochemical consequences of woody plant expansion.*in* E.-D. Schulze, S. P. Harrison, M. Heimann, E. A. Holland, J. Lloyd, I. C. Prentice, and D. Schimel, editors. Global biogeochemical cycles in the climate system. Academic Press, San Diego.

Archer, S., D. S. Schimel, and E. A. Holland. 1995. Mechanisms of shrubland expansion - land-use, climate or CO_2. Climatic Change **29**:91-99.

Archer, S. R. and K. I. Predick. 2014 An ecosystem services perspective on brush management: research priorities for competing land-use objectives. Journal of Ecology **102** 1394–1407.

Arrhenius, S. 1889. Uber die Reaktionsgeschwindigkeit bei der Inversion von Rohrzucker durch Sauren. Zeitschrift fur Physik Chemique **4**:226-248.

Asner, G. P., S. Archer, R. F. Hughes, R. J. Ansley, and C. A. Wessman. 2003. Net changes in regional woody vegetation cover and carbon storage in Texas Drylands, 1937-1999. Global Change Biology **9**:316-335.

Asner, G. P., S. R. Levick, and I. P. J. Smit. 2011. Remote Sensing of Fractional cover and Biochemistry in Savannas.*in* M. J. Hill and N. P. Hanan, editors. Ecosystem function in savannas: Measurement and modeling at landscape to global scales. CRC Press, Boca Raton, FL.

Asner, G. P., C. A. Wessman, and S. Archer. 1998. Scale dependence of absorption of photosynthetically active radiation in terrestrial ecosystems. Ecological Applications **8**:1003-1021.

Baldocchi, D., E. Falge, L. H. Gu, R. Olson, D. Hollinger, S. Running, P. Anthoni, C. Bernhofer, K. Davis, R. Evans, J. Fuentes, A. Goldstein, G. Katul, B. Law, X. H. Lee, Y. Malhi, T. Meyers, W. Munger, W. Oechel, K. T. P. U, K. Pilegaard, H. P. Schmid, R. Valentini, S. Verma, T. Vesala, K. Wilson, and S. Wofsy. 2001. FLUXNET: A new tool to study the temporal and spatial variability of ecosystem-scale carbon dioxide, water vapor, and energy flux densities. Bulletin of the American Meteorological Society **82**:2415-2434.

Ball, J. T., I. E. Woodrow, and J. A. Berry. 1987. A model predicting stomatal conductance and its contribution to the control of photosynthesis under different environmental conditions. Pages 221-224 *in* J. Biggins, editor. Progress in Photosynthesis Research. Springer Netherlands.

Barger, N. N., S. R. Archer, J. L. Campbell, C. Y. Huang, J. A. Morton, and A. K. Knapp. 2011. Woody plant proliferation in North American drylands: A synthesis of impacts on ecosystem carbon balance. Journal of Geophysical Research-Biogeosciences **116**.

Barnes, P. W., S.-Y. Liang, K. E. Jessup, L. E. Ruiseco, P. L. Phillips, and S. J. Reagan. 2000. Soils, Topography and Vegetation of the Freeman Ranch.

Barron-Gafford, G. A., R. L. Scott, G. D. Jenerette, E. P. Hamerlynck, and T. E. Huxman. 2012. Temperature and precipitation controls over leaf- and ecosystem-level CO_2 flux along a woody plant encroachment gradient. Global Change Biology **18**:1389-1400.

Basham, T. S. 2013. Ecophysiology and ecosystem-level impacts of an invasive C4 perennial grass, *Bothriochloa ischaemum*. University of Texas, Austin, TX.

Beer, C., M. Reichstein, E. Tomelleri, P. Ciais, M. Jung, N. Carvalhais, C. Rodenbeck, M. A. Arain, D. Baldocchi, G. B. Bonan, A. Bondeau, A. Cescatti, G. Lasslop, A. Lindroth, M. Lomas, S. Luyssaert, H. Margolis, K. W. Oleson, O. Roupsard, E. Veenendaal, N. Viovy, C. Williams, F. I. Woodward, and D. Papale. 2010. Terrestrial gross carbon dioxide uptake: Global distribution and covariation with climate. Science **329**:834-838.

Bendevis, M. A., M. K. Owens, J. L. Heilman, and K. J. McInnes. 2010. Carbon exchange and water loss from two evergreen trees in a semiarid woodland. Ecohydrology **3**:107-115.

Bernacchi, C. J., E. L. Singsaas, C. Pimentel, A. R. Portis, and S. P. Long. 2001. Improved temperature response functions for models of Rubisco-limited photosynthesis. Plant Cell and Environment **24**:253-259.

Biggs, T. H., J. Quade, and R. H. Webb. 2002. $\delta^{13}C$ values of soil organic matter in semiarid grassland with mesquite (Prosopis) encroachment in southeastern Arizona. Geoderma **110**:109-130.

Bolton, J. and R. H. Brown. 1978. Effects of nitrogen nutrition on photosynthesis and associated characteristics in C3, C4 and intermediate grass species. Plant Physiology **61**:38-38.

Bonan, G. B., K. W. Oleson, M. Vertenstein, S. Levis, X. B. Zeng, Y. J. Dai, R. E. Dickinson, and Z. L. Yang. 2002. The land surface climatology of the community

land model coupled to the NCAR community climate model. Journal of Climate **15**:3123-3149.

Bond, W. J. and G. F. Midgley. 2000. A proposed CO_2-controlled mechanism of woody plant invasion in grasslands and savannas. Global Change Biology **6**:865-869.

Boutton, T. W., S. R. Archer, A. J. Midwood, S. F. Zitzer, and R. Bol. 1998. $\delta^{13}C$ values of soil organic carbon and their use in documenting vegetation change in a subtropical savanna ecosystem. Geoderma **82**:5-41.

Bradley, B. A., R. A. Houghtonw, J. F. Mustard, and S. P. Hamburg. 2006. Invasive grass reduces aboveground carbon stocks in shrublands of the Western US. Global Change Biology **12**:1815-1822.

Cable, J. M., G. A. Barron-Gafford, K. Ogle, M. Pavao-Zuckerman, R. L. Scott, D. G. Williams, and T. E. Huxman. 2012. Shrub encroachment alters sensitivity of soil respiration to temperature and moisture. Journal of Geophysical Research-Biogeosciences **117**.

Cable, J. M., K. Ogle, A. P. Tyler, M. A. Pavao-Zuckerman, and T. E. Huxman. 2009. Woody plant encroachment impacts on soil carbon and microbial processes: results from a hierarchical Bayesian analysis of soil incubation data. Plant and Soil **320**:153-167.

Cambardella, C. A. and E. T. Elliott. 1992. Particulate soil organic matter changes across a grassland cultivation sequence. Soil Science Society of America Journal **56**:777-783.

Campbell, G. S. and J. M. Norman. 1998. Introduction to environmental biophysics. 2nd edition. Springer, New York.

Chen, J. M., C. H. Menges, and S. G. Leblanc. 2005. Global mapping of foliage clumping index using multi-angular satellite data. Remote Sensing of Environment **97**:447-457.

Chen, Q., D. Baldocchi, P. Gong, and T. Dawson. 2008. Modeling radiation and photosynthesis of a heterogeneous savanna woodland landscape with a hierarchy of model complexities. Agricultural and Forest Meteorology **148**:1005-1020.

Christensen, J. H., K. Krishna Kumar, E. Aldrian, S.-I. An, I. F. A. Cavalcanti, M. de Castro, W. Dong, P. Goswami, A. Hall, J. K. Kanyanga, A. Kitoh, J. Kossin, N.-C. Lau, J. Renwick, D. B. Stephenson, X. S.-P., and Z. T. 2013. Climate Phenomena and their Relevance for Future Regional Climate Change. *in* T. F. Stocker, D. Qin, G.-K. Plattner, M. Tignor, S. K. Allen, J. Boschung, A. Nauels, Y. Xia, V. Bex, and P. M. Midgley, editors. Climate Change 2013: The Physical Science Basis. Contribution of Working Group I to the Fifth Assessment Report of the Intergovernmental Panel on Climate Change Cambridge University Press, Cambridge, United Kingdom and New York, NY, USA.

Ciais, P., C. Sabine, G. Bala, L. Bopp, V. Brovkin, J. Canadell, A. Chhabra, R. S. DeFries, J. Galloway, M. Heimann, C. Jones, C. Le Quéré, R. B. Myneni, S. Piao, and P. Thornton. 2013. Carbon and Other Biogeochemical Cycles.*in* T. F. Stocker, D. Qin, G.-K. Plattner, M. Tignor, S. K. Allen, J. Boschung, A. Nauels, Y. Xia, V. Bex, and P. M. Midgley, editors. Climate Change 2013: The Physical

Science Basis. Contribution of Working Group I to the Fifth Assessment Report of the Intergovernmental Panel on Climate Change. Cambridge University Press, Cambridge, United Kingdom and New York, NY, USA.

Colello, G. D., C. Grivet, P. J. Sellers, and J. A. Berry. 1998. Modeling of energy, water, and CO_2 flux in a temperate grassland ecosystem with SiB2: May-October 1987. Journal of the Atmospheric Sciences **55**:1141-1169.

Collatz, G. J., J. T. Ball, C. Grivet, and J. A. Berry. 1991. Physiological and environmental regulation of stomatal conductance, photosynthesis and transpiration - a model that includes a laminar boundary layer. Agricultural and Forest Meteorology **54**:107-136.

Collatz, G. J., M. Ribas-Carbo, and J. A. Berry. 1992. Coupled photosynthesis-stomatal conductance model for leaves of C4 plants. Australian Journal of Plant Physiology **19**:519-538.

Conant, R. T., P. Dalla-Betta, C. C. Klopatek, and J. A. Klopatek. 2004. Controls on soil respiration in semiarid soils. Soil Biology & Biochemistry **36**:945-951.

Cook, G. D., R. J. Williams, L. B. Hutley, A. P. O'Grady, and A. C. Liedloff. 2002. Variation in vegetative water use in the savannas of the North Australian Tropical Transect. Journal of Vegetation Science **13**:413-418.

Cornwell, W. K., J. H. C. Cornelissen, K. Amatangelo, E. Dorrepaal, V. T. Eviner, O. Godoy, S. E. Hobbie, B. Hoorens, H. Kurokawa, N. Perez-Harguindeguy, H. M. Quested, L. S. Santiago, D. A. Wardle, I. J. Wright, R. Aerts, S. D. Allison, P. van Bodegom, V. Brovkin, A. Chatain, T. V. Callaghan, S. Diaz, E. Garnier, D. E. Gurvich, E. Kazakou, J. A. Klein, J. Read, P. B. Reich, N. A. Soudzilovskaia, M. V. Vaieretti, and M. Westoby. 2008. Plant species traits are the predominant control on litter decomposition rates within biomes worldwide. Ecology Letters **11**:1065-1071.

Correia, A. C., F. Minunno, M. C. Caldeira, J. Banza, J. Mateus, M. Carneiro, L. Wingate, A. Shvaleva, A. Ramos, M. Jongen, M. N. Bugalho, C. Nogueira, X. Lecomte, and J. S. Pereira. 2012. Soil water availability strongly modulates soil CO_2 efflux in different Mediterranean ecosystems: Model calibration using the Bayesian approach. Agriculture Ecosystems & Environment **161**:88-100.

Dai, A. G. 2013. Increasing drought under global warming in observations and models. Nature Climate Change **3**:171-171.

Davidson, E. A., I. A. Janssens, and Y. Q. Luo. 2006. On the variability of respiration in terrestrial ecosystems: moving beyond Q_{10}. Global Change Biology **12**:154-164.

Eamus, D., L. B. Hutley, and A. P. O'Grady. 2001. Daily and seasonal patterns of carbon and water fluxes above a north Australian savanna. Tree Physiology **21**:977-988.

Eggemeyer, K. D. and S. Schwinning. 2009. Biogeography of woody encroachment: why is mesquite excluded from shallow soils? Ecohydrology **2**:81-87.

Eldridge, D. J., M. A. Bowker, F. T. Maestre, E. Roger, J. F. Reynolds, and W. G. Whitford. 2011. Impacts of shrub encroachment on ecosystem structure and functioning: towards a global synthesis. Ecology Letters **14**:709-722.

Elkington, R. J., K. T. Rebel, J. L. Heilman, M. E. Litvak, S. C. Dekker, and G. W. Moore. 2014. Species-specific water use by woody plants on the Edwards Plateau, Texas. Ecohydrology **7**:278-290.

Epron, D., L. Farque, E. Lucot, and P. M. Badot. 1999. Soil CO_2 efflux in a beech forest: dependence on soil temperature and soil water content. Annals of Forest Science **56**:221-226.

Farquhar, G. D. 1989. Models of integrated photosynthesis of cells and leaves. Philosophical Transactions of the Royal Society of London Series B-Biological Sciences **323**:357-367.

Fensham, R. J., R. J. Fairfax, and S. R. Archer. 2005. Rainfall, land use and woody vegetation cover change in semi-arid Australian savanna. Journal of Ecology **93**:596-606.

Fierer, N., J. M. Craine, K. McLauchlan, and J. P. Schimel. 2005. Litter quality and the temperature sensitivity of decomposition. Ecology **86**:320-326.

Flexas, J. and H. Medrano. 2002. Drought-inhibition of photosynthesis in C3 plants: Stomatal and non-stomatal limitations revisited. Annals of Botany **89**:183-189.

Fontaine, S., G. Bardoux, D. Benest, B. Verdier, A. Mariotti, and L. Abbadie. 2004. Mechanisms of the priming effect in a savannah soil amended with cellulose. Soil Science Society of America Journal **68**:125-131.

Friedlingstein, P., P. Cox, R. Betts, L. Bopp, W. Von Bloh, V. Brovkin, P. Cadule, S. Doney, M. Eby, I. Fung, G. Bala, J. John, C. Jones, F. Joos, T. Kato, M. Kawamiya, W. Knorr, K. Lindsay, H. D. Matthews, T. Raddatz, P. Rayner, C. Reick, E. Roeckner, K. G. Schnitzler, R. Schnur, K. Strassmann, A. J. Weaver, C. Yoshikawa, and N. Zeng. 2006. Climate-carbon cycle feedback analysis: Results from the (CMIP)-M-4 model intercomparison. Journal of Climate **19**:3337-3353.

Gabbard, B. L. and N. L. Fowler. 2007. Wide ecological amplitude of a diversity-reducing invasive grass. Biological Invasions **9**:149-160.

Gao, Q. and J. F. Reynolds. 2003. Historical shrub-grass transitions in the northern Chihuahuan Desert: modeling the effects of shifting rainfall seasonality and event size over a landscape gradient. Global Change Biology **9**:1475-1493.

González, A. V. 2010. Dynamics of woody plant encroachment in Texas savannas density dependence, environmental heterogeneity, and spatial patterns. University of Texas, Austin, TX.

Grace, J., J. San Jose, P. Meir, H. S. Miranda, and R. A. Montes. 2006. Productivity and carbon fluxes of tropical savannas. Journal of Biogeography **33**:387-400.

Guo, L. B. and R. M. Gifford. 2002. Soil carbon stocks and land use change: a meta analysis. Global Change Biology **8**:345-360.

Hall, M. T. 1952. Variation and hybridization in Juniperus. Annals of the Missouri Botanical garden **39**:1-64.

Hastings, S. J., W. C. Oechel, and A. Muhlia-Melo. 2005. Diurnal, seasonal and annual variation in the net ecosystem CO_2 exchange of a desert shrub community (Sarcocaulescent) in Baja California, Mexico. Global Change Biology **11**:927-939.

Heilman, J. L., M. E. Litvak, K. J. McInnes, J. F. Kjelgaard, R. H. Kamps, and S. Schwinning. 2012. Water-storage capacity controls energy partitioning and water use in karst ecosystems on the Edwards Plateau, Texas. Ecohydrology:n/a-n/a.

Heilman, J. L., M. E. Litvak, K. J. McInnes, J. F. Kjelgaard, R. H. Kamps, and S. Schwinning. 2014. Water-storage capacity controls energy partitioning and water use in karst ecosystems on the Edwards Plateau, Texas. Ecohydrology **7**:127-138.

Heilman, J. L., K. J. McInnes, J. F. Kjelgaard, M. K. Owens, and S. Schwinning. 2009. Energy balance and water use in a subtropical karst woodland on the Edwards Plateau, Texas. Journal of Hydrology **373**:426-435.

Hibbard, K. A., S. Archer, D. S. Schimel, and D. W. Valentine. 2001. Biogeochemical changes accompanying woody plant encroachment in a subtropical savanna. Ecology **82**:1999-2011.

Hibbard, K. A., D. S. Schimel, S. Archer, D. S. Ojima, and W. Parton. 2003. Grassland to woodland transitions: Integrating changes in landscape structure and biogeochemistry. Ecological Applications **13**:911-926.

Hicks, R. A. and W. A. Dugas. 1998. Estimating ashe juniper leaf area from tree and stem characteristics. Journal of Range Management **51**:633-637.

Hogberg, P., A. Nordgren, N. Buchmann, A. F. S. Taylor, A. Ekblad, M. N. Hogberg, G. Nyberg, M. Ottosson-Lofvenius, and D. J. Read. 2001. Large-scale forest girdling shows that current photosynthesis drives soil respiration. Nature **411**:789-792.

Hollister EB, Schadt CW, Palumbo AV, Ansley RJ, Boutton TW. 2010. Structural and functional diversity of soil bacterial and fungal communities following woody plant encroachment in the southern Great Plains. Soil Biology and Biochemistry 42: 1816-1824.

Houghton, R. A. 1999. The annual net flux of carbon to the atmosphere from changes in land use 1850-1990. Tellus Series B-Chemical and Physical Meteorology **51**:298-313.

Houghton, R. A., J. L. Hackler, and K. T. Lawrence. 1999. The US carbon budget: Contributions from land-use change. Science **285**:574-578.

Houghton, R. A., J. I. House, J. Pongratz, G. R. van der Werf, R. S. DeFries, M. C. Hansen, C. Le Quere, and N. Ramankutty. 2012. Carbon emissions from land use and land-cover change. Biogeosciences **9**:5125-5142.

House, J. I., S. Archer, D. D. Breshears, and R. J. Scholes. 2003. Conundrums in mixed woody-herbaceous plant systems. Journal of Biogeography **30**:1763-1777.

Hughes, R. F., S. R. Archer, G. P. Asner, C. A. Wessman, C. McMurtry, J. Nelson, and R. J. Ansley. 2006. Changes in aboveground primary production and carbon and nitrogen pools accompanying woody plant encroachment in a temperate savanna. Global Change Biology **12**:1733-1747.

Huxman, T. E., K. A. Snyder, D. Tissue, A. J. Leffler, K. Ogle, W. T. Pockman, D. R. Sandquist, D. L. Potts, and S. Schwinning. 2004. Precipitation pulses and carbon fluxes in semiarid and arid ecosystems. Oecologia **141**:254-268.

Huxman, T. E., B. P. Wilcox, D. D. Breshears, R. L. Scott, K. A. Snyder, E. E. Small, K. Hultine, W. T. Pockman, and R. B. Jackson. 2005. Ecohydrological implications of woody plant encroachment. Ecology **86**:308-319.

Jackson, R. B., J. L. Banner, E. G. Jobbagy, W. T. Pockman, and D. H. Wall. 2002. Ecosystem carbon loss with woody plant invasion of grasslands. Nature **418**:623-626.

Janssens, I. A., H. Lankreijer, G. Matteucci, A. S. Kowalski, N. Buchmann, D. Epron, K. Pilegaard, W. Kutsch, B. Longdoz, T. Grunwald, L. Montagnani, S. Dore, C. Rebmann, E. J. Moors, A. Grelle, U. Rannik, K. Morgenstern, S. Oltchev, R. Clement, J. Gudmundsson, S. Minerbi, P. Berbigier, A. Ibrom, J. Moncrieff, M. Aubinet, C. Bernhofer, N. O. Jensen, T. Vesala, A. Granier, E. D. Schulze, A. Lindroth, A. J. Dolman, P. G. Jarvis, R. Ceulemans, and R. Valentini. 2001. Productivity overshadows temperature in determining soil and ecosystem respiration across European forests. Global Change Biology **7**:269-278.

Jenerette, G. D., R. L. Scott, G. A. Barron-Gafford, and T. E. Huxman. 2009. Gross primary production variability associated with meteorology, physiology, leaf area, and water supply in contrasting woodland and grassland semiarid riparian ecosystems. Journal of Geophysical Research-Biogeosciences **114**.

Jessup, K. E., P. W. Barnes, and T. W. Boutton. 2003. Vegetation dynamics in a Quercus-Juniperus savanna: An isotopic assessment. Journal of Vegetation Science **14**:841-852.

Jiang, X. Y. and Z. L. Yang. 2012. Projected changes of temperature and precipitation in Texas from downscaled global climate models. Climate Research **53**:229-244.

Johnson, E. H. 2010. The Edwards Plateau. Handbook of Texas Texas State Historical Association.

King, A. W., L. Dilling, G. P. Zimmerman, D. M. Fairman, Richard A. Houghton, G. H. Marland, A. Z. Rose, and T. J. Wilbanks. 2007. The First State of the Carbon Cycle Report (SOCCR) North American Carbon Budget and Implications for the Global Carbon Cycle.

King, A. W., D. J. Hayes, D. N. Huntzinger, T. O. West, and W. M. Post. 2012. North American carbon dioxide sources and sinks: magnitude, attribution, and uncertainty. Frontiers in Ecology and the Environment **10**:512-519.

Kirschbaum, M. U. F. 2000. Will changes in soil organic carbon act as a positive or negative feedback on global warming? Biogeochemistry **48**:21-51.

Kjelgaard, J. F., J. L. Heilman, K. J. McInnes, M. K. Owens, and R. H. Kamps. 2008. Carbon dioxide exchange in a subtropical, mixed C3/C4 grassland on the Edwards Plateau, Texas. Agricultural and Forest Meteorology **148**:953-963.

Knapp, A. K., C. Beier, D. D. Briske, A. T. Classen, Y. Luo, M. Reichstein, M. D. Smith, S. D. Smith, J. E. Bell, P. A. Fay, J. L. Heisler, S. W. Leavitt, R. Sherry, B. Smith, and E. Weng. 2008a. Consequences of more extreme precipitation regimes for terrestrial ecosystems. Bioscience **58**:811-821.

Knapp, A. K., J. M. Briggs, S. L. Collins, S. R. Archer, M. S. Bret-Harte, B. E. Ewers, D. P. Peters, D. R. Young, G. R. Shaver, E. Pendall, and M. B. Cleary. 2008b. Shrub

encroachment in North American grasslands: shifts in growth form dominance rapidly alters control of ecosystem carbon inputs. Global Change Biology **14**:615-623.

Kobayashi, H., D. D. Baldocchi, Y. Ryu, Q. Chen, S. Y. Ma, J. L. Osuna, and S. L. Ustin. 2012. Modeling energy and carbon fluxes in a heterogeneous oak woodland: A three-dimensional approach. Agricultural and Forest Meteorology **152**:83-100.

Kucera, C. L. and D. R. Kirkham. 1971. Soil respiration studies in tallgrass prairie in Missouri. Ecology **52**:912-&.

Kukowski, K. R., S. Schwinning, and B. F. Schwartz. 2013. Hydraulic responses to extreme drought conditions in three co-dominant tree species in shallow soil over bedrock. Oecologia **171**:819-830.

Kurc, S. A. and E. E. Small. 2004. Dynamics of evapotranspiration in semiarid grassland and shrubland ecosystems during the summer monsoon season, central New Mexico. Water Resources Research **40**:15.

Kurc, S. A. and E. E. Small. 2007. Soil moisture variations and ecosystem-scale fluxes of water and carbon in semiarid grassland and shrubland. Water Resources Research **43**.

Kuzyakov, Y., J. K. Friedel, and K. Stahr. 2000. Review of mechanisms and quantification of priming effects. Soil Biology & Biochemistry **32**:1485-1498.

Lasslop, G., M. Reichstein, D. Papale, A. D. Richardson, A. Arneth, A. Barr, P. Stoy, and G. Wohlfahrt. 2010. Separation of net ecosystem exchange into assimilation and respiration using a light response curve approach: critical issues and global evaluation. Global Change Biology **16**:187-208.

Laubach, J. and K. G. McNaughton. 1998. A spectrum-independent procedure for correcting eddy fluxes measured with separated sensors. Boundary-Layer Meteorology **89**:445-467.

Law, B. E., E. Falge, L. Gu, D. D. Baldocchi, P. Bakwin, P. Berbigier, K. Davis, A. J. Dolman, M. Falk, J. D. Fuentes, A. Goldstein, A. Granier, A. Grelle, D. Hollinger, I. A. Janssens, P. Jarvis, N. O. Jensen, G. Katul, Y. Mahli, G. Matteucci, T. Meyers, R. Monson, W. Munger, W. Oechel, R. Olson, K. Pilegaard, K. T. Paw, H. Thorgeirsson, R. Valentini, S. Verma, T. Vesala, K. Wilson, and S. Wofsy. 2002. Environmental controls over carbon dioxide and water vapor exchange of terrestrial vegetation. Agricultural and Forest Meteorology **113**:97-120.

Le Quéré, C., G. P. Peters, R. J. Andres, R. M. Andrew, B. T.A.;, P. Ciais, P. Friedlingstein, R. A. Houghton, G. Marland, R. Moriarty, S. Sitch, P. Tans, A. Arneth, A. Arvanitis, D. C. E. Bakker, L. Bopp, J. G. Canadell, L. P. Chini, S. C. Doney, A. Harper, I. Harris, J. I. House, A. K. Jain, S. D. Jones, Kato E, R. F. Keeling, K. Klein Goldewijk, A. Körtzinger, Koven, N. Lefèvre, F. Maignan, A. Omar, T. Ono, G.-H. Park, B. Pfeil, B. Poulter, M. R. Raupach, P. Regnier, C. Rödenbeck, S. Saito, S. J., S. J., S. B. D., T. T., T. B., v. H. S., V. N., W. R., W. A., and Z. S. 2014. Global carbon budget 2013. Earth System Science Data **6**:235-263.

Liao, J. D., T. W. Boutton, and J. D. Jastrow. 2006. Storage and dynamics of carbon and nitrogen in soil physical fractions following woody plant invasion of grassland. Soil Biology & Biochemistry **38**:3184-3196.

Litvak, M. E., S. Schwinning, and J. L. Heilman. 2011. Woody plant rooting depth and ecosystem function of savannas: A case study from the Edwards Plateau Karst, Texas. Pages 117-134 *in* N. P. H. M.J. Hill, editor. Ecosystem function in Savannas: measuremnt and modeling at landscape to global scales. CRC Press, USA.

Lloyd, J. and J. A. Taylor. 1994. On the temperature dependence of soil respiration. Functional Ecology **8**:315-323.

Lucas, R. M., A. C. Lee, J. Armston, J. M. B. Carreiras, K. M. Viergeven, P. Bunting, D. Clewley, M. Moghaddam, P. Siqueira, and W. I. 2011. Quantifying Carbon in Savannas: the Role of Active Sensors in Measurements of Tree Structure and Biomass.*in* H. M.J. and N. P. Hanan, editors. Ecosystem Function in Savannas: Measurement and Modeling at Landscape to Global Scales. CRC Press, Boca Raton, FL.

Luyssaert, S., I. Inglima, M. Jung, A. D. Richardson, M. Reichstein, D. Papale, S. L. Piao, E. D. Schulzes, L. Wingate, G. Matteucci, L. Aragao, M. Aubinet, C. Beers, C. Bernhofer, K. G. Black, D. Bonal, J. M. Bonnefond, J. Chambers, P. Ciais, B. Cook, K. J. Davis, A. J. Dolman, B. Gielen, M. Goulden, J. Grace, A. Granier, A. Grelle, T. Griffis, T. Grunwald, G. Guidolotti, P. J. Hanson, R. Harding, D. Y. Hollinger, L. R. Hutyra, P. Kolar, B. Kruijt, W. Kutsch, F. Lagergren, T. Laurila, B. E. Law, G. Le Maire, A. Lindroth, D. Loustau, Y. Malhi, J. Mateus, M. Migliavacca, L. Misson, L. Montagnani, J. Moncrieff, E. Moors, J. W. Munger, E. Nikinmaa, S. V. Ollinger, G. Pita, C. Rebmann, O. Roupsard, N. Saigusa, M. J. Sanz, G. Seufert, C. Sierra, M. L. Smith, J. Tang, R. Valentini, T. Vesala, and I. A. Janssens. 2007. CO_2 balance of boreal, temperate, and tropical forests derived from a global database. Global Change Biology **13**:2509-2537.

Ma, S. Y., D. D. Baldocchi, L. K. Xu, and T. Hehn. 2007. Inter-annual variability in carbon dioxide exchange of an oak/grass savanna and open grassland in California. Agricultural and Forest Meteorology **147**:157-171.

Magee, P. 2002. Texas tussockgrass - *Nassella leucotricha (Trin. & Rupr.) Pohl.* - Plant Fact sheet. USDA NRCS National Plant Data Center, Baton Rouge, Louisiana.

Maherali, H., W. T. Pockman, and R. B. Jackson. 2004. Adaptive variation in the vulnerability of woody plants to xylem cavitation. Ecology **85**:2184-2199.

Massman, W. J. 2000. A simple method for estimating frequency response corrections for eddy covariance systems. Agricultural and Forest Meteorology **104**:185-198.

McCole, A. A. and L. A. Stern. 2007. Seasonal water use patterns of Juniperus ashei on the Edwards Plateau, Texas, based on stable isotopes in water. Journal of Hydrology **342**:238-248.

McCulley, R. L., S. R. Archer, T. W. Boutton, F. M. Hons, and D. A. Zuberer. 2004. Soil respiration and nutrient cycling in wooded communities developing in grassland. Ecology **85**:2804-2817.

McCulley, R. L. and R. B. Jackson. 2012. Conversion of Tallgrass Prairie to Woodland: Consequences for Carbon and Nitrogen Cycling. American Midland Naturalist **167**:307-321.

McDowell, N., W. T. Pockman, C. D. Allen, D. D. Breshears, N. Cobb, T. Kolb, J. Plaut, J. Sperry, A. West, D. G. Williams, and E. A. Yepez. 2008. Mechanisms of plant survival and mortality during drought: why do some plants survive while others succumb to drought? New Phytologist **178**:719-739.

Mielnick, P. C. and W. A. Dugas. 2000. Soil CO_2 flux in a tallgrass prairie. Soil Biology & Biochemistry **32**:221-228.

Moore, G. W. and J. L. Heilman. 2011. Proposed principles governing how vegetation changes affect transpiration. Ecohydrology **4**:351-358.

NCDC. http://www.ncdc.noaa.gov/cag/time-series/us. National Climatic Data Center.

Neff, J. C., N. N. Barger, W. T. Baisden, D. P. Fernandez, and G. P. Asner. 2009. Soil carbon storage responses to expanding pinyon-juniper populations in southern Utah. Ecological Applications **19**:1405-1416.

Niinemets, U., J. Flexas, and J. Penuelas. 2011. Evergreens favored by higher responsiveness to increased CO_2. Trends in Ecology & Evolution **26**:136-142.

Niu, S. L., Y. Q. Luo, S. F. Fei, W. P. Yuan, D. Schimel, B. E. Law, C. Ammann, M. A. Arain, A. Arneth, M. Aubinet, A. Barr, J. Beringer, C. Bernhofer, T. A. Black, N. Buchmann, A. Cescatti, J. Q. Chen, K. J. Davis, E. Dellwik, A. R. Desai, S. Etzold, L. Francois, D. Gianelle, B. Gielen, A. Goldstein, M. Groenendijk, L. H. Gu, N. Hanan, C. Helfter, T. Hirano, D. Y. Hollinger, M. B. Jones, G. Kiely, T. E. Kolb, W. L. Kutsch, P. Lafleur, D. M. Lawrence, L. H. Li, A. Lindroth, M. Litvak, D. Loustau, M. Lund, M. Marek, T. A. Martin, G. Matteucci, M. Migliavacca, L. Montagnani, E. Moors, J. W. Munger, A. Noormets, W. Oechel, J. Olejnik, T. P. U. Kyaw, K. Pilegaard, S. Rambal, A. Raschi, R. L. Scott, G. Seufert, D. Spano, P. Stoy, M. A. Sutton, A. Varlagin, T. Vesala, E. S. Weng, G. Wohlfahrt, B. Yang, Z. D. Zhang, and X. H. Zhou. 2012. Thermal optimality of net ecosystem exchange of carbon dioxide and underlying mechanisms. New Phytologist **194**:775-783.

Norman, J. M., C. J. Kucharik, S. T. Gower, D. D. Baldocchi, P. M. Crill, M. Rayment, K. Savage, and R. G. Striegl. 1997. A comparison of six methods for measuring soil-surface carbon dioxide fluxes. Journal of Geophysical Research-Atmospheres **102**:28771-28777.

Owens, M. K. and M. C. Schreiber. 1992. Seasonal gas exchange characteristics of two evergreen trees in a semiarid environment. Photosynthetica **26**:389-398.

Pacala, S. W., G. C. Hurtt, D. Baker, P. Peylin, R. A. Houghton, R. A. Birdsey, L. Heath, E. T. Sundquist, R. F. Stallard, P. Ciais, P. Moorcroft, J. P. Caspersen, E. Shevliakova, B. Moore, G. Kohlmaier, E. Holland, M. Gloor, M. E. Harmon, S. M. Fan, J. L. Sarmiento, C. L. Goodale, D. Schimel, and C. B. Field. 2001. Consistent land- and atmosphere-based US carbon sink estimates. Science **292**:2316-2320.

Polley, H. W., H. S. Mayeux, H. B. Johnson, and C. R. Tischler. 1997. Viewpoint: Atmospheric CO_2, soil water, and shrub/grass ratios on rangelands. Journal of Range Management **50**:278-284.

Raich, J. W. and W. H. Schlesinger. 1992. The global carbon dioxide flux in soil respiration and its relationship to vegetation and climate. Tellus Series B-Chemical and Physical Meteorology **44**:81-99.

Raich, J. W. and A. Tufekcioglu. 2000. Vegetation and soil respiration: Correlations and controls. Biogeochemistry **48**:71-90.

Rasband, W. S. 1997-2014. ImageJ, U. S. National Institutes of Health, Bethesda, Maryland, USA, http://imagej.nih.gov/ij/, 1997-2014. .

Reich, P. B., D. W. Peterson, D. A. Wedin, and K. Wrage. 2001. Fire and vegetation effects on productivity and nitrogen cycling across a forest-grassland continuum. Ecology **82**:1703-1719.

Reich, P. B., M. B. Walters, and D. S. Ellsworth. 1997. From tropics to tundra: Global convergence in plant functioning. Proceedings of the National Academy of Sciences of the United States of America **94**:13730-13734.

Reichstein, M., E. Falge, D. Baldocchi, D. Papale, M. Aubinet, P. Berbigier, C. Bernhofer, N. Buchmann, T. Gilmanov, A. Granier, T. Grunwald, K. Havrankova, H. Ilvesniemi, D. Janous, A. Knohl, T. Laurila, A. Lohila, D. Loustau, G. Matteucci, T. Meyers, F. Miglietta, J. M. Ourcival, J. Pumpanen, S. Rambal, E. Rotenberg, M. Sanz, J. Tenhunen, G. Seufert, F. Vaccari, T. Vesala, D. Yakir, and R. Valentini. 2005. On the separation of net ecosystem exchange into assimilation and ecosystem respiration: review and improved algorithm. Global Change Biology **11**:1424-1439.

Reichstein, M., A. Rey, A. Freibauer, J. Tenhunen, R. Valentini, J. Banza, P. Casals, Y. F. Cheng, J. M. Grunzweig, J. Irvine, R. Joffre, B. E. Law, D. Loustau, F. Miglietta, W. Oechel, J. M. Ourcival, J. S. Pereira, A. Peressotti, F. Ponti, Y. Qi, S. Rambal, M. Rayment, J. Romanya, F. Rossi, V. Tedeschi, G. Tirone, M. Xu, and D. Yakir. 2003. Modeling temporal and large-scale spatial variability of soil respiration from soil water availability, temperature and vegetation productivity indices. Global Biogeochemical Cycles **17**.

Reichstein, M., J. D. Tenhunen, O. Roupsard, J. M. Ourcival, S. Rambal, F. Miglietta, A. Peressotti, M. Pecchiari, G. Tirone, and R. Valentini. 2002. Severe drought effects on ecosystem CO_2 and H_2O fluxes at three Mediterranean evergreen sites: revision of current hypotheses? Global Change Biology **8**:999-1017.

Richards, F. J. 1959. A flexible growth function for empirical use. Journal of Experimental Botany **10**:290-300.

Ryan, M. G. and B. E. Law. 2005. Interpreting, measuring, and modeling soil respiration. Biogeochemistry **73**:3-27.

Sage, R. F. 2004. The evolution of C4 photosynthesis. New Phytologist **161**:341-370.

Sage, R. F. and R. W. Pearcy. 1987. The nitrogen use efficiency of C3 and C4 plants. 2. Leaf nitrogen effects on the gas exchange characteristics of Chenopodium album (L.) and Amaranthus retroflexus (L.). Plant Physiology **84**:959-963.

Sankaran, M., J. Ratnam, and N. P. Hanan. 2004. Tree-grass coexistence in savannas revisited - insights from an examination of assumptions and mechanisms invoked in existing models. Ecology Letters **7**:480-490.

Scheffer, M., S. Carpenter, J. A. Foley, C. Folke, and B. Walker. 2001. Catastrophic shifts in ecosystems. Nature **413**:591-596.

Schenk, H. J. and R. B. Jackson. 2002. Rooting depths, lateral root spreads and below-ground/above-ground allometries of plants in water-limited ecosystems. Journal of Ecology **90**:480-494.

Scholes, R. J. and S. R. Archer. 1997. Tree-grass interactions in savannas. Annual Review of Ecology and Systematics **28**:517-544.

Scholes, R. J. and B. H. Walker. 1993. An African savannas: synthesis of the Nylsvley study. Cambridge University Press, Cambridge, UK.

Schwalm, C. R., C. A. Williams, K. Schaefer, A. Arneth, D. Bonal, N. Buchmann, J. Q. Chen, B. E. Law, A. Lindroth, S. Luyssaert, M. Reichstein, and A. D. Richardson. 2010. Assimilation exceeds respiration sensitivity to drought: A FLUXNET synthesis. Global Change Biology **16**:657-670.

Schwinning, S. 2008. The water relations of two evergreen tree species in a karst savanna. Oecologia **158**:373-383.

Schwinning, S. 2010. The ecohydrology of roots in rocks. Ecohydrology **3**:238-245.

Schwinning, S. 2013. Do we need new rhizosphere models for rock-dominated landscapes? Plant and Soil **362**:25-31.

Schwinning, S., O. E. Sala, M. E. Loik, and J. R. Ehleringer. 2004. Thresholds, memory, and seasonality: understanding pulse dynamics in arid/semi-arid ecosystems. Oecologia **141**:191-193.

Scott, R. L., T. E. Huxman, G. A. Barron-Gafford, G. D. Jenerette, J. M. Young, and E. P. Hamerlynck. 2014. When vegetation change alters ecosystem water availability. Global Change Biology **20**:2198-2210.

Scott, R. L., T. E. Huxman, D. G. Williams, and D. C. Goodrich. 2006. Ecohydrological impacts of woody-plant encroachment: seasonal patterns of water and carbon dioxide exchange within a semiarid riparian environment. Global Change Biology **12**:311-324.

Scott, R. L., G. D. Jenerette, D. L. Potts, and T. E. Huxman. 2009. Effects of seasonal drought on net carbon dioxide exchange from a woody-plant-encroached semiarid grassland. Journal of Geophysical Research-Biogeosciences **114**.

Seager, R., M. F. Ting, I. Held, Y. Kushnir, J. Lu, G. Vecchi, H. P. Huang, N. Harnik, A. Leetmaa, N. C. Lau, C. H. Li, J. Velez, and N. Naik. 2007. Model projections of an imminent transition to a more arid climate in southwestern North America. Science **316**:1181-1184.

Sellers, P. J., J. A. Berry, G. J. Collatz, C. B. Field, and F. G. Hall. 1992. Canopy reflectance, photosynthesis, and transpiration. 3. A reanalysis using improved leaf models and a new canopy integration scheme. Remote Sensing of Environment **42**:187-216.

Sellers, P. J., R. E. Dickinson, D. A. Randall, A. K. Betts, F. G. Hall, J. A. Berry, G. J. Collatz, A. S. Denning, H. A. Mooney, C. A. Nobre, N. Sato, C. B. Field, and A. Henderson-Sellers. 1997. Modeling the exchanges of energy, water, and carbon between continents and the atmosphere. Science **275**:502-509.

Sellers, P. J., S. O. Los, C. J. Tucker, C. O. Justice, D. A. Dazlich, G. J. Collatz, and D. A. Randall. 1996a. A revised land surface parameterization (SiB2) for atmospheric GCMs .2. The generation of global fields of terrestrial biophysical parameters from satellite data. Journal of Climate **9**:706-737.

Sellers, P. J., D. A. Randall, G. J. Collatz, J. A. Berry, C. B. Field, D. A. Dazlich, C. Zhang, G. D. Collelo, and L. Bounoua. 1996b. A revised land surface parameterization (SiB2) for atmospheric GCMs .1. Model formulation. Journal of Climate **9**:676-705.

Smith, D. L. and L. Johnson. 2004. Vegetation-mediated changes in microclimate reduce soil respiration as woodlands expand into grasslands. Ecology **85**:3348-3361.

Smith, D. L. and L. C. Johnson. 2003. Expansion of *Juniperus virginiana L.* in the Great Plains: Changes in soil organic carbon dynamics. Global Biogeochemical Cycles **17**.

Soper FM, Boutton TW, Sparks JP. 2014. Investigating patterns of symbiotic nitrogen fixation during vegetation change from grassland to woodland using fine scale $\delta^{15}N$ measurements. Plant, Cell, and Environment doi: 10.1111/pce.12373.

Storn, R. and K. Price. 1997. Differential evolution - A simple and efficient heuristic for global optimization over continuous spaces. Journal of Global Optimization **11**:341-359.

Sun, Y., L. Gu, R. E. Dickinson, R. J. Norby, S. G. Pallardy, and H. F. M. 2014. Impact of mesophyll diffusion on estimated global land CO2 fertilization - published ahead of print October 13, 2014. Proceedings of the National Academy of Sciences of the United States of America.

Tang, J. W. and D. D. Baldocchi. 2005. Spatial-temporal variation in soil respiration in an oak-grass savanna ecosystem in California and its partitioning into autotrophic and heterotrophic components. Biogeochemistry **73**:183-207.

Thornton, P. E., B. E. Law, H. L. Gholz, K. L. Clark, E. Falge, D. S. Ellsworth, A. H. Golstein, R. K. Monson, D. Hollinger, M. Falk, J. Chen, and J. P. Sparks. 2002. Modeling and measuring the effects of disturbance history and climate on carbon and water budgets in evergreen needleleaf forests. Agricultural and Forest Meteorology **113**:185-222.

Throop, H. L. and S. R. Archer. 2007. Interrelationships among shrub encroachment, land management, and litter decomposition in a semidesert grassland. Ecological Applications **17**:1809-1823.

Throop, H. L. and S. R. Archer. 2008. Shrub (*Prosopis velutina*) encroachment in a semidesert grassland: spatial-temporal changes in soil organic carbon and nitrogen pools. Global Change Biology **14**:2420-2431.

Throop, H. L., L. G. Reichmann, O. E. Sala, and S. R. Archer. 2012. Response of dominant grass and shrub species to water manipulation: an ecophysiological

basis for shrub invasion in a Chihuahuan Desert Grassland. Oecologia **169**:373-383.

Valentini, R., G. Matteucci, A. J. Dolman, E. D. Schulze, C. Rebmann, E. J. Moors, A. Granier, P. Gross, N. O. Jensen, K. Pilegaard, A. Lindroth, A. Grelle, C. Bernhofer, T. Grunwald, M. Aubinet, R. Ceulemans, A. S. Kowalski, T. Vesala, U. Rannik, P. Berbigier, D. Loustau, J. Guomundsson, H. Thorgeirsson, A. Ibrom, K. Morgenstern, R. Clement, J. Moncrieff, L. Montagnani, S. Minerbi, and P. G. Jarvis. 2000. Respiration as the main determinant of carbon balance in European forests. Nature **404**:861-865.

Van Auken, O. W. 2000. Shrub invasions of North American semiarid grasslands. Annual Review of Ecology and Systematics **31**:197-215.

Vesala, T., N. Kljun, U. Rannik, J. Rinne, A. Sogachev, T. Markkanen, K. Sabelfeld, T. Foken, and M. Y. Leclerc. 2008. Flux and concentration footprint modelling: State of the art. Environmental Pollution **152**:653-666.

Vico, G. and A. Porporato. 2008. Modelling C3 and C4 photosynthesis under water-stressed conditions. Plant and Soil **313**:187-203.

Volder, A., M. G. Tjoelker, and D. D. Briske. 2010. Contrasting physiological responsiveness of establishing trees and a C4 grass to rainfall events, intensified summer drought, and warming in oak savanna. Global Change Biology **16**:3349-3362.

Vourlitis, G. L., W. C. Oechel, S. J. Hastings, and M. A. Jenkins. 1993. A system for measuring in-situ CO_2 and CH_4 flux in unmanaged ecosystems - an arctic example. Functional Ecology **7**:369-379.

Waldrop, M. P. and M. K. Firestone. 2006. Seasonal dynamics of microbial community composition and function in oak canopy and open grassland soils. Microbial Ecology **52**:470-479.

Walker, B. H. and I. Noy-Meir. 1982. Aspects of the stability and resilience of savanna ecosystems. Pages 556-590 *in* B. J. Huntley and B. H. Walker, editors. Ecology of tropical savannas

Walter, H. 1954. Shrub encroachment, a phenomenon of subtropical savanna regions and its ecological causes. Vegetatio **5**:6-10.

Ward, D., K. Wiegand, and S. Getzin. 2013. Walter's two-layer hypothesis revisited: back to the roots! Oecologia **172**:617-630.

Webb, E. K., G. I. Pearman, and R. Leuning. 1980. Correction of flux measurements for density effects due to heat and water vapor transfer Quarterly Journal of the Royal Meteorological Society **106**:85-100.

Webster, K. L., I. F. Creed, M. D. Skowronski, and Y. H. Kaheil. 2009. Comparison of the performance of statistical models that predict soil respiration from forests. Soil Science Society of America Journal **73**:1157-1167.

Wigley, B. J., W. J. Bond, and M. T. Hoffman. 2010. Thicket expansion in a South African savanna under divergent land use: local vs. global drivers? Global Change Biology **16**:964-976.

Wilcox, B. P. 2002. Shrub control and streamflow on rangelands: A process based viewpoint. Journal of Range Management **55**:318-326.

Wilcox, B. P., M. K. Owens, R. W. Knight, and R. K. Lyons. 2005. Do woody plants affect streamflow on semiarid karst rangelands? Ecological Applications **15**:127-136.

Williams, A. P., C. D. Allen, A. K. Macalady, D. Griffin, C. A. Woodhouse, D. M. Meko, T. W. Swetnam, S. A. Rauscher, R. Seager, H. D. Grissino-Mayer, J. S. Dean, E. R. Cook, C. Gangodagamage, M. Cai, and N. G. McDowell. 2013. Temperature as a potent driver of regional forest drought stress and tree mortality. Nature Climate Change **3**:292-297.

Williams, C. A. and J. D. Albertson. 2004. Soil moisture controls on canopy-scale water and carbon fluxes in an African savanna. Water Resources Research **40**.

Williams, C. A. and J. D. Albertson. 2005. Contrasting short- and long-timescale effects of vegetation dynamics on water and carbon fluxes in water-limited ecosystems. Water Resources Research **41**.

Williams, C. A., N. Hanan, R. J. Scholes, and W. Kutsch. 2009. Complexity in water and carbon dioxide fluxes following rain pulses in an African savanna. Oecologia **161**:469-480.

Wright, I. J., P. B. Reich, M. Westoby, D. D. Ackerly, Z. Baruch, F. Bongers, J. Cavender-Bares, T. Chapin, J. H. C. Cornelissen, M. Diemer, J. Flexas, E. Garnier, P. K. Groom, J. Gulias, K. Hikosaka, B. B. Lamont, T. Lee, W. Lee, C. Lusk, J. J. Midgley, M. L. Navas, U. Niinemets, J. Oleksyn, N. Osada, H. Poorter, P. Poot, L. Prior, V. I. Pyankov, C. Roumet, S. C. Thomas, M. G. Tjoelker, E. J. Veneklaas, and R. Villar. 2004. The worldwide leaf economics spectrum. Nature **428**:821-827.

Xu, L. K. and D. D. Baldocchi. 2004. Seasonal variation in carbon dioxide exchange over a Mediterranean annual grassland in California. Agricultural and Forest Meteorology **123**:79-96.

Yi, C. X. and D. Ricciuto and R. Li and J. Wolbeck and X. Y. Xu and M. Nilsson and L. Aires and J. D. Albertson and C. Ammann and M. A. Arain and A. C. de Araujo and M. Aubinet and M. Aurela and Z. Barcza and A. Barr and P. Berbigier and J. Beringer and C. Bernhofer and A. T. Black and P. V. Bolstad and F. C. Bosveld and M. S. J. Broadmeadow and N. Buchmann and S. P. Burns and P. Cellier and J. M. Chen and J. Q. Chen and P. Ciais and R. Clement and B. D. Cook and P. S. Curtis and D. B. Dail and E. Dellwik and N. Delpierre and A. R. Desai and S. Dore and D. Dragoni and B. G. Drake and E. Dufrene and A. Dunn and J. Elbers and W. Eugster and M. Falk and C. Feigenwinter and L. B. Flanagan and T. Foken and J. Frank and J. Fuhrer and D. Gianelle and A. Goldstein and M. Goulden and A. Granier and T. Grunwald and L. Gu and H. Q. Guo and A. Hammerle and S. J. Han and N. P. Hanan and L. Haszpra and B. Heinesch and C. Helfter and D. Hendriks and L. B. Hutley and A. Ibrom and C. Jacobs and T. Johansson and M. Jongen and G. Katul and G. Kiely and K. Klumpp and A. Knohl and T. Kolb and W. L. Kutsch and P. Lafleur and T. Laurila and R.

Leuning and A. Lindroth and H. P. Liu and B. Loubet and G. Manca and M. Marek and H. A. Margolis and T. A. Martin and W. J. Massman and R. Matamala and G. Matteucci and H. McCaughey and L. Merbold and T. Meyers and M. Migliavacca and F. Miglietta and L. Misson and M. Moelder and J. Moncrieff and R. K. Monson and L. Montagnani and M. Montes-Helu and E. Moors and C. Moureaux and M. M. Mukelabai and J. W. Munger and M. Myklebust and Z. Nagy and A. Noormets and W. Oechel and R. Oren and S. G. Pallardy and T. P. U. Kyaw and J. S. Pereira and K. Pilegaard and K. Pinter and C. Pio and G. Pita and T. L. Powell and S. Rambal and J. T. Randerson and C. von Randow and C. Rebmann and J. Rinne and F. Rossi and N. Roulet and R. J. Ryel and J. Sagerfors and N. Saigusa and M. J. Sanz and G. S. Mugnozza and H. P. Schmid and G. Seufert and M. Siqueira and J. F. Soussana and G. Starr and M. A. Sutton and J. Tenhunen and Z. Tuba and J. P. Tuovinen and R. Valentini and C. S. Vogel and J. X. Wang and S. Q. Wang and W. G. Wang and L. R. Welp and X. F. Wen and S. Wharton and M. Wilkinson and C. A. Williams and G. Wohlfahrt and S. Yamamoto and G. R. Yu and R. Zampedri and B. Zhao and X. Q. Zhao. 2010. Climate control of terrestrial carbon exchange across biomes and continents. Environmental Research Letters **5**.

Yuan, W., Y. Luo, S. Liang, G. Yu, S. Niu, P. Stoy, J. Chen, A. R. Desai, A. Lindroth, C. M. Gough, R. Ceulemans, A. Arain, C. Bernhofer, B. Cook, D. R. Cook, D. Dragoni, B. Gielen, I. A. Janssens, B. Longdoz, H. Liu, M. Lund, G. Matteucci, E. Moors, R. L. Scott, G. Seufert, and R. Varner. 2011. Thermal adaptation of net ecosystem exchange. Biogeosciences **8**:1453-1463.

Yuste, J. C., D. D. Baldocchi, A. Gershenson, A. Goldstein, L. Misson, and S. Wong. 2007. Microbial soil respiration and its dependency on carbon inputs, soil temperature and moisture. Global Change Biology **13**:2018-2035.

Yuste, J. C., I. A. Janssens, A. Carrara, and R. Ceulemans. 2004. Annual Q_{10} of soil respiration reflects plant phenological patterns as well as temperature sensitivity. Global Change Biology **10**:161-169.

Zhou, X. H., E. S. Weng, and Y. Q. Luo. 2008. Modeling patterns of nonlinearity in ecosystem responses to temperature, CO_2, and precipitation changes. Ecological Applications **18**:453-466.

Zitzer, S. F., S. R. Archer, and T. W. Boutton. 1996. Spatial variability in the potential for symbiotic N-2 fixation by woody plants in a subtropical savanna ecosystem. Journal of Applied Ecology **33**:1125-1136.

Vita

Ann Thijs attended the Catholic University of Leuven (KULeuven, Belgium) from 1994-2000 and received a Bachelors and Masters in Applied Biological Sciences, with a specialization in Environmental Engineering in 2000. From 2000-2003, she worked as a researcher at the Department of Earth and Environmental Sciences at KULeuven. She developed a monitoring network for acidification and eutrophication processes in wetland ecosystems in Belgium, under a grant from the Flemish Government. In 2003, she moved to the US and started graduate school in August 2003.

Permanent email: ann@vancorenland.com

This dissertation was typed by Ann Thijs.